NAVAL MATERIALS SCIENCE - VOL 2 OF 2

Main Category:	Naval Engineering
Sub Category:	-
Course #:	NAV-120
Course Content:	171 pgs
PDH/CE Hours:	8

OFFICIAL COURSE/EXAM
(SEE INSTRUCTIONS ON NEXT PAGE)

NAV-120 EXAM PREVIEW

Instructions:

- At your convenience and own pace, review the course material below. When ready, click "Take Exam!" above to complete the live graded exam. (Note it may take a few seconds for the link to pull up the exam.) You will be able to re-take the exam as many times as needed to pass.
- Upon a satisfactory completion of the course exam, which is a score of 70% or better, you will be provided with your course completion certificate. Be sure to download and print your certificates to keep for your records.

Exam Preview:

1. "Creep" is a progressive plastic deformation that increases with time, even when the stress is below the yield stress of the material. The effects of creep increase as temperature increases, and generally noticeable at above 35% of the melting temperature of the material.
   a. True
   b. False
2. The coordination number is the number of nearest neighbors of an individual atom in a lattice structure. An FCC lattice has a coordination number of 12, while a BCC structure has a coordination number of __.
   a. 8
   b. 10
   c. 16
   d. 20
3. According to the reference material, the compressive strength of concrete varies from ≈ 3-14 ksi. The tensile strength is about 30% of compressive strength.
   a. True
   b. False
4. Alloys of iron and carbon for the system for common steels and cast irons. Generally, steels have a carbon content between 0 and 2 % by weight, while cast irons have a carbon content between _____ % by weight.
   a. 8 and 12
   b. 3 and 7
   c. 6 and 10
   d. 2 and 5

5. Using Fig. 24 Heat Treatment of Eutectic Steel and the surrounding reference material, which of the following cooling techniques produces a fine pearlite structure?
    a. Water quench
    b. Oil quench
    c. Air cool
    d. Furnace cool
6. According to the reference material, in the elastic region, the difference between A and Ao and l and lo is very small so that the "true" stress and strain values are essentially the same as the engineering stress and strain values.
    a. True
    b. False
7. According to the reference material, a typical concrete mixture has 5 main components. Which of the following components contributes the MOST to this mixture?
    a. Portland Cement
    b. Fine Aggregate
    c. Coarse Aggregate
    d. Water
8. There are five material properties that do a good job at describing the characteristics of a material. They are strength, hardness, brittleness, toughness, and ductility. Which of the following properties matches the description: is measure of the materials ability to resist deformation and to maintain its shape.?
    a. Strength
    b. Hardness
    c. Brittleness
    d. Toughness
9. Material properties of wood are generally given for the longitudinal direction and are presented for a standard moisture content of 25%.
    a. True
    b. False
10. The three directional properties of wood vary widely, but in general, if a wood species has a longitudinal strength of ___, its radial strength will be about 5-10 and its tangential strength about 2-10.
    a. 15
    b. 20
    c. 50
    d. 100

CHAPTER 7

MICROSTRUCTURE OF MATERIALS

7.1 Fundamentals
7.2 Bonding
7.3 Crystalline Structure
7.4 Density Calculation
7.5 Direction Indices and Miller Indices
7.6 Polymorphism
7.7 Coordination Number and Packing Factor
7.8 Solidification

7.1 Fundamentals

Materials consist of atoms or molecules (two or more atoms bonded together). In gases, the atoms or molecules are in constant translational motion; in liquids, this motion is greatly reduced; and in solids, there is essentially no translational motion.

    A. Atomic Scale:
        Arrangement of atoms
        Fundamental processes (i.e. molecular bonding and forces, etc.)
    B. Microscopic Scale:
        Properties observable with a microscope (i.e. phases, grains, etc.)
    C. Macroscopic Scale:
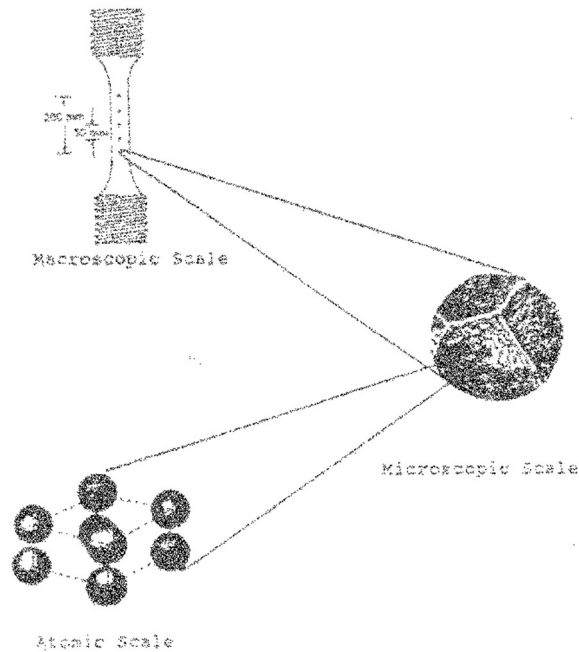   Typical scales of measurement (i.e. cm, inches, yield point, etc.)

Figure 1: Scales of Investigation of Materials

7.2 Bonding

In the solid state, the atoms are held together by <u>ionic, covalent, or metallic bonding</u>.

<u>Ionic Bonding</u>: Bonding force results from an electrical attraction between ions of opposite charge. Most commonly occurs in materials with loosely held electrons or nearly filled outside shells.

<u>Covalent Bonding</u>: Bonding occurs when atoms share electrons, usually to complete the outside shell of one or both of the atoms.

<u>Metallic Bonding</u>: Bonding occurs when a few electrons from an incomplete outer shell break free, forming a "cloud" of free electrons which move about the metal structure. The positively charged "core" maintains an attraction to the negatively charged "clouds," and other similar "cores" are likewise attracted to the "cloud," thus creating a bond between the various atoms within the metallic structure.

Material	Symbol	Type of Bond	Bond Energy, eV (per atom)
Cesium Chloride	CsCl	Ionic	3.4
Sodium Chloride	NaCl	Ionic	4.0
Aluminum Oxide	Al2O3	Ionic	31.4
Magnesium Oxide	MgO	Ionic	20.4
Silicon	Si	Covalent	4.7
Diamond	C	Covalent	7.4
Silicon Carbide	SiC	Covalent	6.4
Mercury	Hg	Metallic	0.7
Aluminum	Al	Metallic	3.4
Iron	Fe	Metallic	4.3
Tungsten	W	Metallic	8.8

7.3 Crystalline Structure

Solids formed by these bonds may be either <u>crystalline</u> or <u>non-crystalline</u> in nature. Crystalline materials have a periodic repeating of the atoms or groups of atoms throughout the material. Non-crystalline materials have a random arrangement of the atoms.

Crystalline solids possess symmetry of atomic arrangement. This symmetry involves a <u>space lattice</u> and a <u>basis</u>.

<u>Space Lattice</u>: Involves the concept of points in space with equal surroundings. Consider the two-dimensional representation of points shown in Figure 2. This represents a simple lattice, since each interior point has identical surroundings. The lattice has associated with it a <u>lattice cell</u> which, in this two dimensional case, is simply a square cell with all sides of equal length "a". Obviously a lattice could be constructed with a rectangular cell shape.

Figure 2: (a) Lattice and (b) Basis

Basis: Suppose we have two atoms, A and B, arranged as shown in figure 3. If we place atom A of the set on each lattice point in Figure 2, we then have a crystalline structure. (A crystalline structure has a set of atoms repeating itself periodically and having identical surroundings as shown in Figure 3). The set of atoms that repeats itself, i.e. A-B, A-B, is known as the basis. The basis may consist of a single atom or a complex group of atoms.
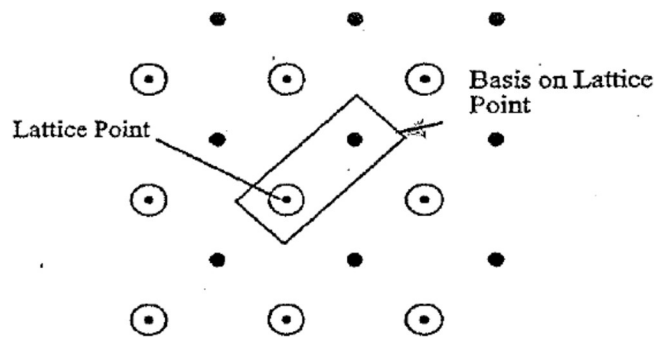

Figure 3: Crystal structure in terms of lattice and basis

The above discussions of the lattice and basis are for the illustrated two-dimensional case, but can easily be expanded into the real world three-dimensional case. In three-dimensions, there are only fourteen possible lattice cells that can exist. Some of the more common of these are illustrated in figure 4.
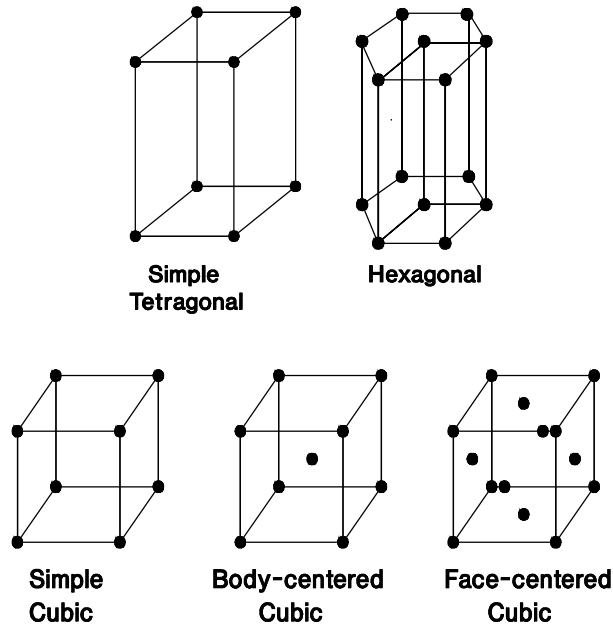
7 - 3

Figure 4: Common Lattice Structures

For metals, the basis often consists of a single atom such that the corresponding crystalline structure consists of the appropriate space lattice with atoms located at its lattice points. For example, iron has a crystalline structure consisting of single atoms located at the points of the body-centered cubic lattice. Aluminum has a structure consisting of single atoms located at the points of a face-centered cubic structure.

An exception to this is the hexagonal close-packed crystalline structure of metals such a zinc and titanium. Here the lattice is hexagonal and its basis consists of two atoms such that there is an intermediate row of atoms between the top and bottom of the hexagonal cell
(Figure 5). This gives rise to the so-called ABAB stacking of atoms. Note that the lattice cells are described by parameters "a" and "c".
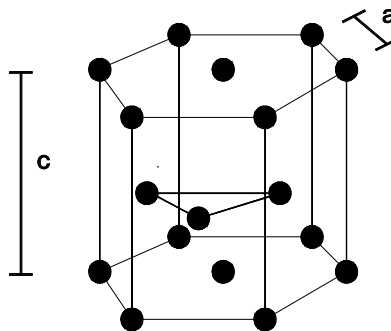

Figure 5: Hexagonal Close Packed Lattice

<u>Hard-Ball Model</u>. If we consider atoms to be hard spheres of definite radius in contact with other atoms in the directions of closest approach, we can relate the atomic radius to lattice parameter. For the face-centered cubic (FCC), the spheres are in contact along the face diagonals. For a body-centered cubic (BCC) the spheres must be in contact along the cube diagonal.

7 - 4

(a)　　　　　　(b)　　　　　　(c)

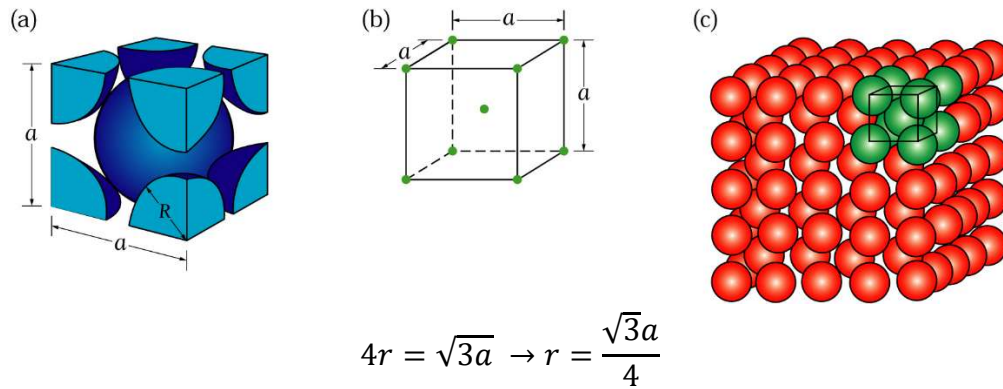$$4r = \sqrt{3a} \ \rightarrow r = \frac{\sqrt{3}a}{4}$$

Figure 6: Body Centered Cubic

(a)　　　　　　(b)　　　　　　(c)

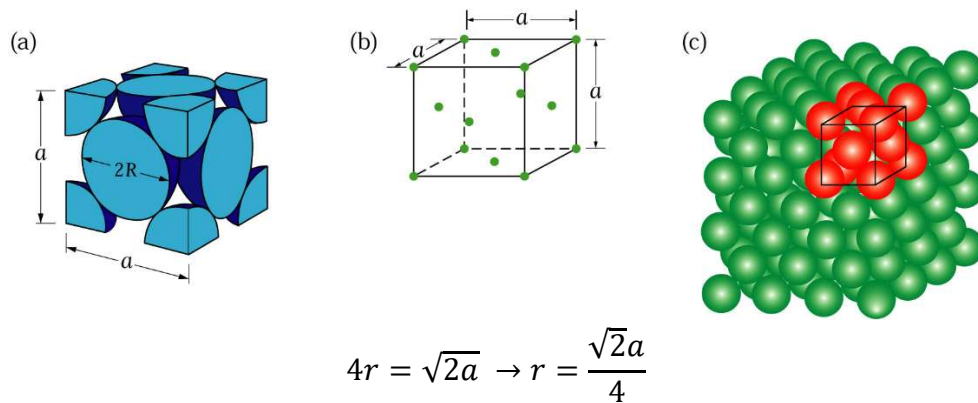$$4r = \sqrt{2a} \ \rightarrow r = \frac{\sqrt{2}a}{4}$$

Figure 7: Face Centered Cubic
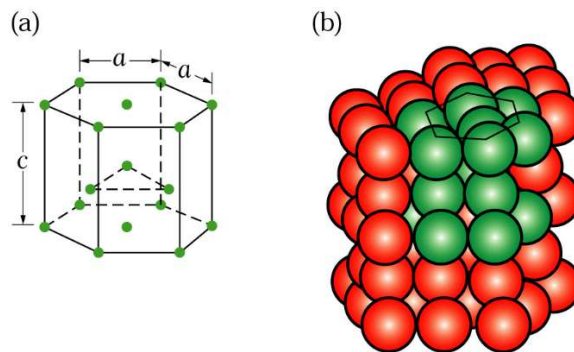
(a)　　　　　　(b)

Figure 8: Hexagonal Close Packed

7 - 5

7.4 Density Calculation

The density of the material may also be calculated from a knowledge of the lattice parameters and the atomic weight (A.W. the weight in grams of Avogadro's Number (6.024×10^{23}) of atoms) of the material. If n = number of atoms in a lattice cell, then

$$\rho = \frac{n \times m}{Volume \ of \ Lattice \ cell}$$

Or, using the weight of one atom,

$$\rho = \frac{n\left(\frac{A.W}{6.024 \ x \ 10^{23}}\right)}{Lattice \ volume \ of \ cell}$$

For metals with cubic arrangement of atoms, the volume of the lattice cell is simply the cube of the lattice parameter (defining the length of the sides of the cells. Noting that lattice cells repeat, and can be considered in contact with one another, it can be seen that an atom at a corner of a cell is actually shared with 7 other cells, so only 1/8 atom belongs to any one cell. The 8 corners of a cell thus provide only one net atom to the cell.

Also, for a FCC cell, the atoms on each face are shared with an adjacent cell, so that the 6 atoms on the faces of any cell provide a net of 3 atoms per cell. The corner and face atoms together thus provide a net number of 4 atoms per cell.

For a BCC cell, the 8 corner atoms contribute the same, namely one atom, while the atom at the center is not shared by any other cell, thus giving a net number of 2 atoms per cell.

Example: Aluminum (A.W. = 26.98 grams)has a FCC lattice cell, with a measured lattice parameter (from x-ray diffraction studies) of a = 4.05 x 10^{-8} cm. Determine its mass density.

$$\rho = \frac{4\left(\frac{26.98}{6.024 \ x \ 10^{23}}\right)}{4.05 \ x \ 10^{-8}}$$

$$\rho = 2.70 \frac{gm}{cm^3} = 0.10 \frac{lb}{inch^3}$$

7.5 Direction Indices and Miller Indices

Direction indices and Miller indices may be used to describe the geometry of a particular lattice structure. Direction indices refer to a specific direction in a cubic unit crystal; whereas Miller indices refer to planes.

<u>Direction indices</u> refer to a specific direction in the cubic unit crystal. By standard convention, the notation is:

$$[h, l, k] = h\hat{x} + l\hat{y} + k\hat{z}$$

Where, h, l, k are vector components of the directions $\hat{x}, \hat{y}, \hat{z}$ reduced to the smallest integer. Negatives are denoted with an overbar, so $\bar{h} = -h$

The method to find the direction indices is as follows:
    1. Locate origin – at the tail of the vector
    2. Find the vector projections in $\hat{x}, \hat{y}, \hat{z}$
    3. if not all integers, multiply by least common denominator
    4. Simplify if needed
    5. Place in brackets

Example: Find the direction indices for the following vector.
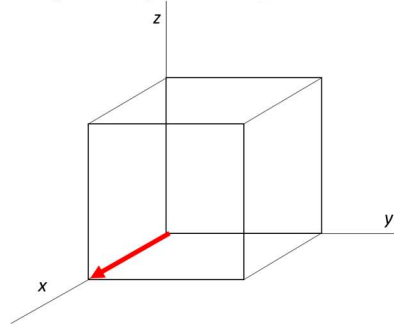
Solution
        1. Origin at (0,0,0)
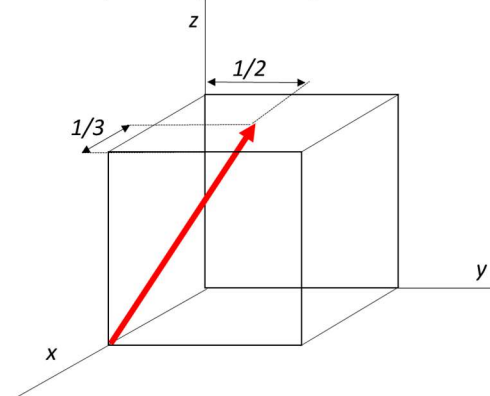   *2. Projections*
        x   y   z
        1   0   0
        3. Integers – Yes!
        4. Simplified- Yes!
        5. Answer [1 0 0]

Example: Find the direction indices for the following vector.

7 - 7

Solution

> *1. Origin at (1,0,0)*
> *2. Projections*
>
> | *x* | *y* | *z* |
> |---|---|---|
> | *-1/3* | *1/2* | *1* |
>
> *3. Integers – No, but multiply by 6 will do*
>
> | *x* | *y* | *z* |
> |---|---|---|
> | *-2* | *3* | *6* |
>
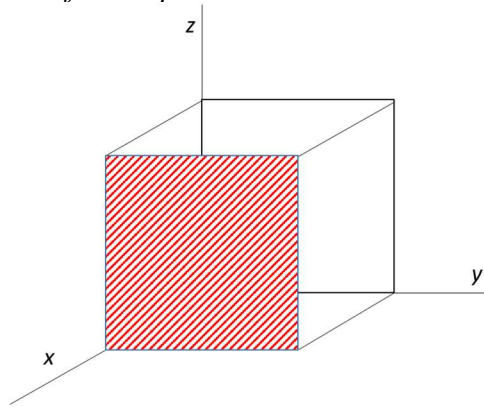> *4. Simplified- Yes!*
> *5. Answer [2̄ 3 6]*

Miller indices refer to a plane in the cubic unit cells.

Method:
1. Choose origin so plane does not pass through it
2. Find axis intercepts with plane in $\hat{x}, \hat{y}, \hat{z}$
3. Take the reciprocal of the intercepts
4. Form integers by multiplying by the least common denominator
5. Simplify by dividing by the least common denominator
6. Place in parentheses

Example: Find the Miller indices for the plane shown below

Solution:

> *1. Find Origin (0,0,0)*
> *2. Projections*
>
> | *x* | *y* | *z* |
> |---|---|---|
> | *+1* | *infinity* | *infinity* |
>
> *3. Reciprocals*
>
> | *x* | *y* | *z* |
> |---|---|---|
> | *+1* | *0* | *0* |
>
> *4. Integers – OK*
> *5. Simplified- OK*
> *6. (1 0 0) ANS*

7 - 8

Example: Find the Miller indices for the plane shown below
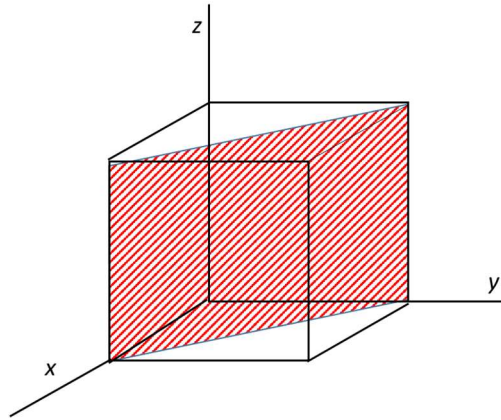
Solution:

1. *Origin (0,0,0)*
2. *Projections*

x	*y*	*z*
1	*1*	*infinity*

3. *Reciprocals*

1	*1*	*0*

4. *Integers -OK*
5. *Simplified – OK*
6. *(1 1 0)*

7.6 Polymorphism.

The ability of a material to have more than one crystalline structure is known as polymorphism. The transition from one structure to another at a specific temperature and pressure is known as a <u>polymorphic change</u>.

A common and important example is iron, which has a BCC cell structure (known as α-Fe) for temperatures up to 910° C. Above this temperature, the structure is FCC (known as γ-Fe) until a temperature of 1400° C is reached. It then reverts back to an BCC structure (known as δ-Fe).

<u>Example</u>: Calculate the change in density of an iron specimen as it changes from BCC to FCC at 910° C. The lattice parameter of iron at 20° C is 2.87 Å and the coefficient of thermal expansion is 15 x 10^{-6}/° C. The lattice parameter of iron at 910° C is 3.65 Å.

Solution:

   Mass = (55.85/6.024 x 10^{23}) = 9.273 x 10^{-23} gm
   n = 2
   BCC lattice parameter at 910° C,

   a = 2.87 + 2.87(15 x 10^{-6})(910-20) = 2.91 Å

   7 - 9

$$\rho_{BCC} = \frac{(2)(9.273 \text{ x } 10^{-23})}{(2.91 \text{ x } 10^{-8})^3}$$

$$\rho_{BCC} = 7.53 \frac{gm}{cm^3}$$

$$\rho_{FCC} = \frac{(4)(9.273 \text{ x } 10^{-23})}{(3.65 \text{ x } 10^{-8})}$$

$$\rho_{FCC} = 7.63 \frac{gm}{cm^3}$$

hence

$$\rho_{FCC} - \rho_{BCC} = 0.10 \frac{gm}{cm^3}$$

$$\frac{\rho_{FCC} - \rho_{BCC}}{\rho_{BCC}} = 1.33\%$$

Example: Using the results above, calculate the change in volume of the iron specimen as it changes from BCC to FCC at 910º C

Solution: Let M = total mass of the specimen and V be its volume. The density ρ is given

ρ = M/V so ρ/V = M (constant)

$\rho_{BCC} / \rho_{FCC} = V_{FCC} / V_{BCC} = 7.53/7.63 = 0.987$

$(V_{FCC} - V_{BCC}) / V_{BCC} = (1 - 0.987)/(1/0.987) = -0.0133 = -1.33\%$

7.7 Coordination Number and Packing Factor

Additional terms of interest include the coordination number and the packing factor.   The coordination number is the number of nearest neighbors of an individual atom in a lattice structure. An FCC lattice has a coordination number of 12, while a BCC structure has a coordination number of 8. The packing factor (p.f.) is the ratio of the volume of atoms (using the hard ball model) to the total volume of the lattice cell structure.

p.f. = Volume of atoms/volume of lattice cell

For a cubic structure with hard-ball radius r

$$\text{p.f.} = n(4/3)(\pi r^3)/a^3$$

where a = lattice parameter.

7 - 11

Example 1: Find the packing factor for aluminum.

Solution: Aluminum is an FCC structure. As shown previously, the lattice parameter was related to the radius r by

$$r = \frac{(\sqrt{2})}{4}a$$

$$n = 4$$

thus

$$p.f. = \frac{(4)(\frac{4}{3})(\pi)(\frac{\sqrt{2}}{4})}{a^3}$$

$$p.f. = 0.74$$

Example 2: Find the packing factor for NaCl.

Solution: NaCl forms an FCC lattice, but now the basis consists of a combination of Na and Cl atoms. As a result the volumes in the equation are different than those in the previous example.
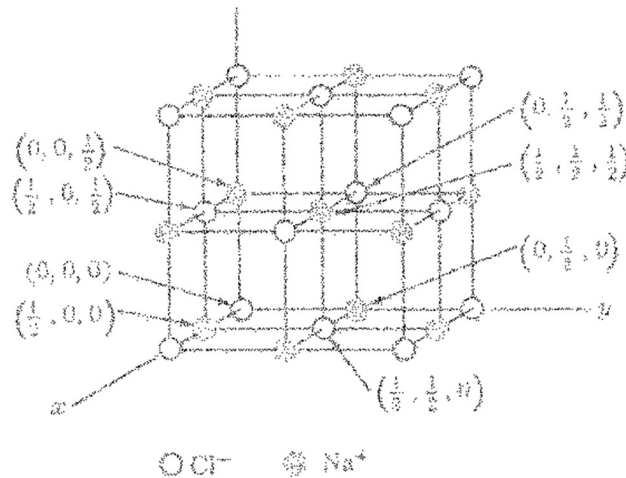
The volume of the atoms V_A is now

$$V_A = (4/3)\pi(r_{Na}{}^3 + r_{Cl}{}^3) = (4/3)\pi(.95^3 + 1.81^3)$$

The volume of the lattice, V_L, has also changed and is now

$$V_L = (2r_{Na} + 2r_{Cl})^3 = (2(0.95) + 2(1.81))^3$$

Thus

$$p.f. = 4(V_A)/(V_L) = 0.67$$

The packing factor is independent of the lattice parameter and the atomic radius <u>provided</u> that only

7 - 12

one atom as present at a lattice site (as is the case for most commom metals of interest in this course). Similar calculations for a BCC structure show p.f. = 0.68, HCP = 0.74, and 0.52 for a simple cubic.

7.8 Solidification

When cooling, metal often solidifies as shown in Figure 9. The stages of solidification include
        a. Crystal Nucleation
        b. and c. Crystal Growth
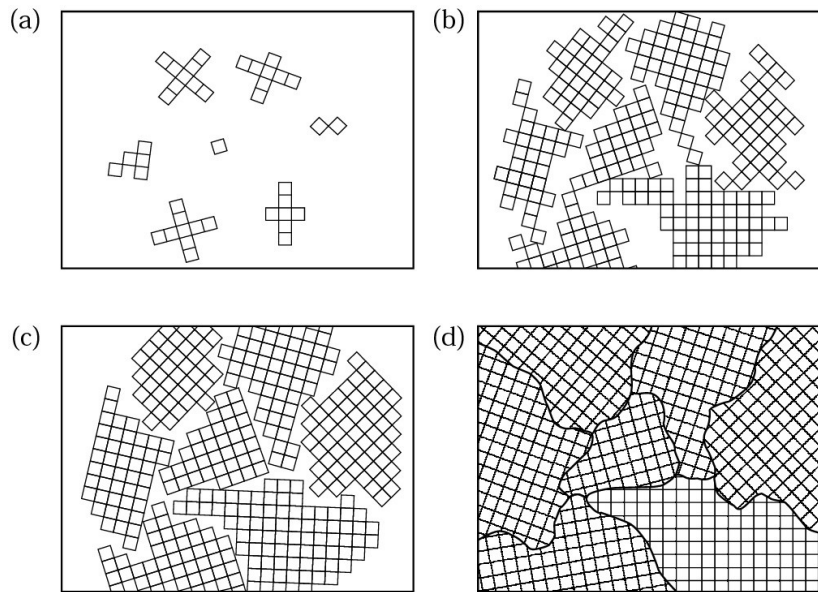   d. Solid Metal with Grain boundaries

Figure 9: Metal Solidification

Polycrystalline Structures
Because of the solidification process shown above, metals generally consist of regions called grains, where the crystalline arrangement of atoms exists. These regions differ from one another only in that the spatial orientation (see figure 10); that is, the orientation of the unit cells describing the crystalline symetry differ from one grain to another. These grains typically have dimensions on the order of 10^{-2} inches or less. They can easily be seen with light microscopes, provided the specimen is smooth enough, since light is reflected differently from the various grains. Photographs showing this "microstructure" are known as photo-micrographs.

In many cases, the grains are randomly oriented relative to one another, so that a specimen with characteristic dimensions of 1 inch will contain many grains. The material will appear isotropic, (properties the same in all directions) even though the grains are anisotropic (different properties in different directions).

Single Crystal
It is possible to control the formation of crystals such that a piece of material has a single crystal structure, rather than the grain boundaries. This is used for solid state devices, and turbine blades.
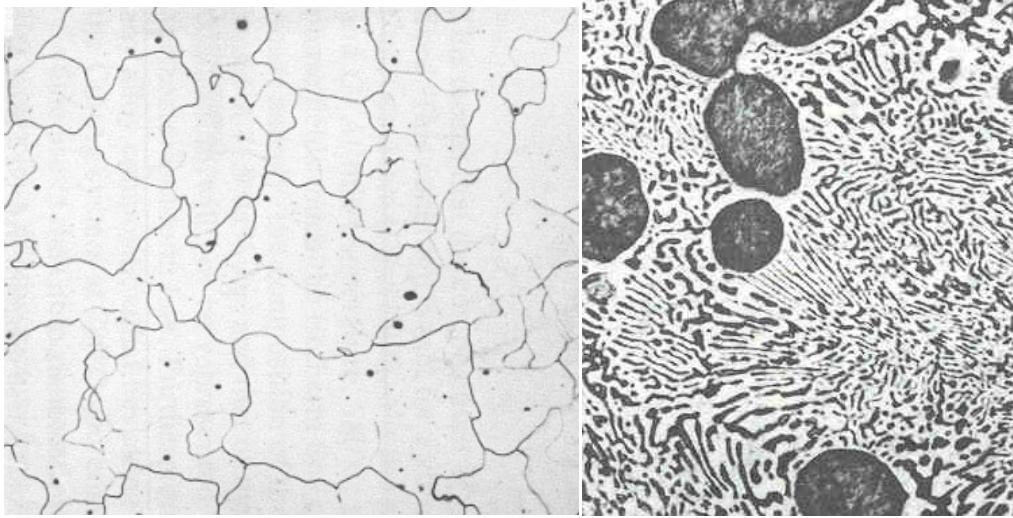
7 - 13

Figure 10: Polycrystalline Structures

CHAPTER 8

METALS AND ALLOYS

Alloys consist of a combination of two or more metal elements in the solid state. In engineering work, alloys, rather than pure metals, are generally used because of their superior properties. Ordinary steels, for example, are alloys of iron and carbon and are preferred to pure iron because of strength and other considerations. Important mechanical properties of alloys are related to the solid phases, or homogenous parts, that form from the combination of elements. Such phases are observable on the microscopic scale, and their study is important in understanding alloy properties.

8.1 Types of Alloying

Interstitial is where the alloy elements are located in spaces between atoms in the unit cell. For instance, when carbon (Atomic radius 0.129 nm) is added to iron (0.075nm), the carbon fits into the gap between the Fe atoms (interstitial site). The solubility depends on the size of these gaps and the crystal structure.

Substitutional is where the alloying elements are located in vacancies in the unit cell. An atom of one element substitutes for another in the crystal structure.
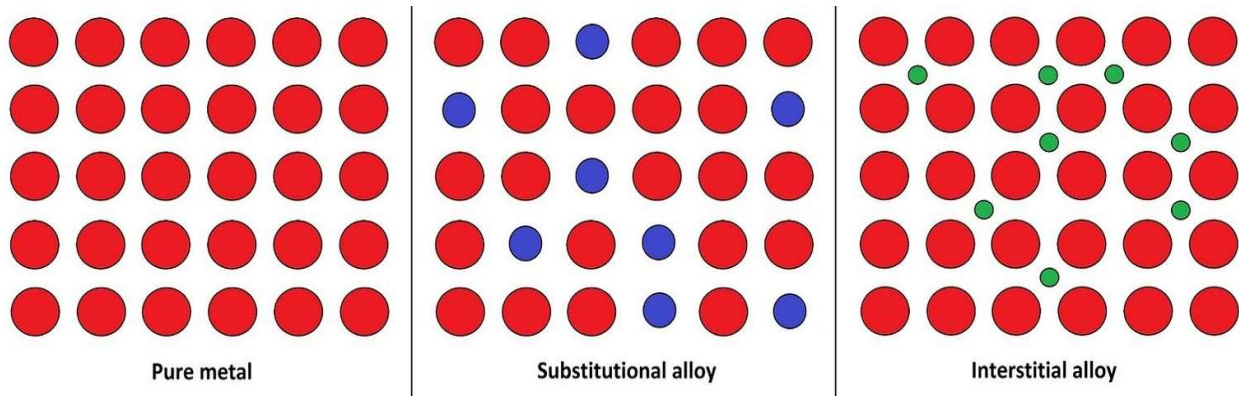
Fig. 1

8.2 Hume-Rothery Rules for Alloying

It is not possible for every combination of materials to form an alloy. The following rules are for maximum solubility in substitutional alloying:

1. Same Crystal Structure (BCC, FCC, HCP for instance)
2. Same Valency Factor
3. Similar Electronegativity – the tendancy for the atom to attract a shared pair of electrons. This depends on the atomic number and the distance at which the valence electrons are from the nucleus.
4. Difference in atomic radius <= 15%

In interstitial alloying, the solute atoms should be <= 59% of the atomic radius of the solvent atoms.

8.3 Material Systems
A <u>material system</u> refers to a definite amount of material or materials.

The <u>components</u> in a system refer to the smallest number or individual substances that must be listed to describe the chemical composition of the system. These may be elements (Pb, Sn, Fe, C, etc.) or compounds (H_2O, NaCl, etc.)

The <u>phases</u> in a system denote the homogenous parts of the system that are made up of its components.

<u>Phase diagrams</u> are graphs showing the phases present under selected conditions of temperature, pressure, and composition when the system is in thermodynamic equilibrium.

A material system may be specified as in the following example:

Example: Suppose we have 8 gms of copper and 2 gms of nickel. This yields a system having 80 w/o copper and 20 w/o nickel (w/o= weight percent). This can also be expressed as mole percent (m/o) or atomic percent (a/o).

8 gm (Cu): (8 gm)/(63.54 gm/mole) = 0.1259 moles
2 gm (Ni): (2 gm)/(58.71 gm/mole) = 0.0341 moles

Since the number of atoms in a mole is constant, the atomic percent is:

8 gm (Cu): 0.1259/(0.1259 + 0.0341) = 78.7 m/o = 78.7 a/o
2 gm (Ni): 0.0341/(0.1259 + 0.0341) = 21.3 m/o = 21.3 a/o

8.4 One-component material systems

The phases possible in a one component system are limited to liquid, solid, and gas states (Fig 2). A phase diagram consists simply of a graph of pressure vs. temperature, with the phase regions indicated.
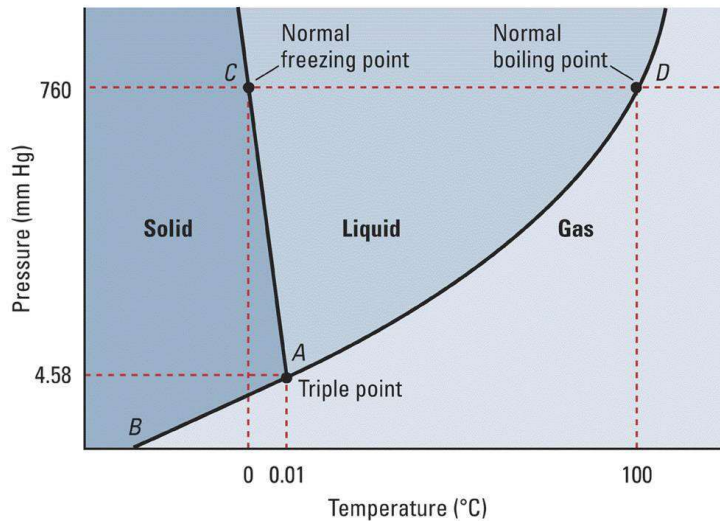
Fig. 2 Phase diagram for a one-component system (water)

8.5 Two component material systems

Materials with two components are called binary systems. They are commonly encountered in engineering materials (brass consisting of copper and zinc, carbon steel consisting of iron and carbon, etc.) The phase diagram of a binary material is customarily displayed in a temperature vs. composition format, with the pressure held fixed at atmospheric.

In the phase diagrams,
L denotes liquid
α, β, γ are various solids
α+ β or L+ γ indicate states where both are present

8 - 3

Two-Components with Complete Solubility: For a system having components completely soluble in the solid state, the phase diagram is especially simple, since only one phase exists in the solid state. See Figure 3 for the phase diagram of the material.

Two-Components with Partial Solubility (Eutectic): For a binary system having components only partially soluble in the solid state, two solid phases will exist, and the phase diagram is much more complex than Figure 3. A special case is an <u>eutectic</u> diagram shown in Figure 4. "Eutectic" means that when the two components are mixed, the melting point is lower than the melting temperatures of the two components separately. At point d, the <u>eutectic</u> reaction Liquid, L → α + β occurs.

Two-Components with Partial Solubility (Eutectoid): When the liquid region is replaced by a third solid phase γ, we have the <u>eutectoid</u> reaction γ → α + β and associated phase diagram. Figure 5 shows such as phase diagram with both a Eutectic and Eutectoid point.

Two-Components with Partial Solubility (Peritectic): For a binary system having components only partially soluble in the solid state, we may also have a phase diagram having a <u>peritectic</u> point P, where the reaction L + β → α occurs (Figure 6)

Two-Components with Partial Solubility (Peritectoid): If the liquid in the peritectic reaction is replaced by a third solid phase, γ, we have a <u>peritectoid</u> reaction α + γ → β. This is illustrated by Figure 7.
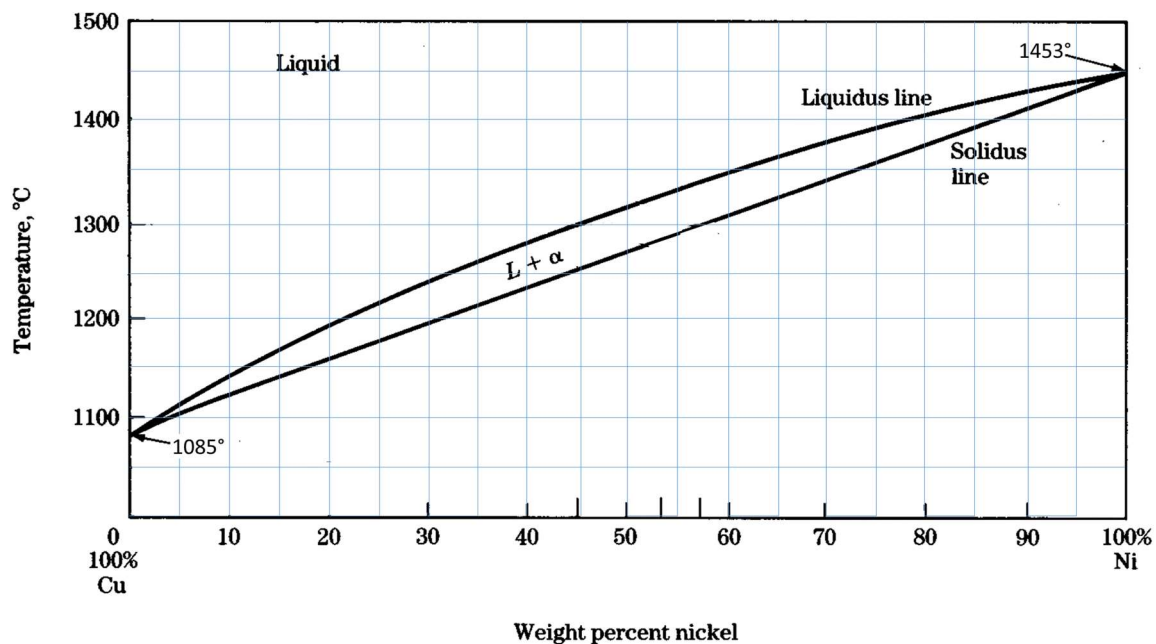
Figure 3: Components with Complete Solubility (Copper-Nickel System)
Melting temperature depends on percentage of nickel. There is a solid phase, then a mixture of liquid and solid (L → α) and then a complete liquid phase L

8 - 4
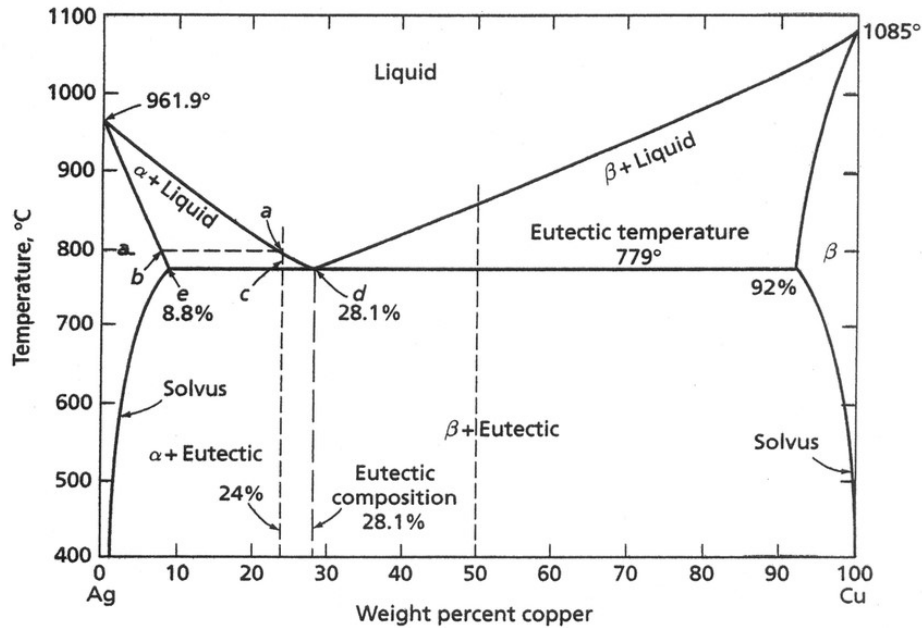
Figure 4: Two Components with Partial Solubility (Silver Alloy Copper System)
At the **Eutectic** point (d) the liquid changes to a solid $L \rightarrow \alpha + \beta$
(This is at a lower temperature than when the separate components become solid)
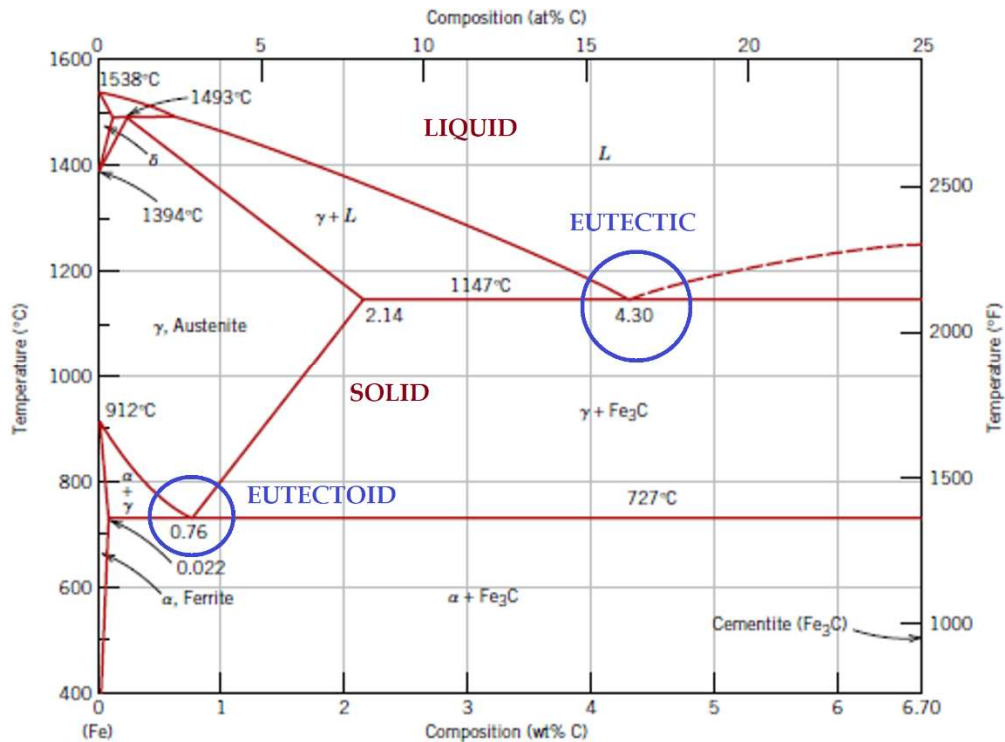
Figure 5: Case 2 - Two Components with Partial Solubility (Iron Carbon System)
At **Eutectic** point, the liquid changes to a solid $L \rightarrow \alpha + \beta$
At the **Eutectiod** point $\gamma \rightarrow \alpha + \beta$
(This is at a lower temperature than when the change occurs for the individual components)

8 - 5
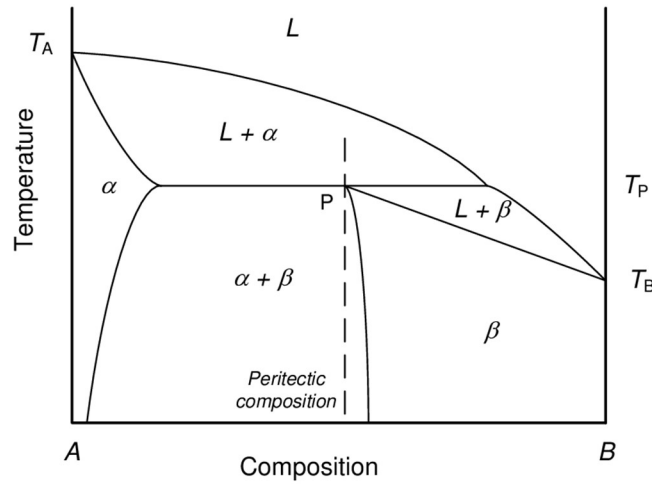
Figure 6: Two Components with Partial Solubility - **Peritectic**
At the Peritectic point, the reaction L + β → α occurs
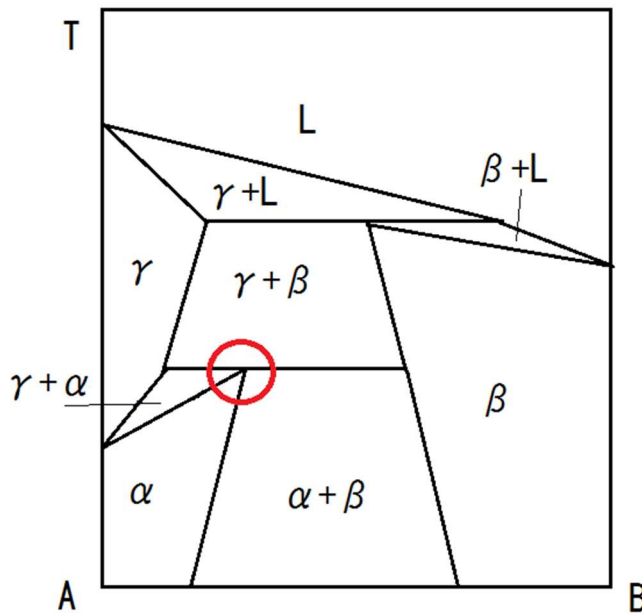
Figure 7: Two components with Partial Solubility- **Peritectoid** Reaction -
<u>peritectoid</u> reaction α + γ → β

8 - 6

8.6 Derivation of Lever Rule

Consider a temperature-composition point in a phase diagram where two phases exist, as shown in Figure 8 for temperature T_1 and composition X_2. The chemical composition of the two phases are:

α - phase: X_1 w/o B, $100 - X_1$ w/o A:
β - phase: X_3 w/o B, $100 - X_3$ w/o A.
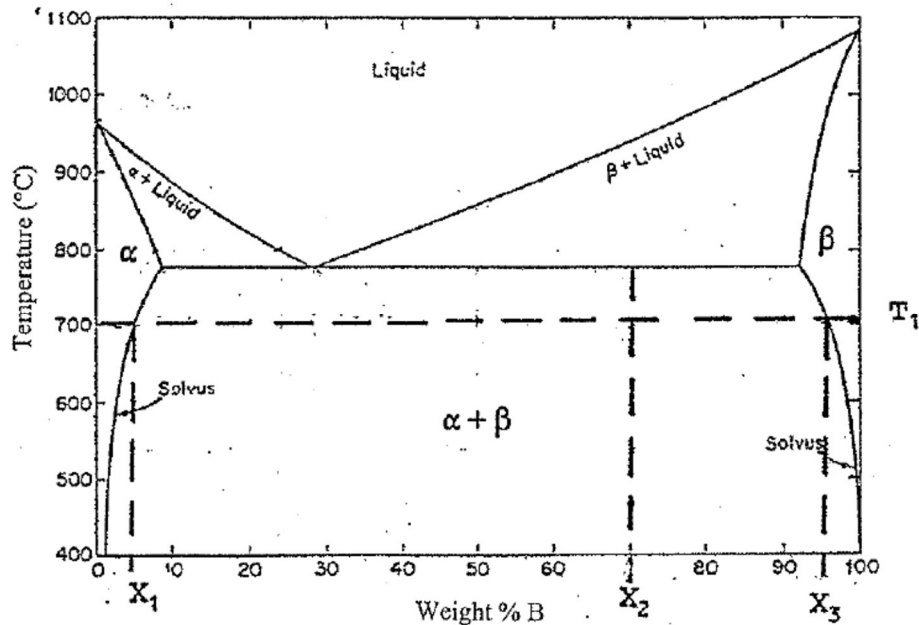
Figure 8: Phase Diagram for Derivation of Lever Rule

This may be seen by imagining that we start with pure A material and add increasing amounts of B. When we reach the composition X_1 w/o B, the α phase has become saturated and can accept no additional amount of B. As we add still more B, the second β phase must appear. The β phase will be saturated, and its composition will be X_3 w/o B, as read from the right side of the diagram.

Now we would like to determine how much α phase and β phase material will exist at a temperature T_1, and the composition X_2 w/o B. To arrive at this, we use the <u>lever rule</u>.

Let A_1 be the amount of α phase present
             A_3 be the amount of β phase present
             A_2 be the total amount of material

8 - 7

The balance of material requires that

$$A_1 + A_3 = A_2$$

And the balance of the B material requires that

$$X_1 A_1 + X_3 A_3 = X_2 A_2$$

Combining these two equations yields

$$\frac{A_1}{A_2} = \frac{(X_3 - X_2)}{(X_3 - X_1)}$$

which is the fractional weight of the α phase, and

$$\frac{A_3}{A_2} = \frac{(X_2 - X_1)}{(X_3 - X_1)}$$

which is the fractional weight of the β phase.

Example: *A Cu-Ni alloy (Fig 9) contains 73% cu and 27% Ni at 1200C. Find (1) Weight % Cu in solid and liquid phases and (2) % of alloy in solid % liquid phases.*
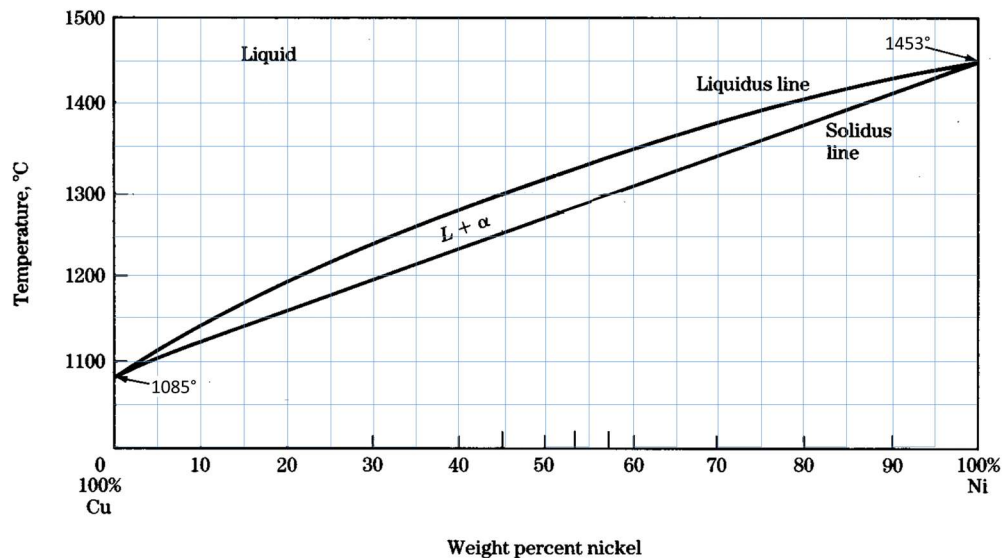
Solution:

Step 1: Draw horizontal tie line at 1200C

Step 2: Project down for Cu

   Liquid, W_L = 80%Cu

   Solid, W_S = 70%Cu

Step 3: For W_O = 27% Nickel, project up to tie line
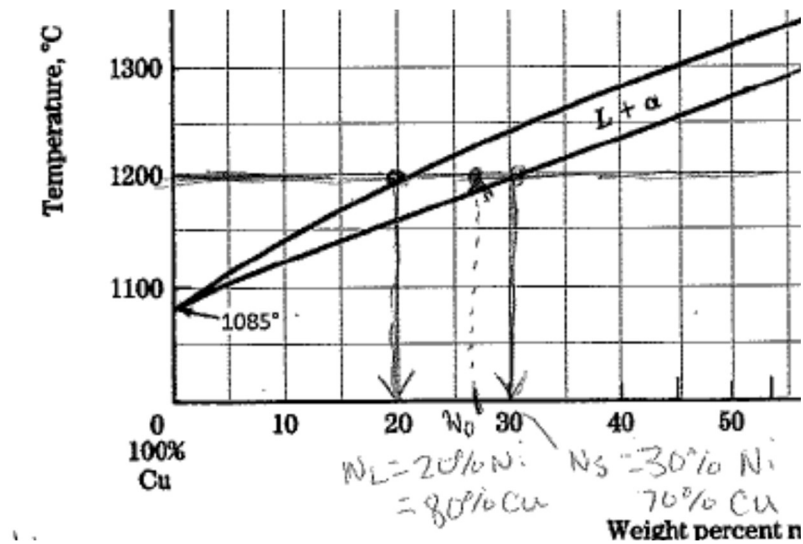
$$X_L = \frac{W_S - W_O}{W_S - W_L} = \frac{30\% \ Ni - 27\%Ni}{30\%Ni - 20\%Ni} = \frac{3}{10} = 0.3$$

Is the fraction of alloy liquid.

$$X_S = \frac{W_O - W_L}{W_S - W_L} = \frac{27\% \ Ni - 20\%Ni}{30\%Ni - 20\%Ni} = \frac{7}{10} = 0.7$$

Is fraction of the alloy that is solid

$X_L + X_S = 1 \quad OK!$

8 - 9

Example: Consider the lead-tin (Pb-Sn) diagram shown in Figure 20. For an alloy consisting of 40 w/o Sn determine the composition and amount of the α and β phases present at 100° C. Also, determine the relative amount of material formed from the eutectic reaction.
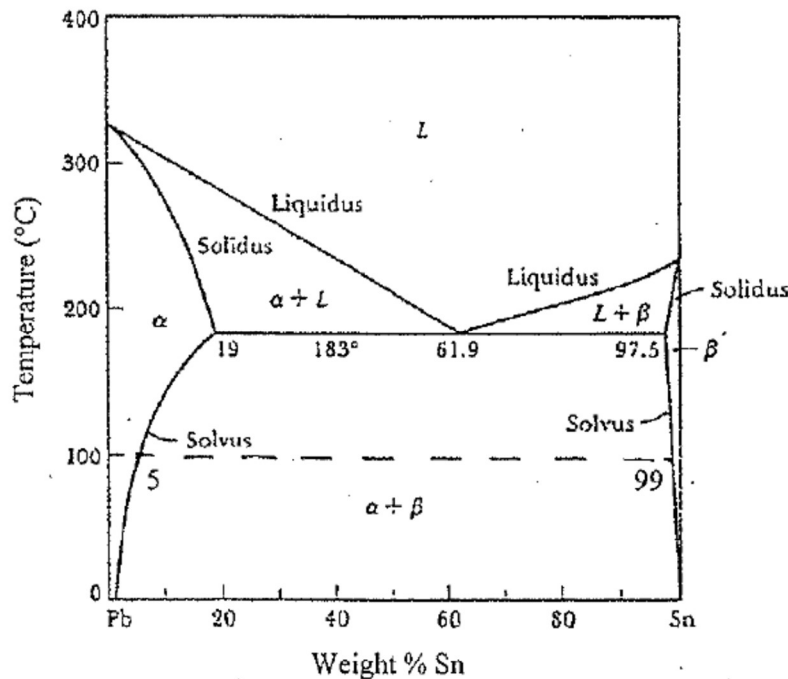
Figure 20: Lead-Tin Phase Diagram

Solution: At T_1 (100° C), the composition of the α phase is
   5 w/o Sn, 95 w/o Pb

The amount of the α phase present is
   $(A_1/A_2) = (99 - 40)/(99 - 5) = 62.8\%$ by weight

The composition of the β phase is
   99 w/o Sn, 1 w/o Pb

The amount of the β phase present is
   $(A_3/A_2) = (40 - 5)/(99 - 5) = 37.2 \%$ by weight

To determine the amount of material that experienced the eutectic reaction, we note that just above the eutectic temperature of 183° C, the remaining liquid had the eutectic composition 62 w/o Sn and 38 w/o Pb. The amount of remaining liquid was (40 - 19)/(62 - 19) = 48.8%. On cooling below the eutectic temperature, this liquid experienced the eutectic reaction $l \rightarrow α + β$. The amount of eutectic material present at 100° C is 48.8 % (by weight). The amount of α and β phase present in the eutectic material at 100° C is (99 - 62)/(99 - 5) = 39.4 % α, 60.6 % β.

8 - 10

Example : Shown in Figure 21 is the phase diagram for the H₂O - NaCl system. Knowing that seawater is 3.5 w/o NaCl, determine:

(a) the amount of NaCl is 100 lbs of seawater,
(b) the relative amount of ice and brine at 10⁰ F, and
(c) the composition of the ice and brine at 10⁰ F.
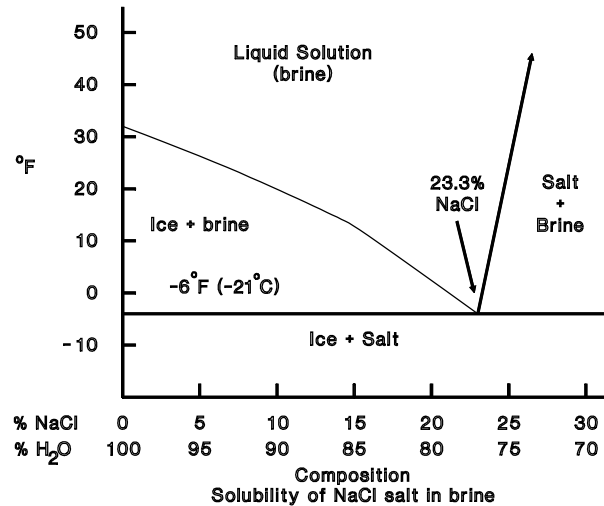
Figure 21: Phase Diagram for Seawater

Solution: *(a) the amount of NaCl in 100 lbs of seawater is*
          (100)(.035) = 3.5 lbs

          (b) the amount of ice and brine at 10⁰ F is
          (16.5 - 3.5)/(16.5) = 78.8% ice
          3.5/16.5 = 21.2% brine

          (c) the compositions are
          0% NaCl in ice and 16.5 % NaCl in the brine.

8 - 11

8.7 Metal Processing

The manufacturing processes can alter crystal microstructure and thus influence the strength, ductility, and impact toughness of a material. While a variety of finishing processes are suited to specific applications, we will focus on casting, hot and cold rolling, extrusion, forging, and drawing.

Casting:
Molten metals can be cast into large ingots in a direct chill casting unit. These large ingots are typically rolled into sheets or plates, or else extruded into structural shapes like I-Beams. Metals can also be cast into smaller, complex shapes using metal or sand molds.

Fig 10 Casting

Hot and Cold Rolling:
To make large sheets or plates, large ingots are often hot-rolled initially (to allow for a larger thickness change). A schematic is shown below. The hot rolling process continues until the plate reaches its desired thickness or until it cools such that rolling becomes impossible. Plates will be reheated and rolled until they reach the desired thickness.
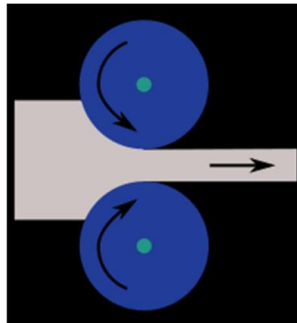
Fig. 11 Hot Rolling

After hot rolling, plates are usually cold rolled. Cold rolling **hardens** and **strengthens** the metal by introducing internal stresses (dislocations) in the material microstructure. To re-soften the material, remove internal stresses, and improve toughness, the material may be reheated in a process called **annealing.**

The amount of cold working is often expressed as a percentage related to the change in a material's thickness, i.e.:

8 - 12

$$\%CW = \frac{th_o - th_f}{th_o} \times 100\%$$

Where %CW indicates the percent cold work done on a material, th_o and th_f indicate the initial and final thickness of the material, respectively.

Extrusion:

Extrusion is the forming of a material through plastic deformation by forcing it though a die under high pressure. Cylindrical rods and hollow tubes of most metals are fabricated this way. This process is often used to form a wide variety of cross sections for aluminum, copper, and their alloys.
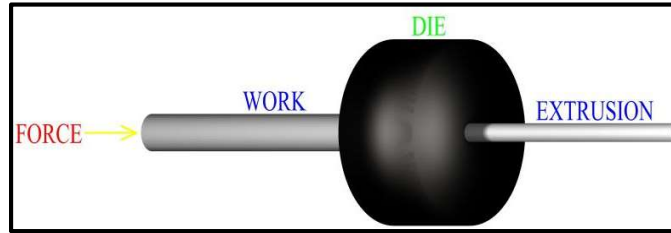
Fig 12 Extrusion

Forging:

Forging is the process of a material being pressed or formed into its desired shape, which can be irregular (unlike rolling or extruding). The temperature of forging is important for the final strength, hardness, and ductility of the material. Typically forged metals are tougher and more durable than cast metals. Forging involves hot and cold working by nature, and can act to reduced voids in the metal's microstructure.

Fig 13 Forging

Drawing:

Drawing is a cold working process typically used to make wire, in which a metal rod (such as copper) is pulled through a carbide nib. Deep drawing is a form of drawing in which a punch and die are used to form cup-shaped objects from sheet metal. Aluminum cans are formed by deep drawing.

Drawing is a form of cold work, and the percentage of cold work can be expressed in a 2-D analogy to the equation for rolling:

$$\%CW = \frac{A_{xc,o} - A_{xc,f}}{A_{xc,o}} \times 100\%$$

8 - 13

Where $A_{xc,o}$ and $A_{xc,f}$ indicate the initial and final cross-sectional areas of the metal rod, respectively.
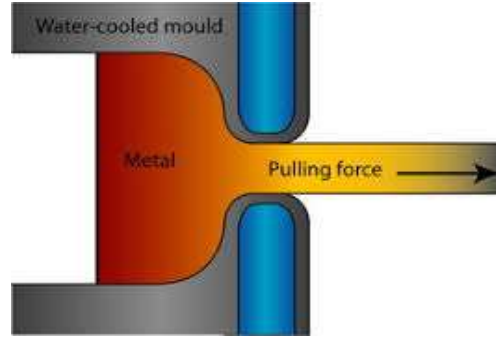
Fig 15 Drawing

8.8 Work Hardening and Annealing

When a material is plastically strained the yield stress is increased. In many of the manufacturing techniques listed earlier, the material is plastically deformed in order to fabricate the desired shape. As Figure 16 shows, although this may significantly increase the yield strength of the material, it also makes it more brittle. This change is a result of the dislocation density, or imperfections in the lattice, increasing as a result of the deformation.
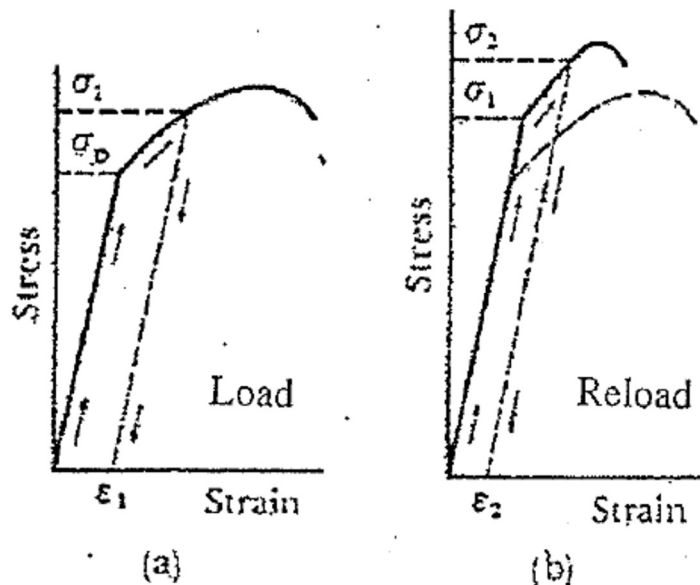
Figure 16: Work Hardening

If we take a work-hardened material and subject it to a sufficiently high temperature for a specified time, we can reduce the dislocation density and the yield stress will return to its initial value. This is known as <u>annealing</u> the material, which is a form of heat treatment. Due to other aspects, such as recrystallization, subjecting the work-hardened material to a high temperature for too long a

8 - 14

time, may result in a material whose yield stress is less than it was before the material was work-hardened.

8.9 Precipitation Hardening of Alloys

Consider the phase diagram below in Figure 17. Suppose we have material held at temperature T_2 and then suddenly quench it to room temperature, T_r. There is insufficient time for the β phase to form and we therefore have an unstable α phase existing at room temperature. Because it is thermodynamically unstable, the β phase would eventually form at room temperature, although it would take many years. If we now heat the material to a temperature T_1, the β will begin to form.

As the β phase begins to form, it transforms the unstable α phase into a stable α phase forming a matrix surrounding numerous extremely small β grains. After some time, the maximum hardness is reached and the material can again be quenched to room temperature, thus yielding a precipitation hardened material (Figure 18).

If the material is held at the treatment temperature for too long, the material will begin to soften. The most important reason for this is that the numerous small β grains which produced the maximum hardness continue to grow. Some of the β grains grow into larger β, obviously decreasing the number of total β grains. Other factors including the strain-energy present and grain boundary depletion are also at work here.
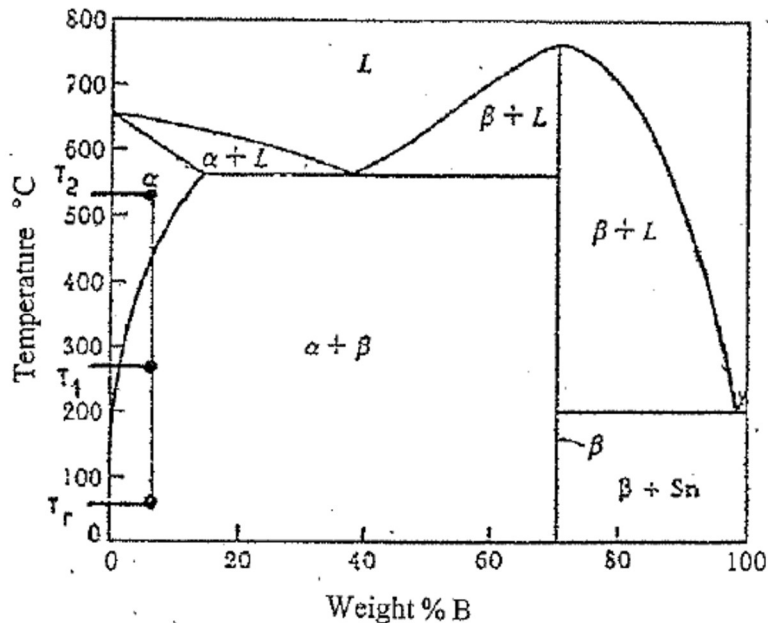
Figure 17: Phase Diagram of Mg-Sn System
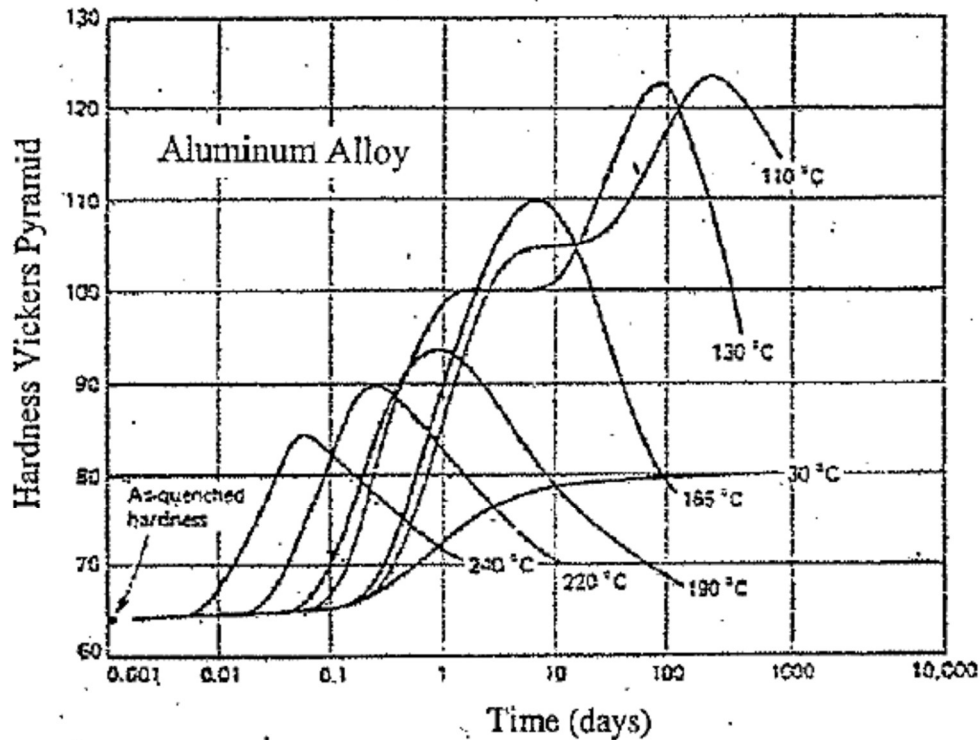
Figure 18: Alloy Hardness vs. Precipitation Time at Elevated Temperatures

8.10 Iron-Carbon Systems

Alloys of iron and carbon for the system for common steels and cast irons. Generally, steels have a carbon content between 0 and 2 % by weight, while cast irons have a carbon content between 2 and 5 % by weight. The iron-carbon phase diagram is shown below in Figure 19.

The phases are defined as follows:
(a) <u>Ferrite α phase</u>: BCC crystalline phase
(b) <u>Austenite γ</u>: FCC crystalline phase
(c) <u>δ phase</u>: high temperature BCC crystalline phase
(d) <u>Cementite or carbide Fe$_3$C</u>: mixture
(e) <u>Pearlite</u>: layered two phase mixture generated by transforming austenite to ferrite and carbide by the eutectoid reaction $\gamma \rightarrow \alpha + Fe_3C$

8 - 16

(f) Martensite: a non-equilibrium phase in steels formed by rapid cooling of austenite. It arises because, with extremely rapid cooling, there is insufficient time for the carbon atoms to realign themselves from their locations within the FCC structure   of austenite to their locations in the BCC structure of ferrite. As a result, the structure is "trapped" between FCC and BCC, and actually results in a body centered tetragonal lattice. Martensite is very hard and brittle, and by itself, has very few practical applications.   Its value lies in combinations of ferrite and martensite obtainable by various heat treatments.

(g) Bainite: mixture of ferrite and cementite formed by isothermal transformation of austenite under selected conditions.
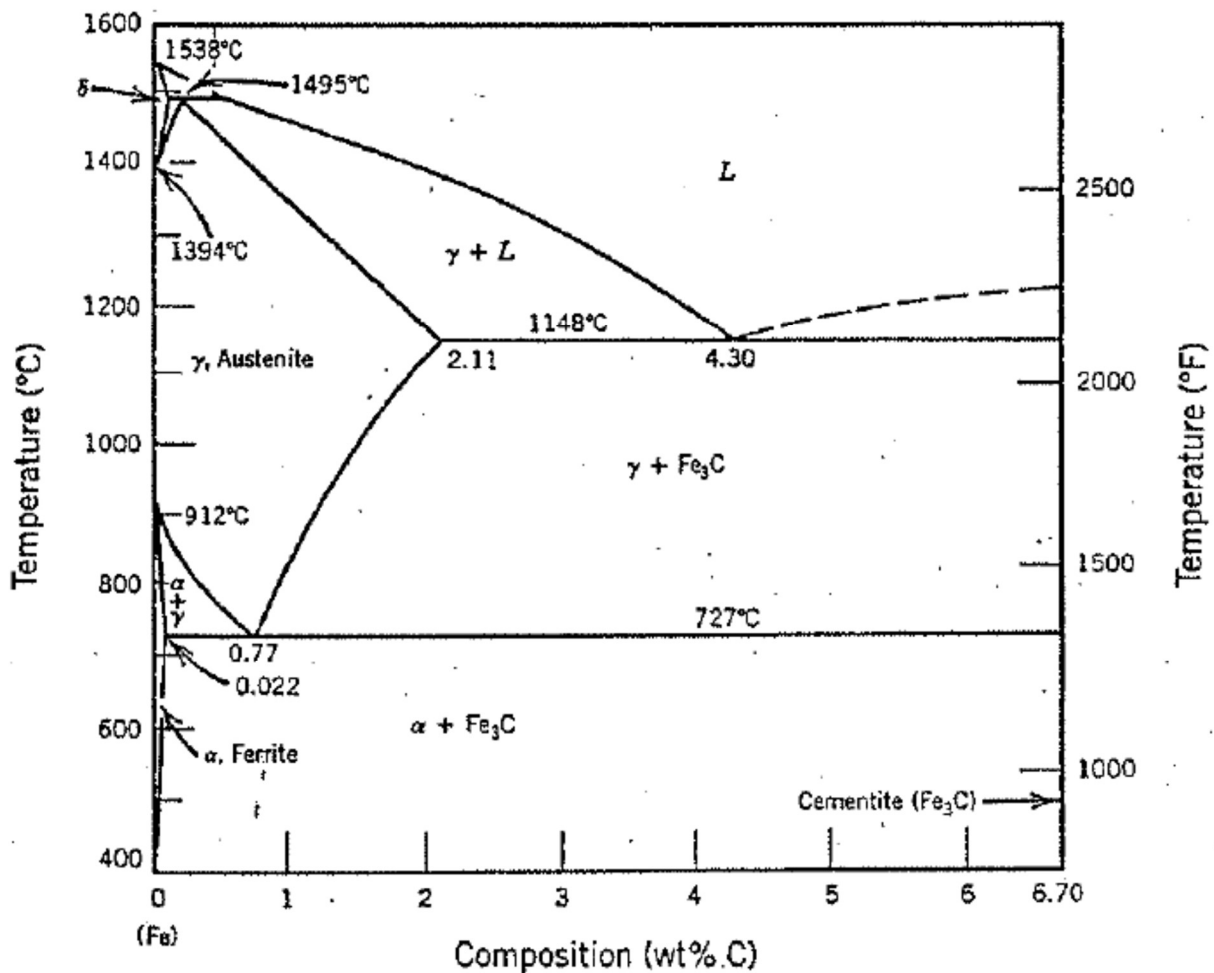
Figure 19: Iron-Carbon Diagram
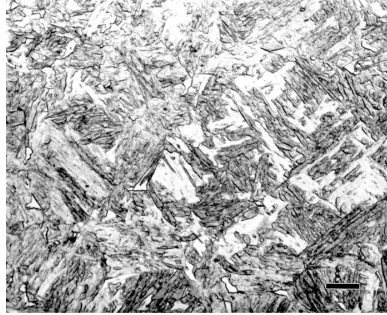
Martensite
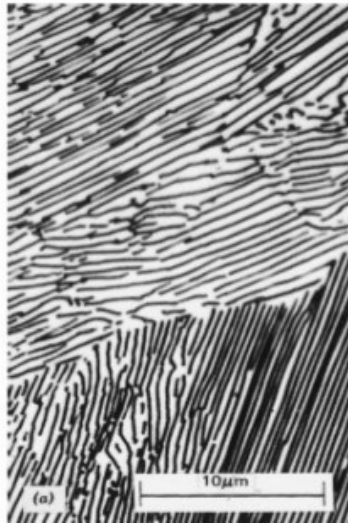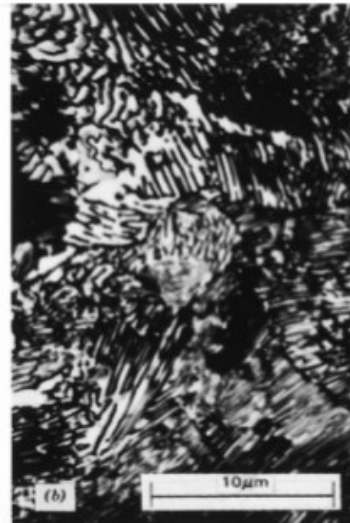
Coarse Pearlite   Fine Pearlite
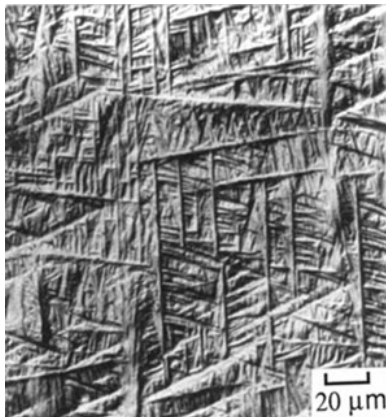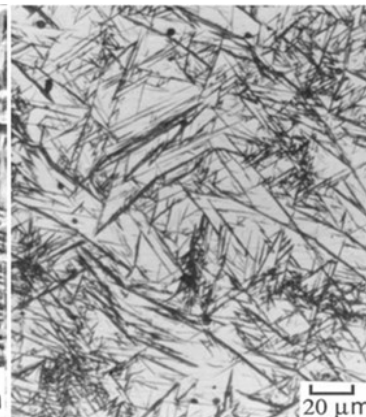
Upper Bainite   Lower Bainite

Fig 20

8.11 Eutectoid Point for Iron-Carbon Systems

The eutectic and eutectoid points on the phase diagram are important for heat treatment. The eutectoid point for Iron-Carbon is at a temperature of 727 C and 0.77% carbon by weight. See the figure below (fig 21) for an enlarged view of this region of the phase diagram.

8 - 18

- Eutectoid steel has exactly 0.77% carbon. When cooling below the eutectoid temperature (727 C) it becomes 100% Pearlite. The resulting steel is high strength and wear resistant, used for things like music wire or railway track.
- Hyper-Eutectoid has more than 0.77% carbon content. When cooling below the eutectoid temperature, it forms a combination of cementite and pearlite. This is more brittle.
- Hypo-Eutectoid has less than 0.77% carbon content. When cooled below the eutectoid temperature, it forms a combination of pearlite and ferrite. This is more ductile.

The lever rule, discussed earlier, can be used to determine the proportions.
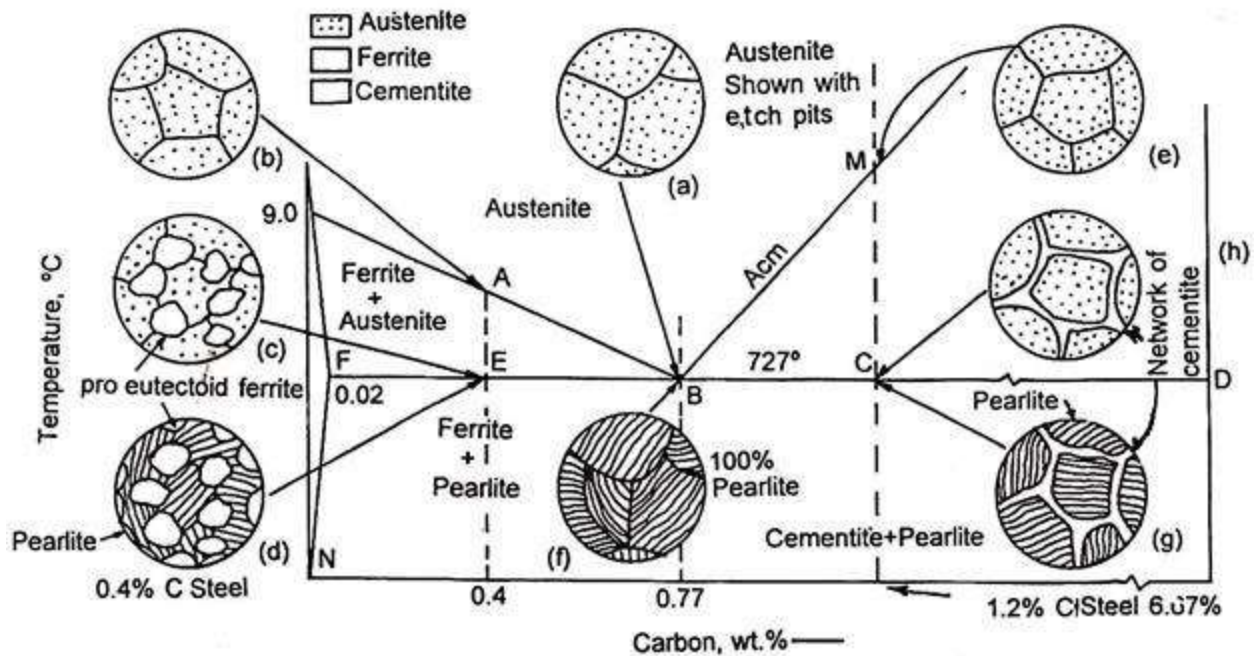
Fig. 3.37. Fe-Fe₃C phase diagram illustrating eutectoid reaction.

Fig 21

8.12 Time-Temperature-Transformation (TTT) Diagrams for Iron-Carbon Systems

Suppose we rapidly cool steel of eutectoid composition (0.8 % C) from the austenitic range down to some temperature where α and Fe_3C are the stable phases. If we could observe the resulting transformation process, we would find that, initially, the material is 100% unstable austenite. After some time, the ferrite and cementite would begin to form (either as pearlite or bainite) and after sufficient time, the transformation of the austenite would be complete. This process is represented by the so-called Time-Temperature- Transformation (TTT) diagram shown in Figure 22.

Notice that, if we suddenly cool the austenite to a temperature M_s (martensite start) or less, some martensite will form. The remaining austenite will then transform to bainite. If we suddenly cool the material to temperature M_f (martensite finish), we will have 100% martensite and no further transformation will occur.
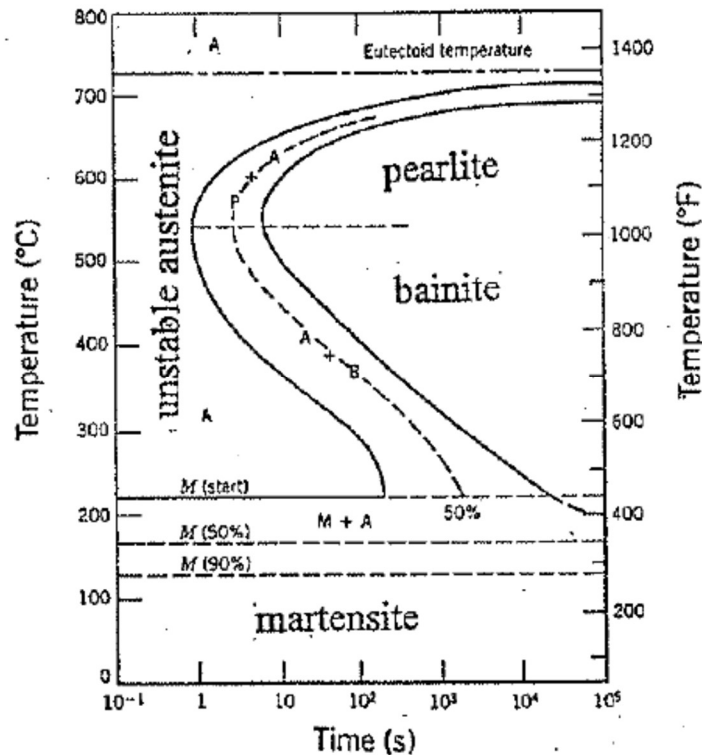
Figure 22: TTT Diagram for Steel

8 - 20

8.12 Continuous-Cooling Transformation Diagram for Iron-Carbon Systems

The TTT diagram refers strictly to the cases where the steel is suddenly cooled from the austenite (γ) range down to some new temperature. In most instances, the cooling is not instantaneous, but rather occurs at a finite rate. As an approximation, the TTT diagram may also be used in this case, but a more accurate Continuous-Cooling Transformation (CCT) Diagram should be used when available. This diagram is shown in Figure 23 for a eutectoid steel.
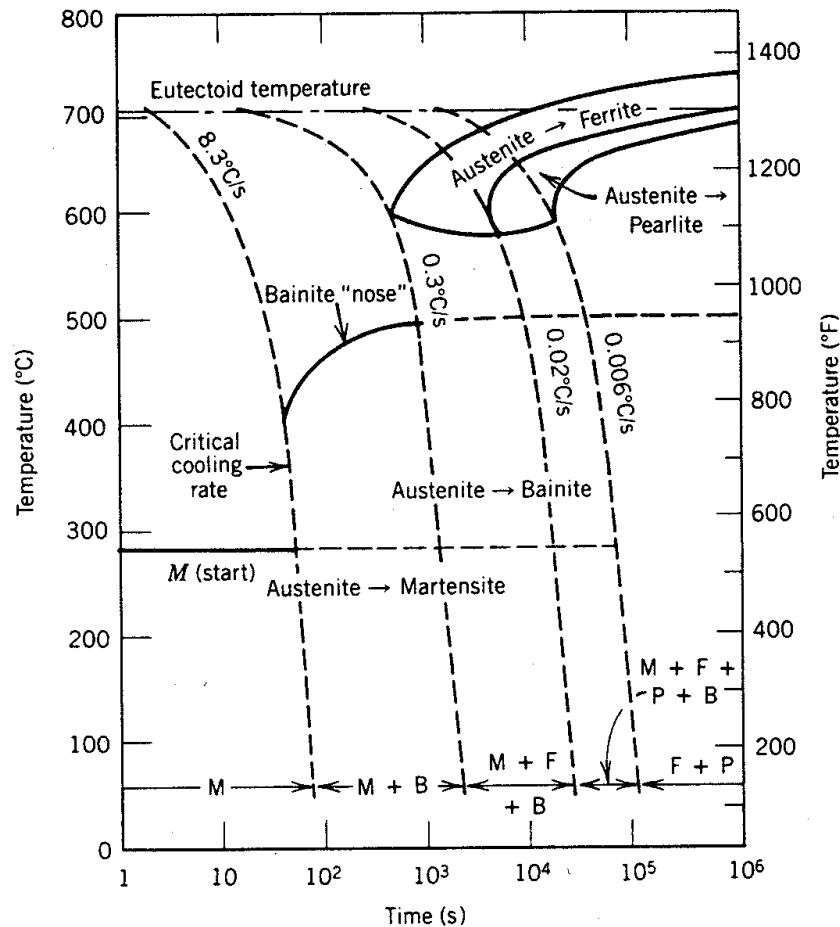
Figure 23: Continuous Cooling Transformation for Steel

If we suddenly cool the material at such a rapid rate, that when plotted on the TTT diagram the time vs temperature line does not intersect the γ + α + carbide phase (also known as "missing the knee" but instead goes straight from the γ_{stable} through the $\gamma_{unstable}$ region to a temperature M_f (martensite finish), we will have martensite with no additional phase. When the cooling rate is such that both the beginning and end curves are reached before reaching the martensitic zone, no (or very little) martensite will form.

8 - 21

8.13 Heat Treatment of Steel

By varying the amount of martensite present in the material, the mechanical properties of the steel can be varied. Martensite alone is very hard and strong but also is extremely brittle. A compromise between strength and ductility can be reached by varying the amount of martensite present in equilibrium with ferrite and carbide.

	Martensite	Very fine pearlite	Fine pearlite	Coarse pearlite
Tens. str. (psi)	250,000	160,000	125,000	76,000
Yld. str. (psi)		80,000	40,000	20,000
Rock. C hard	50	35	25	15
Red. of area (%)	low	22	27	30
Approx. transf. Temp. (°C)	120	540	650	723
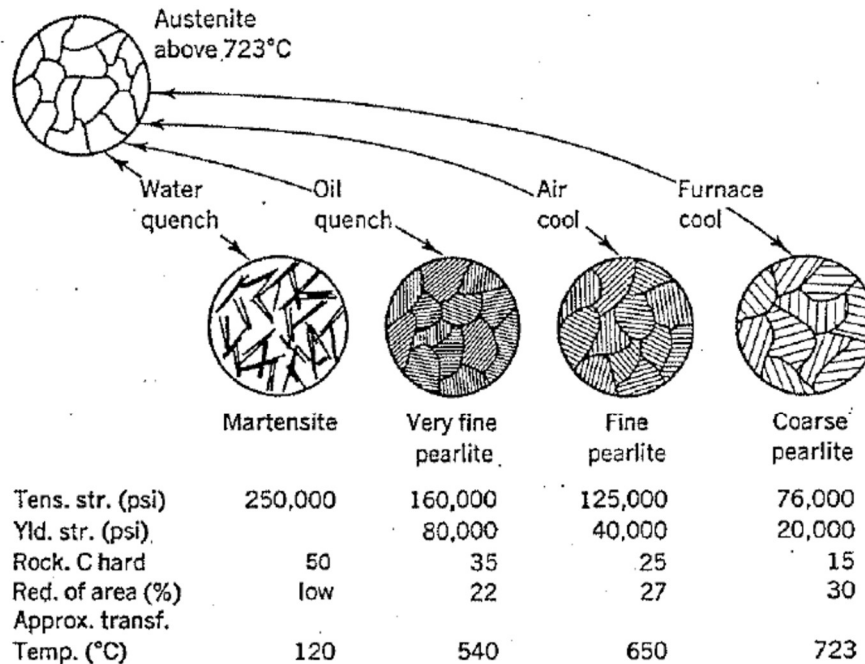
Schematic interpretation of the effect of cooling rate on approximate transformation temperature, microstructure, and properties of a eutectoid carbon steel. C.O. Smith, *The Science of Engineering Materials*, Prentice-Hall (1977)

Fig. 24 Heat Treatment of Eutectic Steel

The procedure for forming this mixed material is called "heat treatment." First, the material is rapidly cooled (quenched) so as to form nearly 100% martensite. At room temperature, this non-equilibrium phase is, for all practical purposes, stable and will not further transform to ferrite and carbide. If we then take the 100% martensite and heat it to an elevated temperature (say 700° C) and hold it there for some length of time (tempering), the martensite can be softened (stress relieved) and decompose. The changes that occur are temperature dependent and range from merely a reduction in strain-energy and dislocation density to microstructural changes within the martensite itself. The end result is a material that retains some of the high strength and hardness characteristics of pure martensite while restoring some ductility.

As shown in Figure 25, the hardness obtainable with martensite is dependent on the carbon content. Since it is the "trapping" of the carbon atoms which forms martensite, and thus hardens the metal, pure iron can not be hardened by quenching

8 - 22
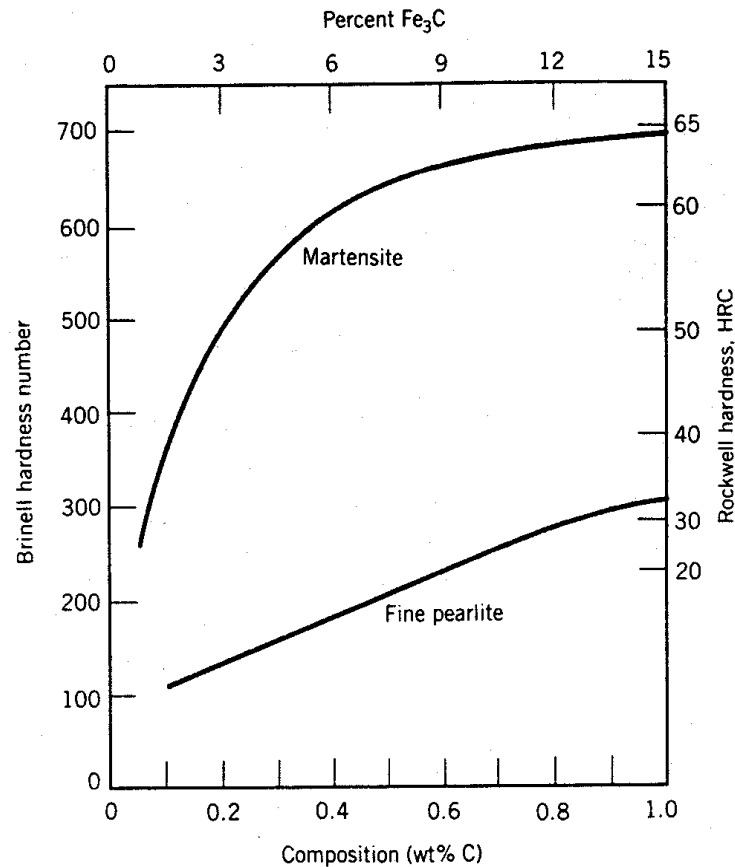
Figure 25: Hardness

8.14 Specifics of Quenching Process for Iron-Carbon Systems

The rate of cooling affects the resulting grain structure and thus the hardness, ductility, and strength of the steel specimen. **Quenching** is typically achieved in one of the following mediums. From fastest to slowest, steel can be quenched in brine (fastest), water (second fastest), air, or molten salt (slowest). We often use Time-Temperature-Transformation curves (TTT Curves), described earlier, to predict a steel's properties after heat treatment. The following discussion uses figure 26, below.

The first step in any heat treatment process is to heat the material above 727.ºC. This step is called **austenitizing.**

The dark blue curved lines on the diagram indicate the start and end of the transformation from austenite to pearlite. Each of the lines labeled (a)—(g) indicate idealized cooling curves (remember that the rate of cooling affects the transformation rate):

> **Curve (a)** shows a steel sample rapidly quenched in brine or water. The idealized cooling curve never approaches the transformation to pearlite, and therefore all austenite (ϒ) is converted to **Martensite. Martensite** is an extremely hard and strong crystal structure with

8 - 23

a very low ductility. It is rarely used structurally without tempering. The temperature at which austenite will transform to martensite is around 250ºC

Curve (b) shows a steel that is heated to 727 ºC, hot quenched (in molten salt) to ~695 ºC, and held at that temperature for over 2 hours to form **100% coarse pearlite. 100% coarse pearlite** is very ductile as hot quenching removes strain-induced stresses, but it is also soft and weak.

Curve (c) shows a steel that is heated to 727 ºC, hot quenched to 610 ºC, and held at that temperature for over 3 minutes to form 100% fine pearlite. **100% fine pearlite** has a uniform structure and higher strength than coarse pearlite. The cutoff between coarse and fine pearlite varies but is around 650 ºC.

Curve (d) shows a steel that is heated to 727 ºC, hot quenched to 580 ºC, held for ~5 seconds then water quenched to form a structure of **50% fine pearlite and 50% martensite**.

Curve (e) shows a steel that is heated to 727 ºC, quenched to ~475ºC, and held for over 3 minutes to form **upper bainite. Bainite** is an intermediate structure between pearlite and martensite. It forms between 250 - 550 ºC. **Upper Bainite** is distinguished by its coarser cementite particles. IT forms between 330 – 550 ºC.

Curve (f) shows a steel that is heated to 727 ºC, quenched to ~295ºC, and held for over 2 hours to form **lower bainite. Lower bainite** is characterized by its finer cementite particles.

Curve (g) shows a steel that is heated to 727 ºC, cooled to ~300 ºC, and held for 30 minutes then rapid quenched (in water) to form 50% lower bainite and 50% martensite.

8 - 24
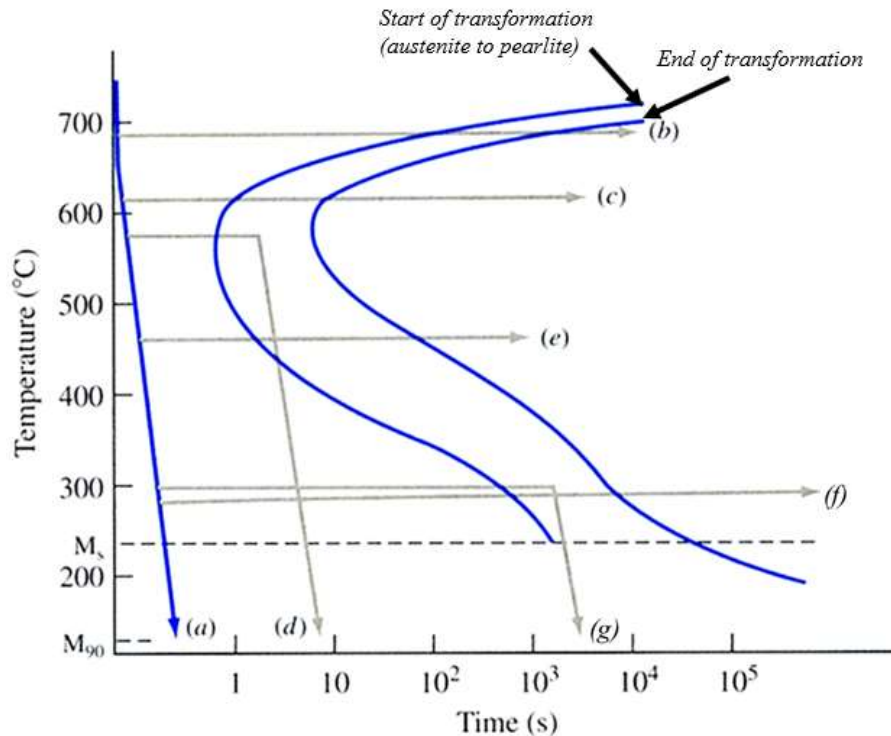
Fig 26: TTT Diagram of Eutectoid Steel

8.15 Case Hardening of Steel

Case Hardening is when metal is placed inside a carbon-rich environment. It is heated to very high temperatures to introduce carbon to the outside of the structure. This results in a hard outer surface, but a tough and strong inner surface. The process involves diffusion, following Fick's Second Law.

Fick's second law tells us that when case hardening steel, the carbon concentration in air at the surface, C_s, the carbon concentration at some distance x into the surface, C_x, and the initial carbon concentration of the steel, C_o, can be related according to:

$$\frac{C_s - C_x}{C_s - C_o} = erf\left(\frac{x}{2\sqrt{Dt}}\right)$$

where D is the diffusivity constant in m²/s and t is time.

A plot of the error function (*erf*) is shown in the Figure 27 below. Typically, this is tabulated for increasing values of z as shown in the following table.

8 - 25
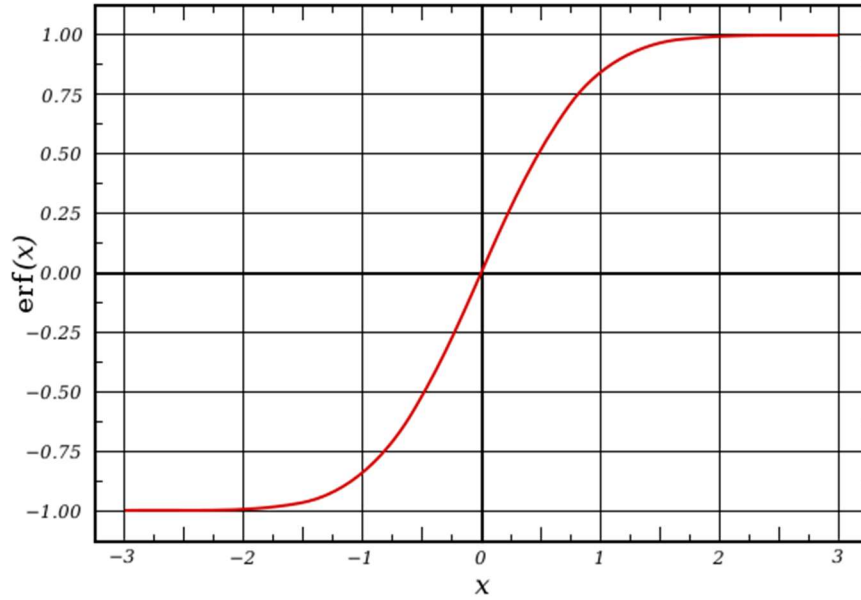
Figure 27: *erf(x)* vs. *x*

Tabulated values for *erf(z)*

z	erf(z)	z	erf(z)	z	erf(z)
0	0	0.55	0.5633	1.3	0.9340
0.025	0.0282	0.60	0.6039	1.4	0.9523
0.05	0.0564	0.65	0.6420	1.5	0.9661
0.10	0.1125	0.70	0.6778	1.6	0.9763
0.15	0.1680	0.75	0.7112	1.7	0.9838
0.20	0.2227	0.80	0.7421	1.8	0.9891
0.25	0.2763	0.85	0.7707	1.9	0.9928
0.30	0.3286	0.90	0.7970	2.0	0.9953
0.35	0.3794	0.95	0.8209	2.2	0.9981
0.40	0.4284	1.0	0.8427	2.4	0.9993
0.45	0.4755	1.1	0.8802	2.6	0.9998
0.50	0.5205	1.2	0.9103	2.8	0.9999

8 - 26

CHAPTER 9

STRESS

9.1 General Stress State and Principal Stresses
9.2 Determination of Principal Stresses (Two Dimensional) and Mohr's Circle
9.3 Determination of Principal Stresses (Three dimensional*)*
9.4 Maximum Shear Stress

9.1 General Stress State and Principal Stresses

The mechanical properties of materials are best described in terms of the state of stress which the material experiences. For example, the "break-down" in the elastic behavior of a bar under simple tension loading is described by the condition that the break-down will occur when the stress in the bar equals the yield stress of the material. For general loading, rather than simple tension, a similar but more complex law applies involving the magnitudes of the various stresses existing.

To describe mechanical properties, we thus first need to consider the general concept of stress at a point in a material.

A general stress state of a point in a solid consist of three normal stresses σ_x, σ_y, σ_z and six shearing stresses τ_{xy}, τ_{yx}, τ_{xz}, τ_{zx}, τ_{yz}, and τ_{zy} as shown in figure 1.
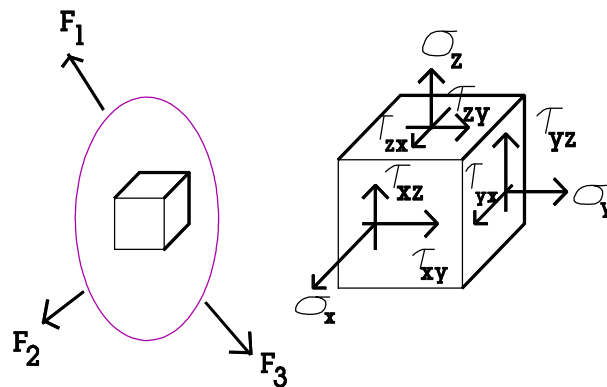
Figure 1: General Stress State

Each of the stresses (or stress components) represents a force per unit area acting on the small cube of material. By equilibrium, it is easily seen that $\tau_{xy} = \tau_{yx}$, $\tau_{xz} = \tau_{zx}$, $\tau_{yz} = \tau_{zy}$
(if $\tau_{xy} \neq \tau_{yx}$ etc, the block would try to rotate) so that three normal and three shearing stresses are needed to describe a general stress state.

<u>Principal Stresses:</u> Planes on which only normal stresses act are referred to as principal planes and the normal stresses as principal stresses. For any stress state, we may always find principal planes and principal stresses, as described below.

9.2 Determination of Principal Stresses (Two Dimensional) and Mohr's Circle

First, consider the two-dimensional plane stress case. At any point the stresses will be as shown in figure 2.
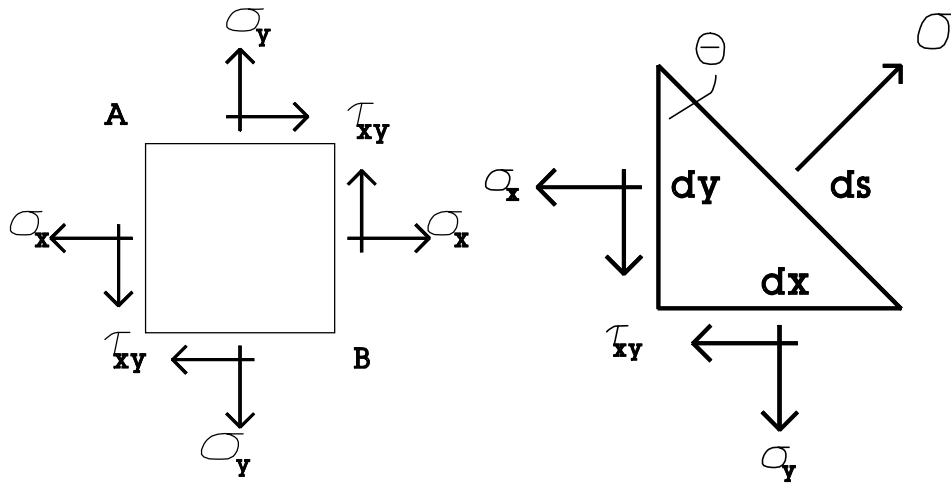
Figure 2: 2-D Principal Stresses

For principal stresses, we wish to find surfaces on which only normal stresses act. Considering the element of figure 3, which is part of figure 2, let σ be the principal stress acting on the plane δs. Equilibrium requires that:

$$\sigma n_x = \sigma_x n_x + \tau_{xy} n_y$$
$$\sigma n_y = \tau_{xy} n_x + \sigma_y n_y$$

where $n_x = \cos\theta$ and $n_y = \sin\theta$

rewriting the equations as

$$(\sigma_x - \sigma)n_x + \tau_{xy} n_y = 0$$
$$\tau_{xy} n_x + (\sigma_y - \sigma)n_y = 0$$

it is seen that for a non-trivial solution for n_x, n_y, we must require that

9 - 2

$$\begin{vmatrix} \sigma_x - \sigma & \tau_{xy} \\ \tau_{xy} & \sigma_y - \sigma \end{vmatrix} = 0$$

which provides the quadratic equation

$$\sigma^2 - (\sigma_x + \sigma_y)\sigma + \sigma_x \sigma_y - \tau_{xy}^2 = 0$$

with solutions

$$\sigma_{1,2} = \frac{\sigma_x + \sigma_y}{2} \pm \sqrt{\left(\frac{\sigma_x - \sigma_y}{2}\right)^2 + \tau_{xy}^2}$$

The directions of the normals to the planes having these principal stresses can be found since $\tan\theta = n_y/n_x$.

$$\tan\theta = \frac{\sigma - \sigma_x}{\tau_{xy}}$$

Example. *Consider the two-dimensional stress state shown below in figure 4 and determine the principal stresses and the planes on which the act.*
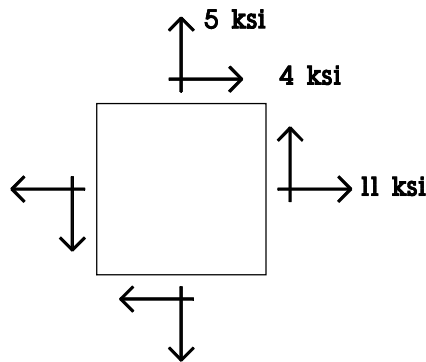
Figure 4

Solution. *From eq. (3), we find that σ₁ = 13 ksi, σ₂ = 3 ksi. Using eq. (4), we then find that for σ₁ = 13, tan θ₁ = (13-11)/4 = 0.5 and θ₁ = 26.6°. Similarly, for σ₂ = 3, tan θ₂ = -2 and θ₂ = -63.4°. These planes are shown in figure 5.*

9 - 3
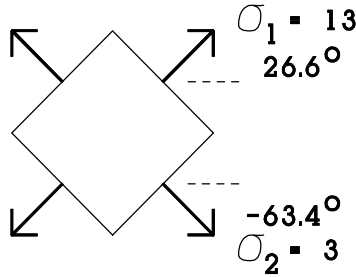
Fig. 5

Notice that the planes are perpendicular to one another. This can be shown to be true in general, and we thus see that if we had chosen the element with the orientation of figure 5 initially, the shear stresses would have been zero and only normal principal stresses would be involved.

Example: Consider the previous example using Mohr's circle

Solution: The above equations are easily seen to yield the Mohr's circle method for principal stress determination. Taking horizontal and vertical axes with normal stress plotted along the horizontal and a shear stress along the vertical, we have (adopting the convention that normal stress is plotted positive on the σ-axes and shear stress, tending to rotate the element clockwise, is plotted on the positive (τ axes) on the sketch shown in figure 6.
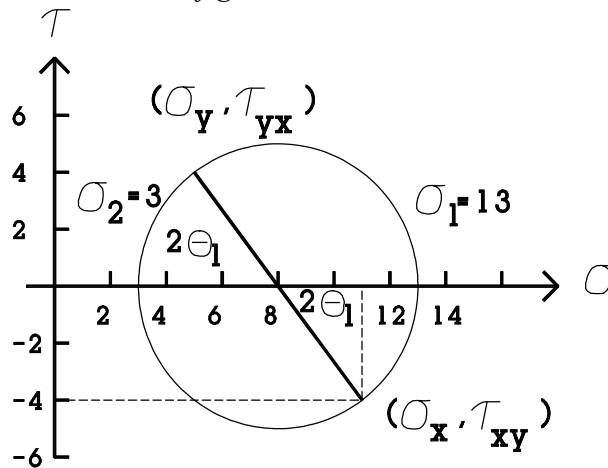
$$c = \frac{\sigma_x + \sigma_y}{2}$$

$$r = \sqrt{(\sigma_x - c)^2 + \tau_{xy}^2}$$

$$\tan 2\theta_1 = \frac{\tau_{xy}}{\sigma_x - c}$$

$$\sigma_1 = c + r, \ \sigma_2 = c - r$$

Figure 6: Mohr's Circle

9 - 4

9.3 Determination of Principal Stresses (Three dimensional*)*

To find the principal stresses for the general three-dimensional case, we define direction cosines n_x, n_y, and n_z of the normal n to the principal plane as shown in figure 7.

$$n_x = \cos \theta_x$$
$$n_y = \cos \theta_y$$
$$n_z = \cos \theta_z$$
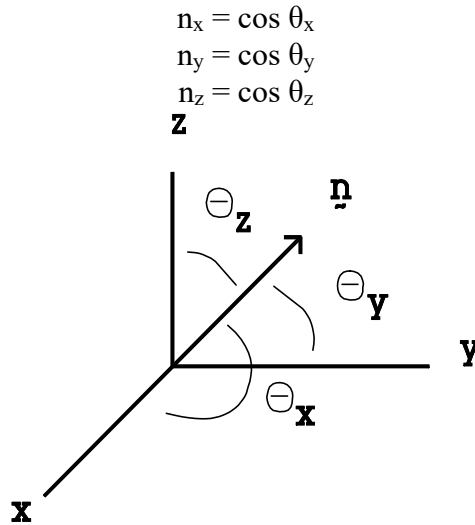
Figure 7

The equilibrium equations are

$$(\sigma_x - \sigma)n_x + \tau_{xy}n_y + \tau_{xz}n_z = 0$$
$$\tau_{xy}n_x + (\sigma_y - \sigma)n_y + \tau_{yz}n_z = 0$$
$$\tau_{xz}n_x + \tau_{yz}n_y + (\sigma_z - \sigma)n_z = 0$$

For a non-trivial solution for n_x, n_y, and n_z, the determinate of coefficients must vanish. Thus

$$\begin{bmatrix} (\sigma_x-\sigma) & \tau_{xy} & \tau_{xz} \\ \tau_{xy} & (\sigma_y-\sigma) & \tau_{yz} \\ \tau_{xz} & \tau_{yz} & (\sigma_z-\sigma,) \end{bmatrix} = 0$$

Expanding this determinant yields a cubic equation whose roots are the principal stresses.

$$\sigma^3 - A\sigma^2 + B\sigma - C = 0$$

9 - 5

Where

$$A = \sigma_x + \sigma_y + \sigma_z$$

$$B = \sigma_x \sigma_y + \sigma_y \sigma_z + \sigma_x \sigma_z - \tau_{xy}^2 - \tau_{yz}^2 - \tau_{xz}^2$$

$$C = \sigma_x \sigma_y \sigma_z + 2\tau_{xy}\tau_{yz}\tau_{zx} - \sigma_x \tau_{yz}^2 - \sigma_y \tau_{xz}^2 - \sigma_z \tau_{xy}^2$$

The roots of the equation, usually determined numerically, are the principal stresses. To find the direction cosines, n_x, n_y, and n_z of the plane in which, say σ_1 acts, we may use the above equations with $\sigma = \sigma_1$, together with the geometric condition

$$n_x{}^2 + n_y{}^2 + n_z{}^2 = 1$$

Similar procedures apply for σ_2 and σ_3.

9.4 Maximum Shear Stress

It is not difficult to show, using methods of analysis similar to those applied above, that the maximum shear stress existing at a point is given by the greatest of the quantities

$$\left| \frac{\sigma_1 - \sigma_2}{2} \right| , \left| \frac{\sigma_2 - \sigma_3}{2} \right| , \left| \frac{\sigma_3 - \sigma_1}{2} \right|$$

if we label the principal stresses such that $\sigma_1 > \sigma_2 > \sigma_3$, then

$$\tau_{max} = \left| \frac{\theta_1 - \theta_3}{2} \right|$$

This greatest shear stress acts on a plane perpendicular to the principal plane associated with σ_2 and at 45° to those associated with σ_1 and σ_3.
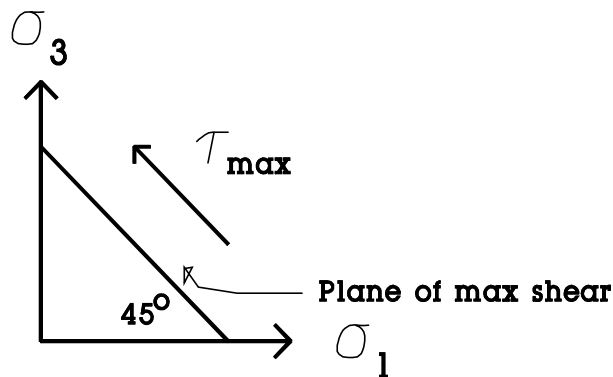
Example. *Consider the stress state defined by*

$$\sigma_x = 2 \ ksi, \ \ \sigma_y = \sigma_z = 0$$
$$\tau_{xy} = \tau_{yz} = 0, \ \tau_{xz} = 1 \ ksi$$

Solution. *We find the three principal stresses as*

$$\sigma_1 = 2.414 \ ksi, \ \sigma_2 = 0, \ \sigma_3 = -0.414 \ ksi$$

To find the directions associated with each, use the first two equilibrium equations and the relation
$n_x^2 + n_y^2 + n_z^2 = 1.$

> *For $\sigma = \sigma_1$*
> $\qquad$ *-0.414 n_x + n_z = 0*
> $\qquad$ *-2.414 n_y = 0*
> $\qquad$ *$n_x^2 + n_y^2 + n_z^2 = 1$*
> *thus we find*
> $\qquad$ *n_x = ± 0.9237*
> $\qquad$ *n_y = 0*
> $\qquad$ *n_z = ± 0.3826*
> *and*
> $\qquad$ *θ_{1x} = 22.5° or 157.5°*
> $\qquad$ *θ_{1y} = 90°*
> $\qquad$ *θ_{1z} = 67.5° or 112.5°*
> *Similarly, for σ_2 we find $n_x = n_z = 0$, $n_y = ± 1$, so that*
> $\qquad$ *θ_{2x} = 90°*
> $\qquad$ *θ_{2y} = 0° or 180°*
> $\qquad$ *θ_{2z} = 90°*
> *And for σ_3 we find $n_x = ± 0.3826$, $n_z = ± 0.9237$*
> $\qquad$ *θ_{3x} = 112.5° or 67.5°*
> $\qquad$ *θ_{3y} = 90°*
> $\qquad$ *θ_{3z} = 22.5° or 157.5°*

9 - 7

CHAPTER 10

DEFORMATION

Consider the bar in figure 1 subjected to a simple tension loading F.

Figure 1: Bar in Tension

Engineering Stress (σ) is the quotient of load (F) and area (A). The units of stress are normally pounds per square inch (psi).

$$\sigma = \frac{F}{A}$$

where:
σ is the stress (psi)
F is the force that is loading the object (lb)
A is the cross sectional area of the object (in^2)

When stress is applied to a material, the material will deform. Elongation is defined as the difference between loaded and unloaded length

$$\Delta l = L - L_o$$

where:
Δl is the elongation (ft)
L is the loaded length of the cable (ft)
L_o is the unloaded (original) length of the cable (ft)

10-1

Strain is the concept used to compare the elongation of a material to its original, undeformed length. Strain (ε) is the quotient of elongation (e) and original length (L_0). Engineering Strain has no units but is often given the units of in/in or ft/ft.

$$\varepsilon = \frac{\Delta l}{L_o}$$

where: ε   is the strain in the cable (ft/ft)
              Δl is the elongation (ft)
              L_o is the unloaded (original) length of the cable (ft)

Example   *Find the strain in a 75 foot cable experiencing an elongation of one inch.*

Solution:

$$Strain(\varepsilon) = \frac{e(ft)}{L_o(ft)} = \frac{1\ in\ (1ft/12in)}{75\ ft} = 1.11x10^{-3}\ ft/ft$$

10.1 Stress-Strain Diagrams and Material Behavior

Stress and strain are calculated from easily measurable quantities (normal load, diameter, elongation, original length) and can be plotted against one another as in Figure 2. Such Stress-Strain diagrams are used to study the behavior of a material from the point it is loaded until it breaks. Each material produces a different stress-strain diagram.

Point 1 on the diagram represents the original undeformed, unloaded condition of the material. As the material is loaded, both stress and strain increase, and the plot proceeds from Point 1 to Point 2. If the material is unloaded before Point 2 is reached, then the plot would proceed back down the same line to Point 1.

If the material is unloaded anywhere between Points 1 and 2, then it will return to its original shape, like a rubber band. This type of behavior is termed *Elastic* and the region between Points 1 and 2 is the *Elastic Region*.

The Stress-Strain curve also appears linear between Points 1 and 2. In this region stress and strain are proportional. The constant of proportionality is called the *Elastic Modulus* or *Young's Modulus (E)*. The relationship between stress and strain in this region is given by Equation 5-4.

$$E = \frac{\sigma}{\varepsilon} \qquad or \qquad \sigma = E\varepsilon$$

where: σ   is the stress (psi)
              E   is the Elastic Modulus (psi)
              ε   is the strain (in/in)

The Elastic Modulus is also the slope of the curve in this region, solved by taking the slope between data points (0,0) and (σ_y, ε_y).
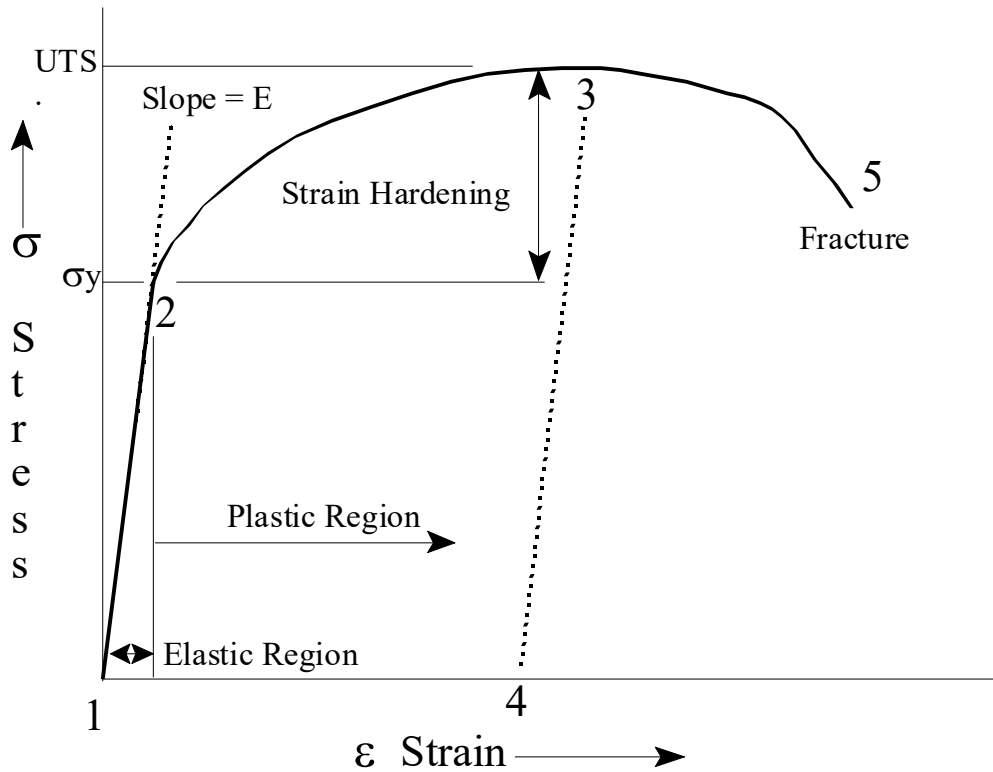
Figure 2 Stress/Strain Diagram

Point 2 is called the *Yield Strength* (σ_y). If it is passed, the material will no longer return to its original length. It will have some permanent deformation. This area beyond Point 2 is the *Plastic Region.* Consider, for example, what happens if we continue along the curve from Point 2 to Point 3, the stress required to continue deformation increases with increasing strain. If the material is unloaded the curve will proceed from Point 3 to Point 4. The slope (Elastic Modulus) will be the same as the slope between Points 1 and 2. The difference between Points 1 and 4 represents the permanent strain of the material.

If the material is loaded again, the curve will proceed from Point 4 to Point 3 with the same Elastic Modulus (slope). The Elastic Modulus will be unchanged, but the Yield Strength will be increased. Permanently straining the material in order to increase the Yield Strength is called *Strain Hardening.*

If the material is strained beyond Point 3 stress decreases as non-uniform deformation and necking occur. The sample will eventually reach Point 5 at which it fractures.

10-3

The largest value of stress on the diagram is called the *Tensile Strength (TS)* or *Ultimate Tensile Strength (UTS)*. This is the most stress the material can support without breaking.

Example: (This is from the FE Exam) A Steel rod (E=200 GPa) has a circular cross section and is 10m long. Determine the minimum diameter if the rod must hold a 30 kN tensile force without deforming more than 5mm. Assume the steel stays in the elastic region. Note, 1 GPa = 10^9 Pa.

Solution:

Knowing the initial length and the change in length permits the calculation of strain.

$$\varepsilon = \frac{\Delta l}{l_o} = \frac{5mm(\frac{1m}{1000mm})}{20m} = 0.0005$$

In the elastic region, the stress σ is directly proportional to the strain ε, by the Modulus of Elasticity, E

$$\frac{F}{A_o} = \sigma = E\varepsilon$$

Rearranging, substituting values and converting units,

$$\sigma = E\varepsilon = (200 \ GPa)0.0005 = 0.1 \ GPa = 0.1 \times 10^9 Pa = 0.1 \times 10^9 \ N/m^2$$

The definition of stress $\sigma = \frac{F}{A_o}$ can be used to find the required cross section area.

$$A_O = \frac{F}{\sigma} = \frac{30kN\left(\frac{1000N}{kN}\right)}{0.1 \times 10^9 \ N/m^2} = 0.0003m^2(\frac{1000mm}{m})(\frac{1000mm}{m}) = 300mm^2$$

The diameter, d_o is solved from the area of a circle

$$A_o = \frac{\pi d_o^2}{4}$$

$$d_o^2 = \frac{A_o 4}{\pi}$$

$$d_o = \sqrt{\frac{A_o 4}{\pi}} = \sqrt{\frac{300mm^2 * 4}{3.14}} = 19.5mm$$

10-4

10.2 Material Characteristics

There are five material properties that do a good job at describing the characteristics of a material. They are <u>strength, hardness, brittleness, toughness, and ductility</u>. Each of these will be discussed in more detail in the upcoming chapters.

Strength is measure of the materials ability to resist deformation and to maintain its shape. Strength can be quantified in terms of yield stress or ultimate tensile strength. Both yield stress and ultimate tensile strength can be determined from tensile test data by plotting a stress strain curve.

Hardness is a measure of the materials ability to resist indentation, abrasion and wear. Hardness is quantified by arbitrary hardness scales such as the Rockwell hardness scale or the Brinell hardness scale. These measurements are obtained by a special apparatus that uses an indenter that is loaded with standard weights. The indenter can have various shapes such as a pyramid or a sphere and is pressed into the specimen. Either the depth of penetration or the diameter of the indentation made is measured to quantify material hardness. Hardness and strength correlate well because both properties are related to inter-molecular bonding. Figure 3 illustrates the test and gives conversion scales for relating values to tensile strength.

Ductility is a measure of materials ability to deform before failure. Ductility can be quantified by reading the value of strain at the fracture point on the stress strain curve or by doing a percent reduction in area calculation. Low carbon steels, pure aluminum, copper, and brass are examples of ductile materials.

Brittleness is a measure of a material inability to deform before failure. Brittleness is the opposite of ductility. Brittleness is not quantified since it is the inability to deform. However, ductility is quantified as discussed above. Examples of brittle materials include glass, cast iron, high carbon steels, and many ceramic materials. Figure 4 shows the difference between ductile and brittle behavior on a stress-strain diagram. This will be discussed in more detail in the chapter on fracture.

Toughness is a measure of a materials ability to absorb energy. There are two measures of toughness. Material Toughness and Impact Toughness. <u>Material Toughness</u> can be measured by calculating the area under the stress strain curve from a tensile test (Fig 5). The units on this measure of toughness are in-lb/in3. These are units of energy per volume. *Material Toughness* equates to a slow absorption of energy by the material. <u>Impact Toughness</u> is measured by doing a Charpy V-notch Test, discussed further in the chapter on Fracture.

The <u>material toughness</u> can be expressed as the work W required to strain a bar to engineering strain ε.

$$W = \int_{l_o}^{l} F dl = A_o l_o \int_0^{\varepsilon} \sigma d\varepsilon$$

or if w denotes the work per unit volume of material $W/A_o l_o$, then

10-5

$$w = \int_0^{\varepsilon} \sigma d\varepsilon$$

Thus, the area under the engineering stress-strain curve is a direct measure of the amount of work per unit volume of the material needed to effect a given engineering strain ε.
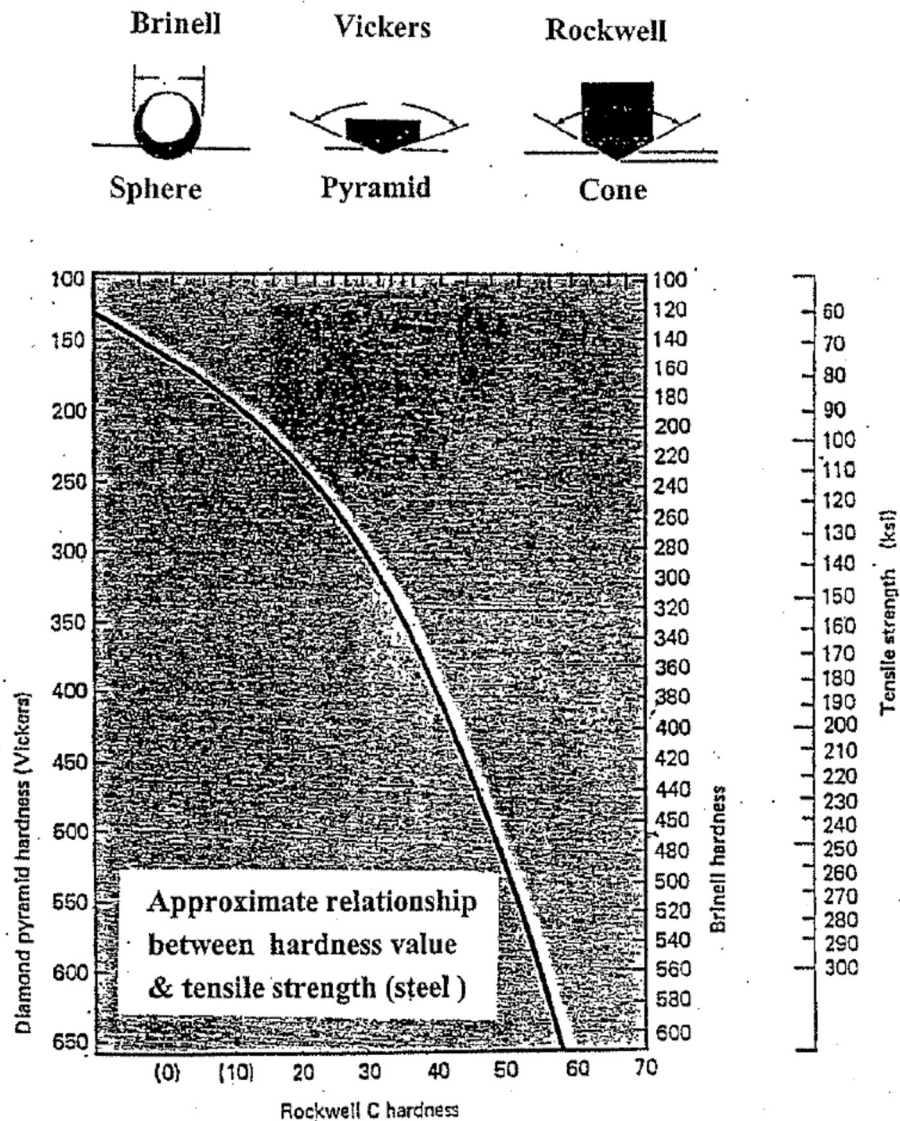
Figure 3: Hardness Tests

10-6
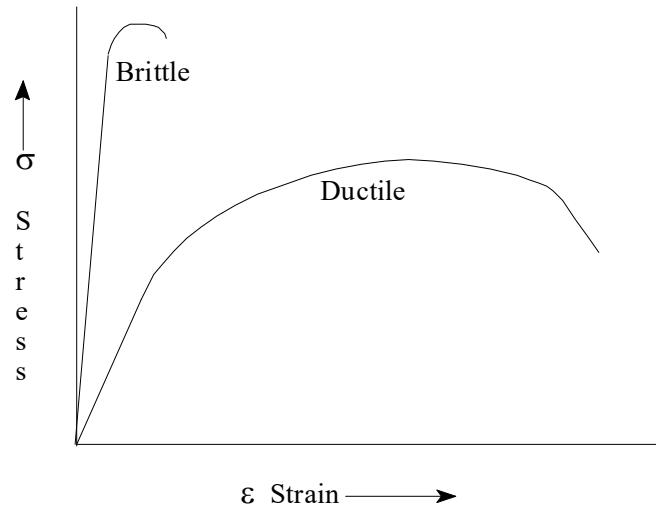
Figure 4. Ductile and Brittle Behavior
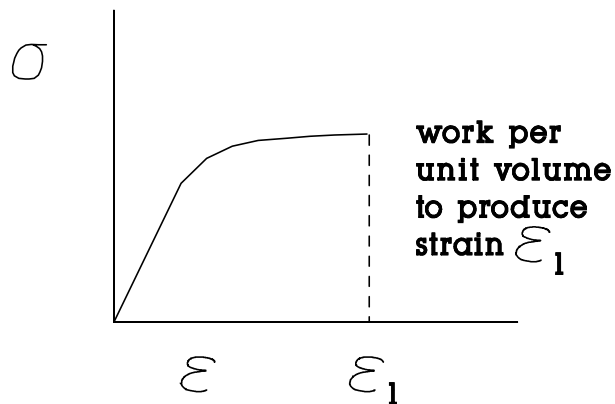
Fig. 5

10.3 Elastic-Plastic Response of Metals

When an ordinary piece of metal is subjected to a force of gradually increasing intensity, the atoms within the individual grains are simply displaced from their initial positions in an elastic fashion; if the force is reduced, the atoms will return to their initial positions.

When the force becomes sufficiently large, the atoms essentially shift from their elastically distorted initial positions to new, identical positions within the lattice, resulting in permanent plastic strain. Thus, in the ordinary tensile test of a metal, we may think of the elastic region as the region where the atoms are slightly displaced from initial positions, whereas the plastic region, planes of atoms are actually slipping over one another, resulting in permanent, plastic deformation.

The actual mechanism by which the atoms slip over one another is generally thought to involve the idea of dislocations or imperfections in the otherwise perfect crystalline arrangement of the atoms. These imperfections (Fig 6) make the slipping (Fig 7) relatively easy.

The two general types of locations are edge dislocations and screw dislocations (Fig. 8). Edge dislocations exist when an extra plane of atoms exists in a portion of the lattice structure. Screw dislocations result when a plane of atoms shifts its orientation from one plane to another.

Force analyses show that slipping of the plates can occur with much lower stress than would be required if the arrangement of atoms was perfect. In fact, theoretical calculations accounting for a given <u>dislocation density</u> are consistent with those found experimentally.
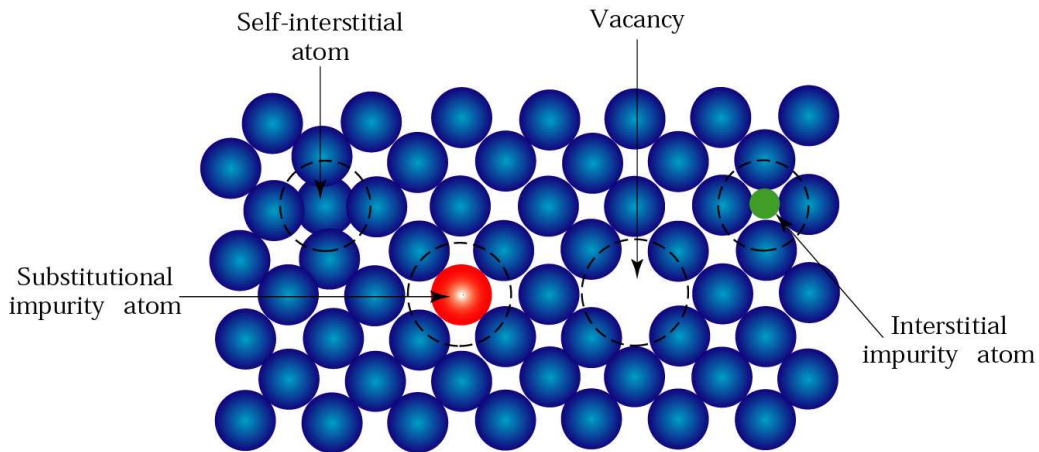
Fig. 6 Interstitial Atoms and Vacancies
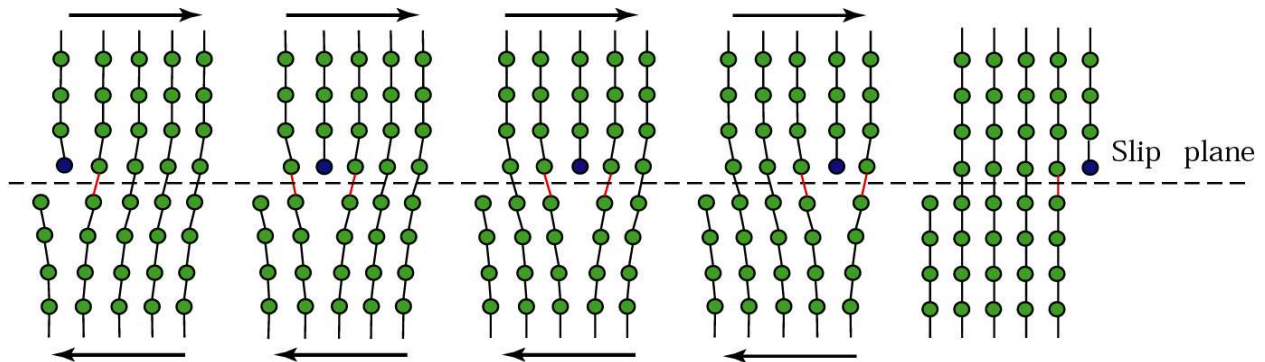
Fig.7 Movement of Edge Dislocations

(a)

(b)
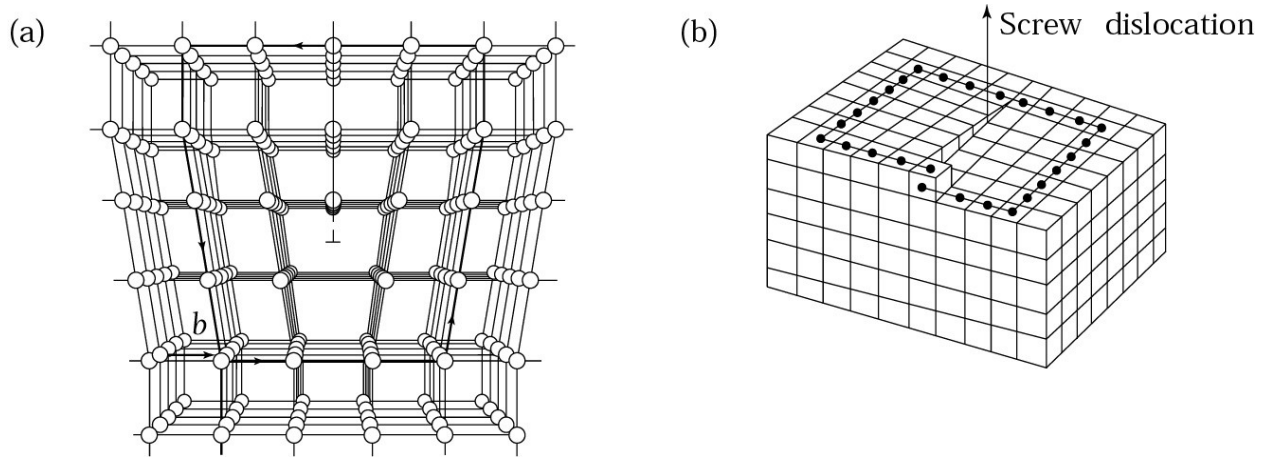
Screw dislocation

Fig. 8 Edge Dislocation (a) and Screw Dislocation (b)

10.4 True stress and strain measures.

Instead of using engineering stress and strain measures, we may use the so-called "true" stress, σ_T, and "true" strain, ε_T, measures. These are defined as

$$\sigma_T = \frac{F}{A}$$

$$\varepsilon_T = \int_{l_o}^{l} \frac{dl}{l} = \ln\left(\frac{l}{l_o}\right)$$

where A denotes the deformed area of the specimen at load F and l denotes the deformed length of the specimen associated with a small increase in extension dl.

In the elastic region, the difference between A and A_o and l and l_o is very small so that the "true" stress and strain values are essentially the same as the engineering stress and strain values. When large plastic deformation takes place, the difference is no longer negligible and it is necessary to specify which stress and strain measures are used.

For plastic deformations where the difference between A and l and A_o and l_o are important, it has been shown experimentally that the volume of the specimen remains essentially constant such that

$$Al = A_o l_o$$

We also have by the definition of engineering strain

$$l = l_o(1 + \varepsilon)$$

Combining the above equations gives us "true" stress and strain expressible as

$$\sigma_T = \sigma(1 + \varepsilon), \quad \varepsilon_T = \ln(1 + \varepsilon)$$

These equations are useful for determining "true" stress-strain response. Notice, however, that since the "true" stress and strain are expressible in terms of the engineering stress and strain, in the real sense one is no more true than the other. One set can be obtained from the other simply by computation. Figure 9 shows a comparison between engineering and "true" stress-strain response.
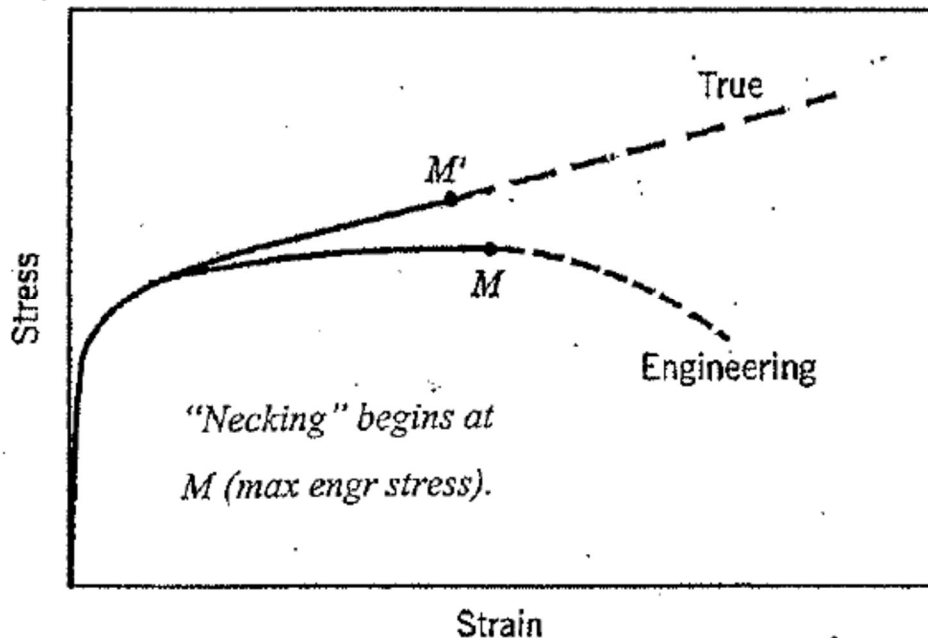
Figure 9: True vs Engineering Stress

10.5 Yielding of a Ductile Metal under a General Stress State - Mises Yield Condition.

The work done per unit volume of material by the stress in a simple tension test is determined by the area under the stress-strain curve up to the level of strain experienced at max stress. In the elastic region (assuming linear behavior) this is given by

$$W = \tfrac{1}{2}\sigma\varepsilon$$

All of this work is stored as "elastic energy" in the material, which is released at unloading. Once the material is in the plastic region a part of this work is associated with changing the materials volume while the rest is associated with changing its shape (distorting).

This same division is also true in a general stress loading and forms the basis for the Mises Yield Condition expressing the condition for yielding, or elastic break-down, under general stress loading. The Mises Condition can be interpreted as requiring that yielding occurs when the strain energy of distortion in a general stress state equals the strain energy of distortion at yielding in a simple tension test on the same material.

To develop the mathematical form of this expression, we consider a general cubic element of material having principal stresses σ_1, σ_2, and σ_3 acting on it and experiencing associated strain ε_1,

ε_2, and ε_3. The work (or strain energy) per unit volume of material associated with these strains is given, by analogy with eq. (17) as

$$w = \tfrac{1}{2}\sigma_1\varepsilon_1 + \tfrac{1}{2}\sigma_2\varepsilon_2 + \tfrac{1}{2}\sigma_3\varepsilon_3$$

Now, from the elastic stress strain relations we have

$$\varepsilon_1 = \frac{\sigma_1}{E} - \frac{v}{E}(\sigma_2 + \sigma_3)$$

$$\varepsilon_2 = \frac{\sigma_2}{E} - \frac{v}{E}(\sigma_1 + \sigma_3)$$

$$\varepsilon_3 = \frac{\sigma_3}{E} - \frac{v}{E}(\sigma_1 + \sigma_2)$$

where E is Young's modulus, v is Poisson's ratio, both constants for a given material. Substituting we find

$$w = \frac{1}{2E}(\sigma_1{}^2 + \sigma_2{}^2 + \sigma_3{}^2) - \frac{v}{E}(\sigma_1\sigma_2 + \sigma_2\sigma_3 + \sigma_1\sigma_3)$$

Now consider the volume of the small element of material. If its sides were initially of length a, its initial volume was a^3 and its final volume is $a^3(1 + \varepsilon_1)(1 + \varepsilon_2)(1 + \varepsilon_3)$. For small strains, we thus have for the change in unit volume per unit initial area

$$\Delta = (1 + \varepsilon_1)(1 + \varepsilon_2)(1 + \varepsilon_3) - 1 \approx \varepsilon_1 + \varepsilon_2 + \varepsilon_3$$

We also see that

$$\Delta = \frac{1-2v}{E}(\sigma_1 + \sigma_2 + \sigma_3)$$

Hence, the change in volume is related directly to the sum $\sigma_1 + \sigma_2 + \sigma_3$. We may then define the mean stress $\overline{\sigma}$ as

$$\overline{\sigma} = \frac{1}{3}(\sigma_1 + \sigma_2 + \sigma_3)$$

The element stresses can be thought of as being composed of this mean stress $\overline{\sigma}$ and an additional stress dependent on the mean stress; i.e.
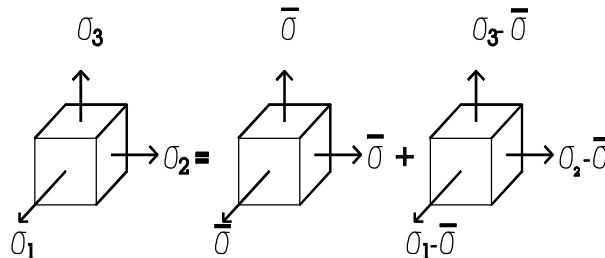
Figure 10

It is clear that the stress $\bar{\sigma}$ is associated with the total volume change of the material and the stresses $\sigma_1 - \bar{\sigma}$, $\sigma_2 - \bar{\sigma}$, $\sigma_3 - \bar{\sigma}$ are associated only with its distortion. Hence, the strain energy associated with the volume change is determined by substituting $\sigma_1 = \bar{\sigma}$, $\sigma_2 = \bar{\sigma}$, $\sigma_3 = \bar{\sigma}$ into the equation, we find

$$w_v = \frac{3}{2E}(1 - 2v)\bar{\sigma}^2$$

Subtracting this from the total strain energy w we find (using the definition of $\bar{\sigma}$) the strain energy of distortion given by

$$w - w_v = \frac{1+v}{3E}(\sigma_1^2 + \sigma_2^2 + \sigma_3^2 - \sigma_1\sigma_2 - \sigma_2\sigma_3 - \sigma_1\sigma_3)$$

The value of this expression at yielding in a simple tension test ($\sigma_1 = \sigma_Y$, $\sigma_2 = \sigma_3 = 0$) is

$$w - w_v = \frac{1+v}{3E}\sigma_Y^2$$

By equating the right-hand side of the previous equation to this value, we have the Mises Yield Condition in the form

$$\sigma_1^2 + \sigma_2^2 + \sigma_3^2 - \sigma_1\sigma_2 - \sigma_2\sigma_3 - \sigma_1\sigma_3 = \sigma_Y^2$$

An alternate form of this equation is

$$(\sigma_1 - \sigma_2)^2 + (\sigma_2 - \sigma_3)^2 - (\sigma_3 - \sigma_1)^2 = 2\sigma_Y^2$$

In two dimensional plane stress

$$\sigma_1^2 + \sigma_2^2 - \sigma_1\sigma_2 = \sigma_Y^2$$

If we use for the two-dimensional case

$$\sigma_{1,2} = \frac{\sigma_x + \sigma_y}{2} \pm \sqrt{\frac{\sigma_x - \sigma_y}{2}^2 + \tau_{xy}^2}$$

we find the Mises Yield Condition expressible as

$$\sigma_x^2 + \sigma_2^2 - \sigma_x\sigma_y + 3\tau_{xy}^2 = \sigma_Y^2$$

Example: A cylindrical pressure vessel of 15 inches in diameter has a wall thickness of 0.25 inches. The yield stress of the material is 40,000 psi. Determine the internal pressure required for yielding using the Mises Condition.
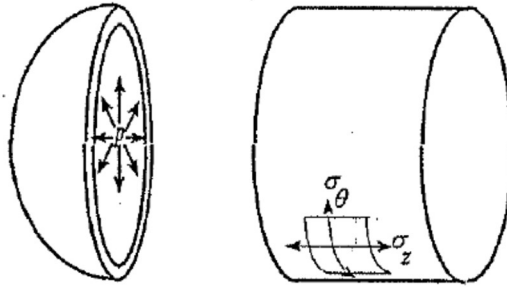
The stresses are

$$\sigma_\theta = (pr)/t, \ \sigma_z = (pr)/2t$$

where r = radius, t = wall thickness, p = net internal pressure. (these formulae are valid only for thin walled pressure vessels).

Solution: On substituting for r and t we have $\sigma_\theta = 30\,p$ and $\sigma_z = 15p$. These are principal stresses. Substituting into the Mises Condition, eq. (30), we have

$$900p^2 + 225p^2 - 450p^2 = \sigma_Y = 40000 \ psi$$
$$\boldsymbol{or} \ p = 1540 \ psi$$

This is the net internal pressure, i.e. the difference between internal and external pressure.

Example. A circular steel shaft is subjected to a bending moment of 3000 in-lb and a twisting moment of 8000 in-lb. Determine the required diameter of the shaft if the yield stress in a simple tension test in 36,000 psi.

10-13
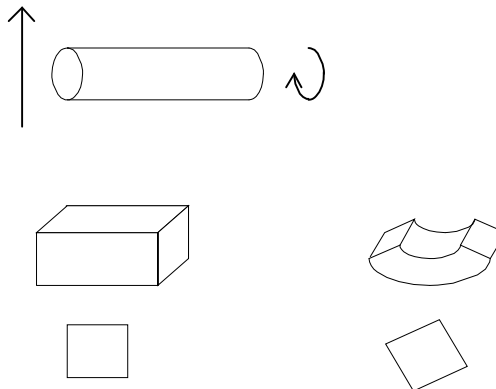
Solution: the maximum bending stress σ_x is

$$\sigma_x = M_b r/I$$

where M_b is the bending moment and I is the moment of inertia of the cross-sectional area with respect to the neutral axis. Therefore

$$\sigma_x = (3000)(r)/(\pi r^4/4) = 3820/r^3$$

The maximum shear stress is $\tau_{xy} = (M_t r)/(J)$ where M_t is the twisting moment and J is the polar moment of inertia. Therefore

$$\tau_{xy} = (8000)(r)/(\pi r^4/2) = 5093/r^3$$

Substituting into the Mises relation

$$\sigma_x^2 + \sigma_2^2 - \sigma_x\sigma_y + 3\tau_{xy}^2 = \sigma_Y^2$$

with $\sigma_y = 0$, we have

$$(\frac{3820}{r^3})^2 \; + \; 3(\frac{5093}{r^3})^2 \; = \; (36000)^2$$

Hence $r^6 = 0.0710 \ in^6 \Rightarrow r = 0.644 \ in$ and the required diameter is 1.29 in.

10.6 Maximum shear stress condition.

A theory for the yielding of ductile metals which is sometimes used in place of the Mises Yield Condition is the maximum shear stress condition. This theory assumes that elastic breakdown will occur when the maximum shear stress in a general stress state reaches the value it has in a simple tension test at yielding. Thus, if τ_{max} denotes the maximum shear stress in a general stress loading, we have

$$\tau_{max} = \tfrac{1}{2}\sigma_Y$$

where $\tfrac{1}{2}\sigma_Y$ is the maximum stress in a simple tension loading at yield.

Example: Reconsider the pressure vessel from the previous example using the maximum shear stress condition.

Solution: The principal stresses are $\sigma_1 = pr/t$, $\sigma_2 = pr/2t$, $\sigma_3 = 0$. The maximum shear stress is thus

$$\tau_{max} = \left|\frac{\sigma_1 - \sigma_3}{2}\right| = \frac{pr}{2t}$$

$$pr/2t = \tfrac{1}{2}\sigma_Y \ or \ p = 1333 \ psi.$$

10-14

Note that this is about 13% less than that given by the Mises equation and thus provides a more conservative estimate. Experimentally, the Mises Yield Condition has proven to be the most accurate.

10.7 Creep

"Creep" is a progressive plastic deformation that increases with time, even when the stress is below the yield stress of the material. The effects of creep increase as temperature increases, and generally noticeable at above 35% of the melting temperature of the material. Figure 11, below shows the effects of creep, in term of strain versus time.

- Initially, the rate of creep (slope) is high. In this initial stage, effects analogous to strain hardening reduce the rate of creep with time.
- In the second stage, the creep achieves a constant rate due to a balance between work hardening and annealing (thermal softening).
- In the third stage, necking of the material causes the strain to increase more rapidly, leading to rupture.
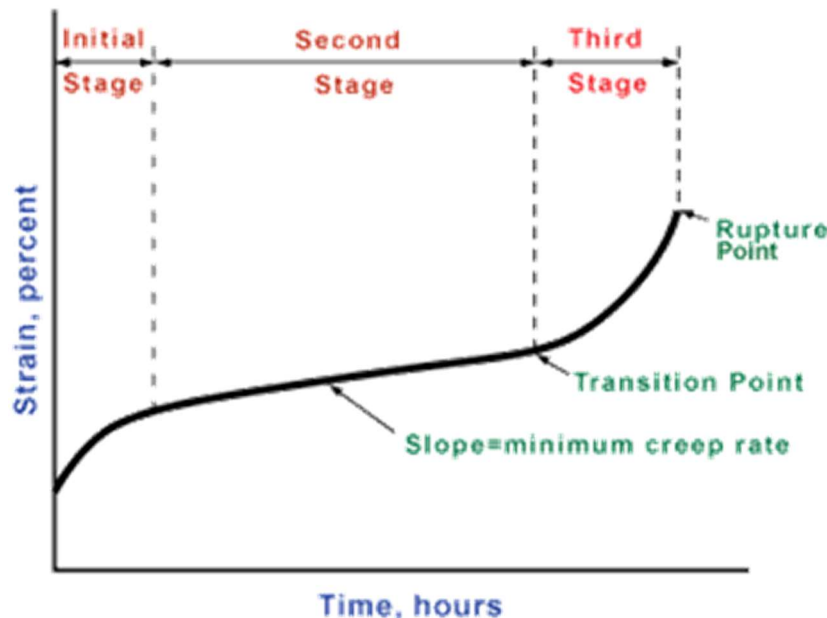
Figure 11: Stages of Creep

A well-known example of material creep was the World Trade Center Collapse. The stress on the materials increased because of the reduced structural capacity of the damaged building and added weight due to planes. The burning jet fuel increased the temperature, causing thermal creep. This lead to a reduced cross section of the material and eventual failure.

10-15
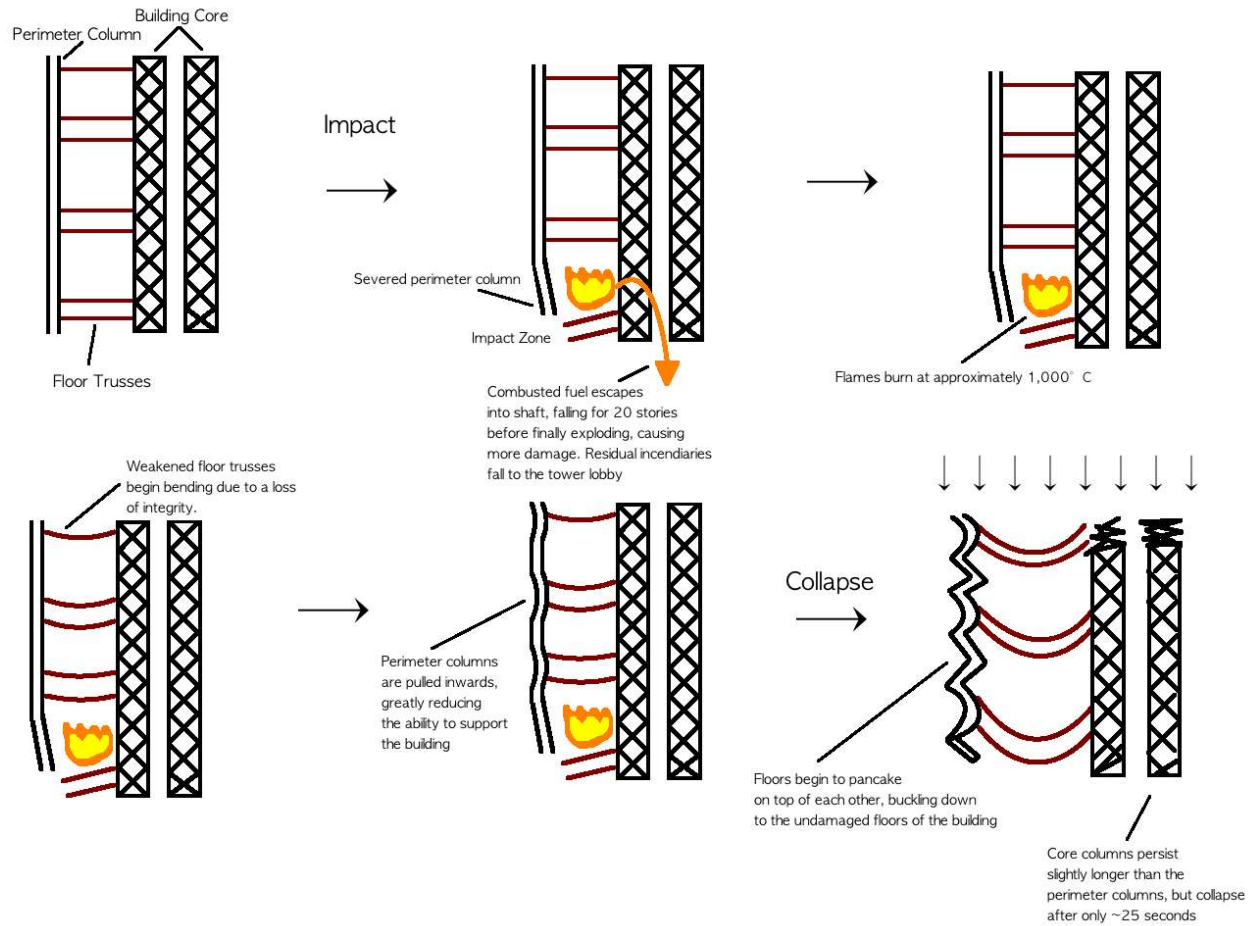
Figure 12: Creep and Failure mechanism in World Trade Center Collapse
(From TLC "Anatomy of Collapse")

10-16

CHAPTER 11

FRACTURE OF MATERIALS

11.1 Brittle vs. Ductile Fracture
11.2 Temperature Effects and Fracture Analysis Diagram
11.3 Griffith Theory of Brittle Fracture.
11.4 Fracture mechanics of high-strength materials
11.5 Connection with Fracture Mechanics
11.6 Stress Corrosion Cracking (SCC)
11.7 Non-Destructive Testing

11.1 Brittle vs. Ductile Fracture

Fracture involves the forced separation of a material into two or more parts. Brittle Fracture involves fracture without any appreciable plastic deformation (i.e. energy absorption). Ductile Fracture in the converse and involves large plastic deformation before separation. The difference between brittle and ductile fracture is illustrated in figures 1 and 2. Remembering that the area under the σ - ε curve, Fig. 1, represents energy, we can see that much less energy is expended in brittle fracture than in ductile fracture.
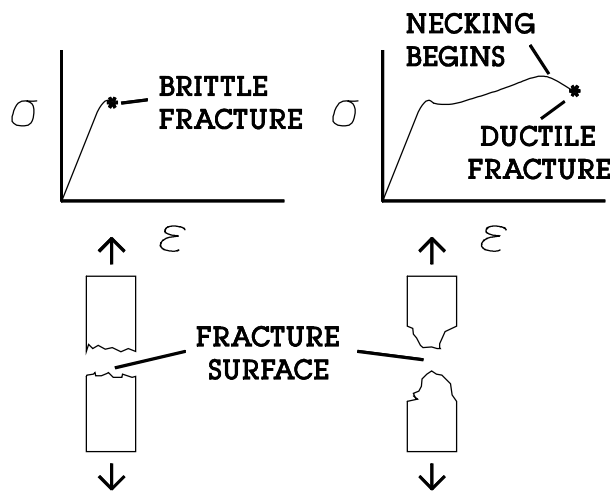
Figure 1: Brittle vs Ductile Fracture

brittle fracture   cup-and-cone fracture
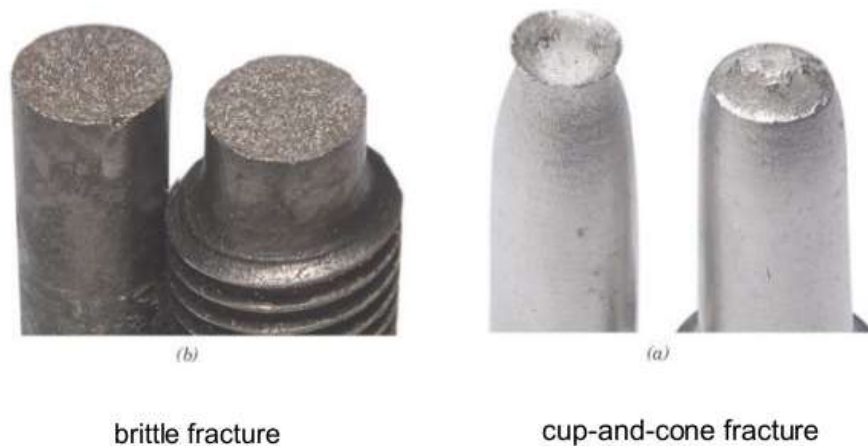
Figure 2. Photos of Tensile Specimens (Left) Brittle, (right) Ductile

Toughness is a measure of a material's ability to absorb energy before failure. Formally, the toughness is the integral under the stress-strain curve up to the fracture point. The Charpy Impact test is often used to determine the material toughness (or relative fracture performance) in the presence of notches and temperature changes. This test is illustrated in figure 3, along with typical result for steel and aluminum.

The figure also shows the temperature effect. Reducing the temperature below the "transition temperature" causes the material to change from ductile to brittle. For example, during World War II, Liberty Ships operating in the North Atlantic had failures due to brittle fracture because the water temperature was below the transition temperature of the material (Fig. 4).
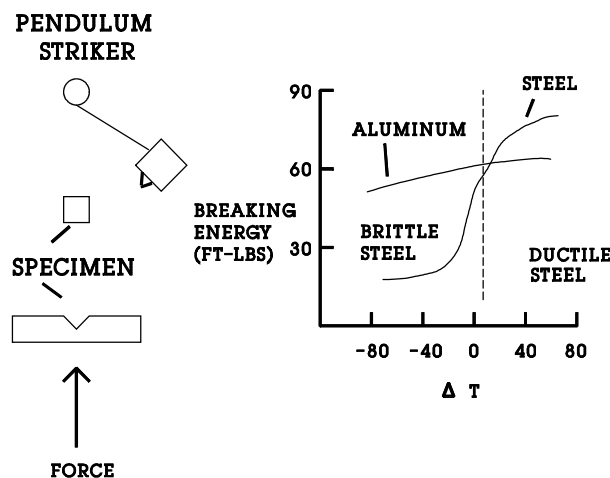
Figure 3: Charpy Impact Test

11 - 2
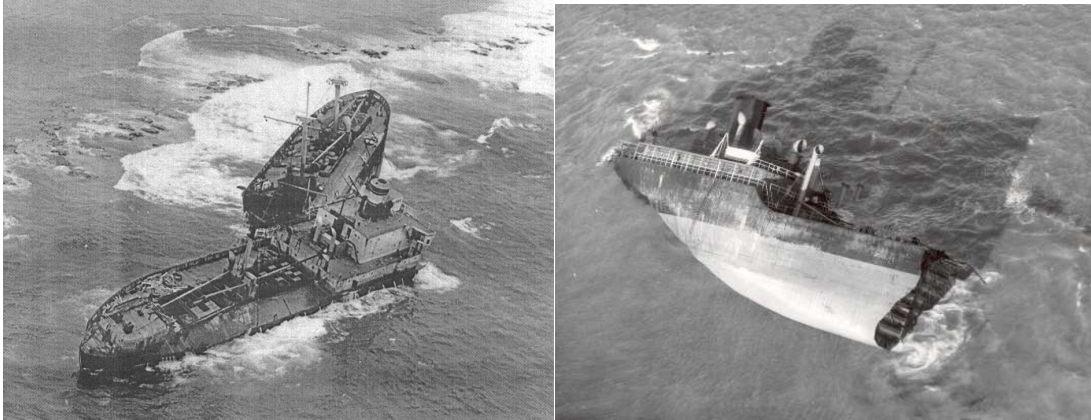
Figure 4. Fractured Hull of Liberty Ship

Brittle fracture is generally governed by the maximum tensile principal stress. A simple illustration is a piece of chalk in torsion (Fig 5). Here the plane of the principal tensile stress is at 45º to the axis of the chalk, and thus is the plane of the fracture.
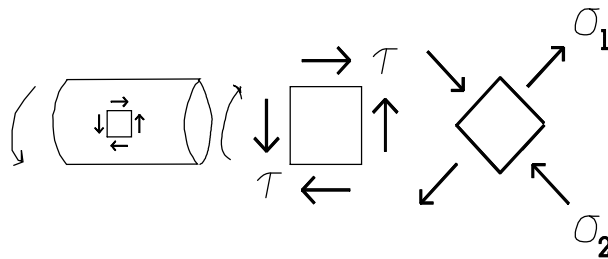
Fig 5: Principal Tensile Stress for Chalk in Torsion

11.2 Temperature Effects and Fracture Analysis Diagram

We have noted earlier in connection with the Charpy impact test that the fracture of steel is very sensitive to the testing temperature within certain temperature ranges. To illustrate this point further, consider a material with a certain crack size present. Below a certain temperature, called the Nil Ductility transition Temperature (NDT temperature), the fracture will be completely brittle in nature. At temperature greater than the NDT temperature, some plastic deformation will accompany the fracture and the fracture will be ductile to some degree. The stress required to cause brittle fracture will be less than that to cause ductile fracture in the same material and the fracture stress vs temperature behavior will be as indicated in figure 25 for a given crack size.

If we consider a number of crack sizes, we will generate a family of curves similar to that shown in figure 6. This leads to the Fracture Analysis Diagram. Such a diagram is shown in Figure 7 for a low carbon construction steel. The vertical axis in the fracture analysis diagram represents the operating stress and the horizontal axis represents the operating temperature, expressed as:

11 - 3

$$T = T_{NDT} + \Delta T \quad \text{therefore,} \quad T - T_{NDT} = \Delta T$$

with the origin denoting $\Delta T = 0$.
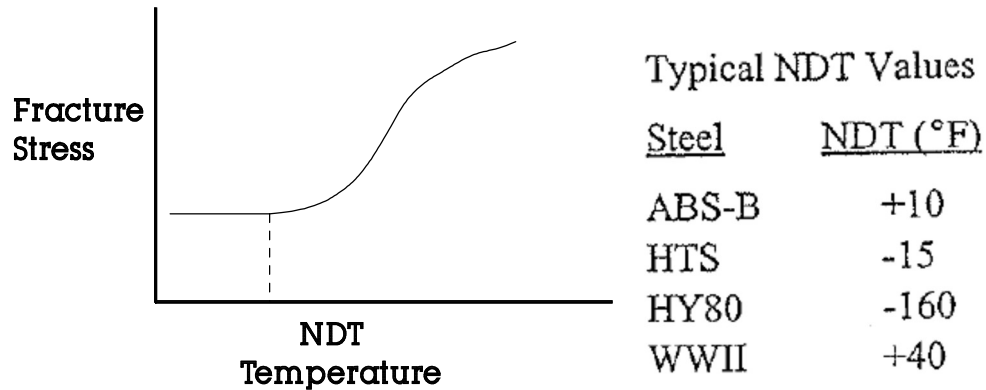
Figure 6 Illustration of Typical Fracture Behavior for Steels
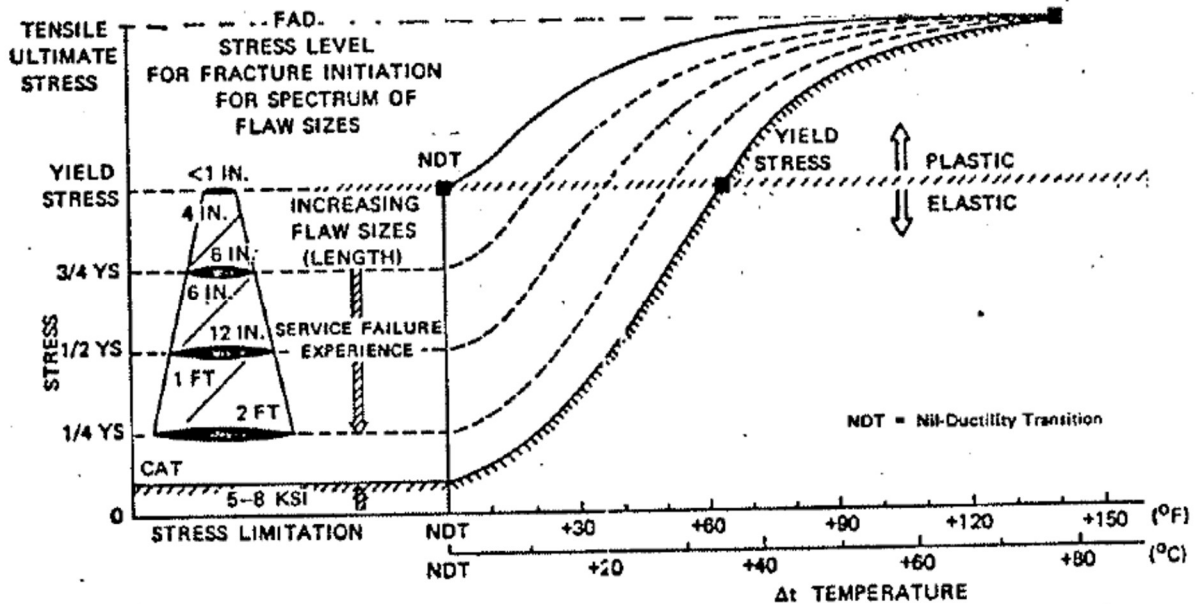
Figure 7: Fracture Analysis Diagram

Example. The walls of a submersible are to be made of a steel having a yield stress of 45 ksi. For this material, under a nominal stress of 30 KSI and an operating temperature of 35ºF, determine the NDT temperature where a "stress concentration factor" of 1.5 exists, if (a) 8 inch cracks are to be arrested and (b) if 12 inch cracks are to be arrested.

11 - 4

Solution. Because of the stress concentrations the operating stress will be (1.5)(30) = 45 ksi, which equals the yield stress. Reading horizontally across from the yield-stress value in Figure 28 to the intersection of the dotted curve for 8inch cracks we find the temperature NDT + 25. This must equal the operating temperature of 35ºF so the required NDT temperature is 10ºF. Similarly for 12 inch cracks, NDT = 0ºF.

Example. For a steel with an operating stress equal to 1/2 of the yield stress, determine the smallest crack size which could cause brittle fracture at 40ºF if the steel has a NDT of 15ºF.

Solution. Reading horizontally in Figure 28 at a stress level of 1/2 yield stress and vertically up from a temperature of NDT + 25ºF, we find the intersection at an interpolated fracture curve of about 18 inches. Hence cracks of 18 inches or longer would result in fracture.

11.3 Griffith Theory of Brittle Fracture.

Consider a thin plate of length l having a thru-crack of length 2c, as shown in figure 8.
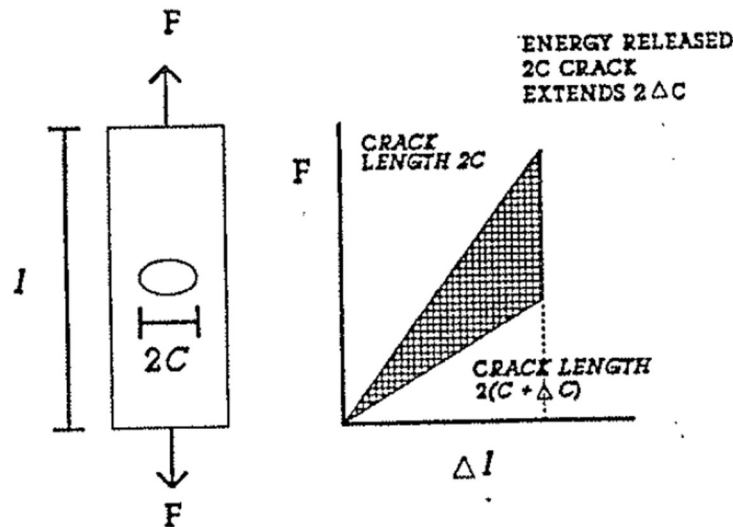
Fig. 8 Fracture with Thru Crack

For a non-extending crack of length 2c, the force-deflection curve will be as the upper curve shown in Figure 8. For a non-extending crack of length 2(c + Δc), the curve will be as the lower curve in Figure 8. The area between these curves thus represents the energy released as the crack extends from 2c to 2(c + Δc).

11 - 5

Using elasticity theory Griffith showed that the energy **released** per unit thickness during a crack growth of 2Δc is

$$\Delta w_e = \frac{2\pi\sigma^2}{E} c\Delta c$$

The creation of additional crack surface **requires** surface energy per unit thickness given by

$$\Delta w_s = 2\gamma_s(2\Delta c) = 4\gamma_s \Delta c$$

where γ_s is the surface energy per unit area.

Now, if $\Delta w_e < \Delta w_s$ the crack will not grow since the released energy will be less than that required to create a new surface.

11 - 6

If, on the other hand, $\Delta w_e \geq \Delta w_s$, crack growth will occur since adequate energy is available for creating the new surface. Hence for crack growth and subsequent failure we must have the condition

$$\frac{2\pi\sigma^2}{E} c\Delta c \geq 4\gamma_s \Delta c$$

The critical fracture stress σ_c is therefore

$$\sigma_c = \sqrt{\frac{2E\gamma_s}{\pi c}}$$

Thus, the critical stress is inversely proportion to $c^{\frac{1}{2}}$. Hence, the smaller the flaw, the greater the value of σ_c. (The entire concept of crack growth is based on the natural tendency for things (midshipmen included) to seek the lowest energy state available. Thermodynamically, there is a 'hump' which must be overcome in order for this to occur. In the case of crack propagation the energy supplied during the loading of the material must be sufficient enough to overcome the 'hump').

The Griffith theory is good for very brittle material, such as glass, in which no plastic deformation accompanies the fracture. When there is some plastic deformation associated with the crack extension, we must add the plastic work γ_p expended in making the surface to the surface energy term γ_s to obtain

$$\sigma_c = \sqrt{\frac{2E(\gamma_s + \gamma_p)}{\pi c}}$$

This formula forms the starting point for modern fracture mechanic analysis as discussed below.

11 - 7

11.4 Fracture mechanics of high-strength materials

High strength steels (yields stresses of 100,000 psi or greater) have a low toughness, and designs using theses materials must employ fracture mechanics methods of analysis to insure against failure by brittle fracture. Using the Griffith formulation, we define a new property of the material:

$$\sigma_c\sqrt{\pi c} = k_c$$

where K_c is known as the <u>fracture toughness</u> of the material and is equal to

$$k_c = \sqrt{2E(\gamma_s + \gamma_p)}$$

and has the units of

$$\frac{lbf}{inch^2}\sqrt{inch}$$

The quantity K_c can be measured in a simple test by simply measuring the size of an induced crack and measuring the resulting fracture stress, as shown in Figure 9(a). Figure 9(b) shows the effect of varying the thickness of the test plate. It will be seen that K_c falls of as plate thickness increases and reaches a constant value of K_{IC} at thickness t*. This critical thickness, t*, varies with the material under consideration but usually is 1/2 inch or less. In using equation for an interior crack, it is always conservative to take $K_c = K_{IC}$. The variation of K_{IC} with the yield strength for steels is illustrated in figure 10.

The <u>critical defect size</u> is

$$C_c = \frac{K_{IC}^2}{\pi\sigma^2}$$

where σ is the applied stress and $2C_c$ is the flaw or crack size needed for brittle fracture. For surface and interior cracks that do not extend through the plate thickness, we have the geometry shown in figure 11.

11 - 8

(a)   (b)
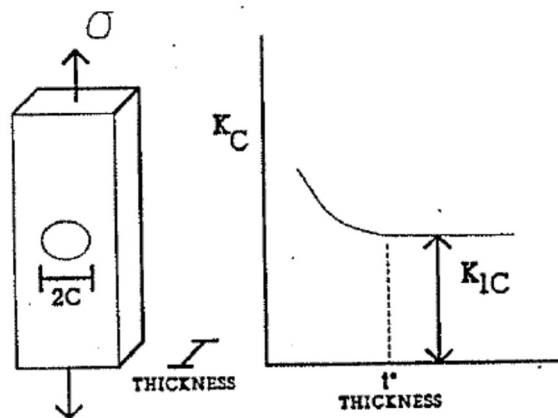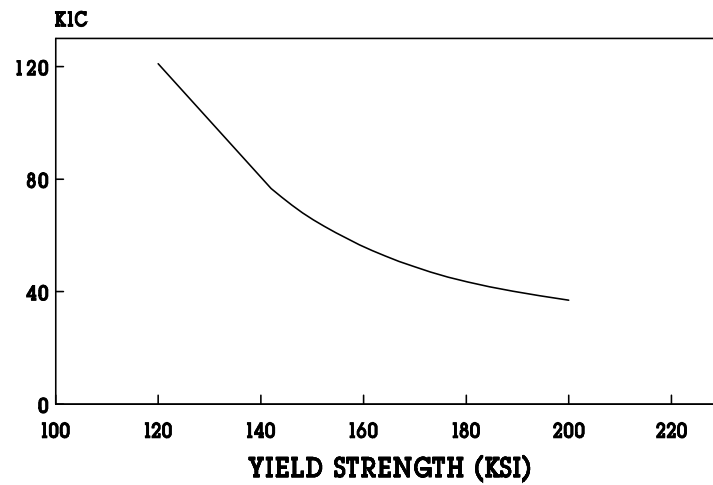
Figure. 9

Figure 10: Fracture Toughness vs Yield Strength for Steel
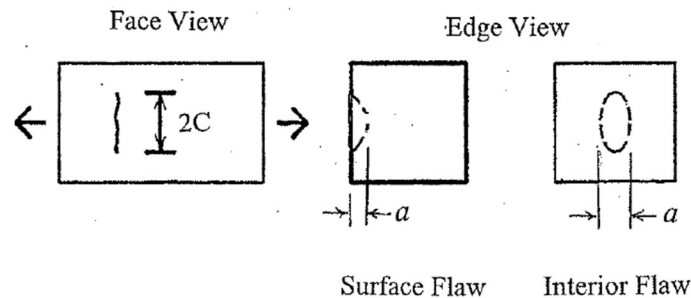
Fig. 11 Flaw Geometry

Typical Fracture-Toughness Values for Selected Engineering Alloys

Material	K_{IC}		$\sigma_{yield\ strength}$	
	MPa$\sqrt{m}$	ksi$\sqrt{in}$	MPa	ksi
Aluminum alloys:				
2024-T851	26.4	24	455	66
7075-T651	24.2	22	495	72
7178-T651	23.1	21	570	83
Titanium alloy:				
Ti-6A1-4V	55	50	1035	150
Alloy steels:				
4340 (low-alloy steel)	60.4	55	1515	220
17-7 pH (precipitation hardening)	76.9	70	1435	208
350 maraging steel	55	50	1550	225

11 - 9

Approximate formulas for the critical flaw size for cracks which do not initial extend thru the plate thickness are:

for a **surface crack**:

$$a_c = \frac{K_{IC}^2}{\pi\sigma^2}\left[\frac{\varphi^2 - 0.2(\sigma/\sigma_y)^2}{1.2}\right]$$

for an **interior crack**:

$$a_c = \frac{K_{IC}^2}{\pi\sigma^2}[\varphi^2 - 0.2(\sigma/\sigma_y)^2]$$

where φ depends on the ratio a/c as given below.

a/c	φ
0	1.0
0.2	1.05
0.4	1.15
0.6	1.28
0.8	1.42
1.0	1.57

Example. For a "thumb-nail" surface flaw, a/c = 0.4. Hence φ = 1.15. Suppose the operating stress to be equal to $\frac{1}{2}\sigma_y$, we thus have the critical flaw size for fracture given as

$$a_c = \frac{K_{IC}^2}{\pi\sigma^2}\left[\frac{(1.15)^2 - (0.2)(0.5)^2}{1.2}\right] = 1.06\frac{K_{IC}^2}{\pi\sigma^2}$$

Example. A pressure vessel is to be made using a steel with K_{IC} = 41 ksi - $(in)^{1/2}$ and σ_y = 220 ksi. Assuming surface cracks of 0.05 inches or less and $\sigma = \sigma_y$, determine whether the chosen material is adequate from fracture considerations.
  Assume first that a/c = 0.4 (thumb nail flaw). then φ = 1.15 and $\sigma = \sigma_y$, we have

$$K_{IC}^2 = \frac{1.2a_c\pi\sigma_y^2}{\varphi^2 - 0.2} = 8130$$

Hence K_{IC} = 90 ksi-$in^{1/2}$. But for the material, K_{IC} is only equal to 41 ksi-$in^{1/2}$. Thus fractures will occur for thumb-nail cracks.

Next assume a/c = 1.0; we then find that K_{IC} = 66 ksi-in$^{\frac{1}{2}}$. This is still higher than K_{IC} for the material. Hence to ensure against fracture, we must select a material with a greater fracture toughness or reduce the operating stress.

<u>*Example.*</u> *A pressure vessel has material properties σ_y = 65 ksi and K_{IC} = 35 ksi -in$^{\frac{1}{2}}$. If the diameter is 20 in and the wall thickness is 1 inch, determine the maximum pressure the tube can withstand before failure if thumbnail cracks of depth 0.1 inches exist.*
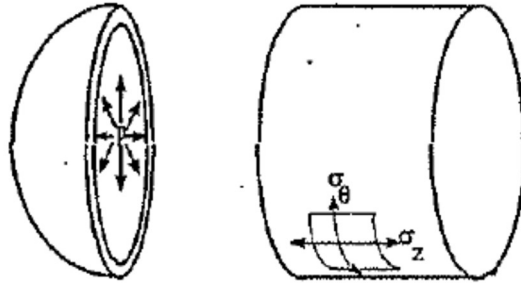
<u>*Solution:*</u>

$$\sigma_\theta = \frac{Pa}{t} = 10p, \ \sigma_z = \frac{Pa}{2t} = 5p$$

First check the maximum pressure required for yielding. The Mises condition gives

$$\sigma_\theta^2 + \sigma_z^2 - \sigma_\theta \sigma_z = \sigma_y^2$$

Hence
$$75p^2 = \sigma_y^2$$
and
p = 7.50 ksi (for yielding).

Next check the maximum pressure for fracture. Here only σ_θ enters since fracture is determined by the greatest tensile principal stress. We have

$$K_{ic}^2 \left[\varphi^2 - 0.2 \left(\frac{\sigma_\theta}{\sigma_Y} \right)^2 \right] = 1.2a\pi\sigma_Y^2 \left(\frac{\sigma_\theta}{\sigma_Y} \right)^2$$

$$1620 - 245 \left(\frac{\sigma_\theta}{\sigma_Y} \right)^2 = 1593 \left(\frac{\sigma_\theta}{\sigma_Y} \right)^2$$

$$\frac{\sigma_\theta}{\sigma_Y} = 0.939$$

11 - 11

Therefore, fracture will occur when $\sigma_\theta = 0.939\ \sigma_y$ or when $p = 0.1(0.939)\sigma_Y$ and $p = 6.10$ ksi which is before the yielding.

Example. A thin-walled cylindrical pressure vessel is to have a wall thickness of 0.5 inches and a radius of 10 inches. The material used has K_{IC} vs σ_y fracture characteristics as shown. Surface cracks in the material may be assumed no deeper than 0,025 inches. Select the appropriate σ_y value which will allow the greatest safe pressure loading. What is the pressure value?
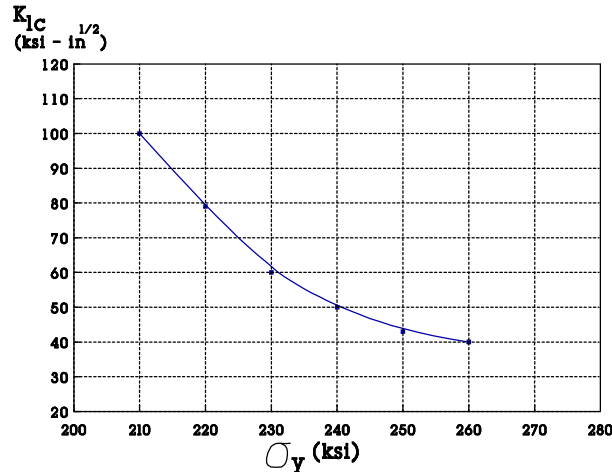
Solution:

Fracture Characteristics for Example

We assume thumbnail flaws with $a/c = 0.4$ and $\varphi = 1.15$. From the surface flaw equation we have

$$K_{ic}^2 = \frac{1.2a\pi\sigma_\theta^2}{\varphi^2 - 0.2(\frac{\sigma_\theta}{\sigma_y})^2}$$

From the Mises yield condition we also have

$$\sigma_\theta^2 + \sigma_z^2 - \sigma_\theta\sigma_z = \sigma_z^2$$

Therefore for yielding we have (with $\sigma_\theta = 20p$, $\sigma_z = 10p$)

$$p = 0.0577\sigma_y$$

Constructing the following table:

σ_y	P	σ_θ	K_{ic}	Remarks
200	11.55	231	68.8	too low
240	13.85	277	82.4	too high
220	12.69	254	75.6	ok

Thus at $\sigma_y = 220$ ksi the allowable pressure is 12.69 ksi.

11 - 12

11.5 Connection with Fracture Mechanics

The above results imply, in terms of modern fracture mechanics, that the "fracture toughness" (or critical stress intensity factor) varies with the relative temperature T - T_{NDT}. Such variation has been given in the ASME (American Society of Mechanical Engineers) Boiler and Pressure Vessel Code used in the design of such vessels.

This variation is shown in Figure 12 for steels used in pressure vessels such as containment vessels for nuclear reactors. (Yield stresses $\approx$ 50 - 70 ksi at room temperature). The values plotted are the <u>minimum</u> values from individual tests showing scatter.
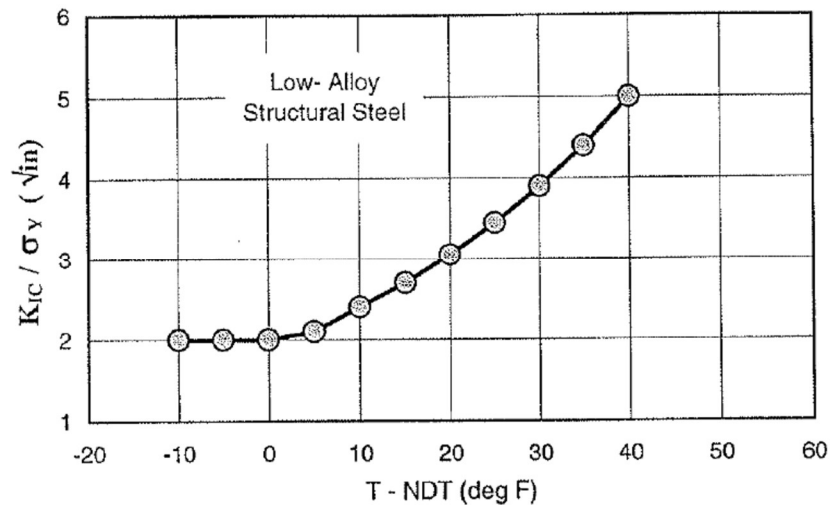
Figure 12. Variation in Fracture Toughness with Temperature

Using the above fracture toughness data ($K_{IC} = K_{IR}$), curves such as shown earlier on the Failure Analysis Diagram can be constructed for this steel using the thru-crack equation. (Fig 13)

$$\sigma = \frac{K_{IC}}{\pi\sqrt{C}}$$

11 - 13
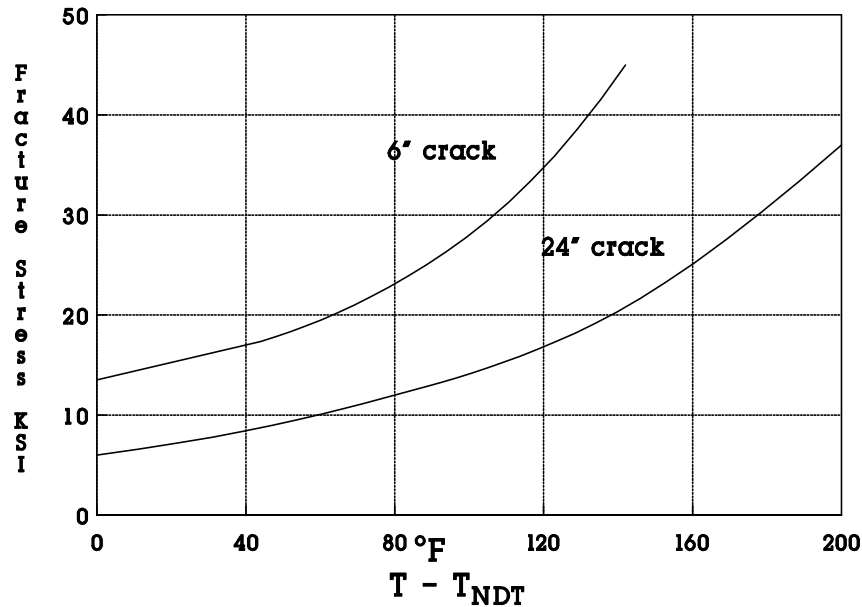
Figure 13: Fracture Toughness with Temperature

Example. *A confining vessel for a nuclear reactor is designed to withstand a net pressure of 2000 psi. The outside radius in 80 inches and the wall thickness is 9 inches. The material is steel with a yield stress of 40 ksi at an operating temperature of 500ºF. A hypothetical surface flaw is postulated (as part of the safety code requirements) with a depth of 1/9 the wall thickness and a length 2/3 times the thickness.*

> *(a) What is K_{IC}?*
> *(a) If the operating temperature is 500ºF, what is the required NDT?*
> *(b) What about at 300ºF?*

Solution. We have the equation

$$\sigma = \frac{K_{IC}}{\sqrt{\pi a}} [\frac{\varphi^2 - 0.2(\sigma - \sigma_y)^2}{1.2}]^{1/2}$$

The values of the crack dimensions are a = (1/9)(9) = 1 in and 2c = (2/3)(9) = 6. Therefore a/c = 0.33 and φ = 1.1. The stress is

$$\sigma = \frac{Pr}{t} = \frac{(2000)(80)}{9} = 17,800 (p.s.i)$$

or 17.8 ksi. Solving for K_{IC}, we find K_{IC} = 47.9 ksi $in^{1/2}$. From the curve of fracture toughness (figure 13) and the intersection of a horizontal line from σ = 17.8 KSI and the 6 inch curve, we then have T - $T_{NDT} \approx 55$

> *(a) for T = 500ºF we require T_{NDT}= 445ºF (or lower).*

11 - 14

(b) for T = 300ºF we require T_{NDT}= 2450ºF (or lower).

Initially T_{NDT} may be low (say -50ºF), but with radiation embrittlement it can increase to 250 - 350ºF over a 20 year period. If it has increased to 280ºF and a sudden cooling of the reactor water to 300ºF occurred, brittle fracture could result. This problem is very obviously one of great concern. This phenomenon is known as "pressurized thermal shock".

11.6 Stress Corrosion Cracking (SCC)

Stress corrosion cracking refers to the fracture of metals and alloys under tensile stress in a corrosive environment when the applied stress is below the yield stress for the material. The fracture does not occur immediately, but instead occurs after a finite amount of time. During this time localized corrosion, caused by a specific combination of electrolyte and metal, results in the formation of cracks. Continued corrosion and solid formation within the crack combine to, in effect, increase the applied tensile load. As shown in figure 14, the allowable stress decreases the longer the particular environment exists. The phenomenon can be expressed in terms of modern fracture mechanics in terms as follows: A "stress intensity" factor is defined for a thru crack as

$$K_q = \sigma\pi(c)^{\frac{1}{2}}$$

where σ is the applied stress and c is one-half the width of the crack. We have already seen that fracture will occur when $K = K_c$.
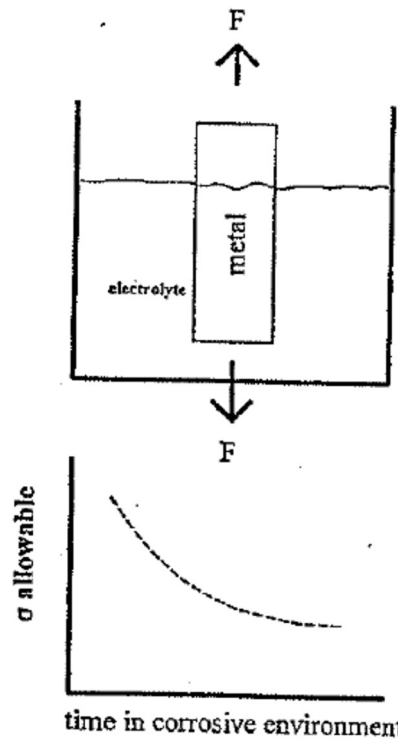
Figure 14: Stress Corrosion Cracking

Experiments have shown that with certain high-strength steels, as well as stainless steels and aluminum alloys, crack growth can occur when the material is under stress and in a corrosive environment. In this case, the stress intensity, which is a function of flaw geometry, can increase with time until it reaches the critical K_c value and failure occurs. If the stress intensity K is initially less than a critical value K_{scc} for the material, no crack growth will occur. This is illustrated in figure 15.
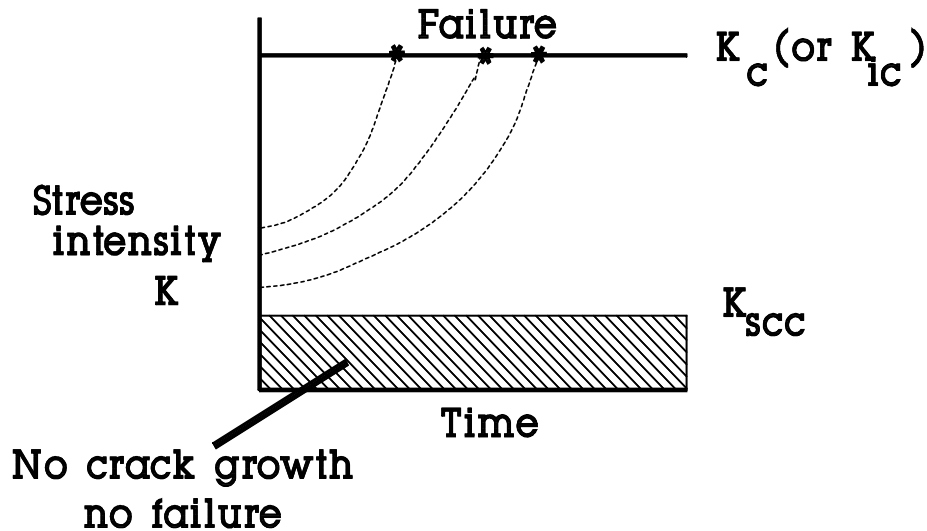
Figure 15: Stress Corrosion Cracking

11.7 Non-Destructive Testing

Nondestructive testing (NDT) methods are inspections for material defects, such as the cracks discussed in this chapter.

<u>External (Surface) Inspection Techniques</u>

The three most commonly used external (surface) inspection techniques currently in use are the Visual Test, Dye Penetrant Test, and Magnetic Particle Test.

- **Visual Testing (VT)** should be done during all phases of maintenance. It can usually be performed quickly and easily and at virtually no cost. Sometimes photographs are made as a permanent record. Visual inspections only allow the inspector to examine the surface of a material.
- **Dye Penetrant Testing (PT)** uses dyes in order to make surface flaws visible to the naked eye. It can be used as a field inspection for glass, metal, castings, forgings, and welds. The technique is simple and inexpensive and is shown schematically at Figure 5.10. Only surface defects may be detected, and great care must be taken to ensure cleanliness.

Underbead crack — Weld — Cleaned surface of a weld which has a crack in the heat-affected zone

Penetrant — Liquid penetrant is drawn into crack by capillary action

Trapped penetrant — After the surface is cleaned, penetrant remains trapped in the crack

Developer — Trapped penetrant — Developer is sprayed onto the surface

Indication of crack — Penetrant migrates from the crack, reacts with the developer, and causes a color change which identifies the crack location

The elements of the dye penetrant test, used to detect cracks that penetrate to the surface.

Fig 16: Dye Penetrant Testing

- **Magnetic Particle Testing (MT)** is only used on ferromagnetic materials. This method involves covering the test area with iron filings and using magnetic fields to align the filings with defects. Figure 17 shows the deformation of a magnetic field by the presence of a defect. Magnetic particle tests may detect surface and shallow subsurface flaws, and weld defects. It is simple and inexpensive to perform, however a power source is required to apply the magnetic field.
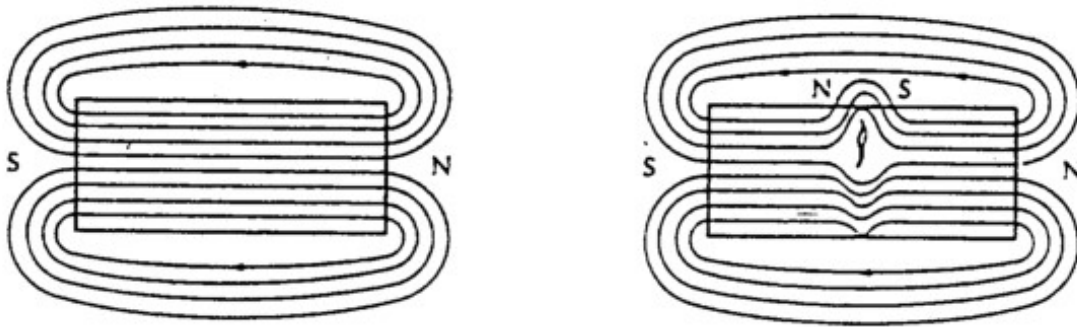
Figure 17 Magnetic Particle Testing

11 - 17

Internal (Sub-surface) Inspection Techniques

The three most common internal (subsurface) techniques are the Ultrasonic Testing, Radiographic Testing, and Eddy Current Testing.

- **Radiographic Testing (RT)** is accomplished by exposing photographic film to gamma or x-ray sources. This type of testing detects a wide variety if internal flaws of thin or thick sections and provides a permanent record. These methods of testing require trained technicians and present radiation hazards during testing.
- **Ultrasonic Testing (UT)** utilizes a transducer to send sound waves through a material. It may be used on all metals and nonmetallic materials. UT is an excellent technique for detecting deep flaws in tubing, rods, brazed and adhesive-joined joints. The equipment is portable, sensitive and accurate. Interpretation of the results requires a trained technician. Figure 18 shows an ultrasonic transducer configuration.
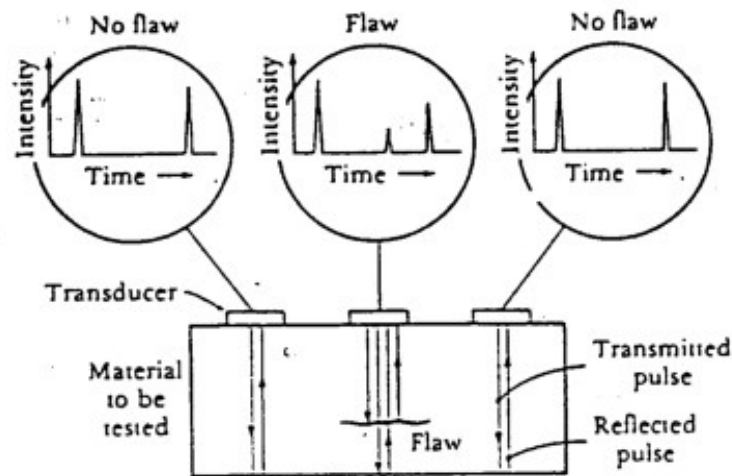
Figure 18 Ultrasonic Testing

- **Eddy Current Testing** involves the creation of a magnetic field in a specimen and reading field variations on an oscilloscope. It is used for the measurement of wall thicknesses and the detection of longitudinal seams and cracks in tubing. Test results may be affected by a wide variety of external factors. This method can only be used on very conductive materials, and is only good for a limited penetration depth. Once very common, it is being replaced by the increasing usage of ultrasonic testing.

Figure 19 summarizes these non-destructive testing techniques.

11 - 18

TEST	MEASURES	USED FOR	ADVANTAGES	LIMITATIONS
Visual Test (VT)	1. Finish 2. Surface Defects	ALL	1. Cheap 2. Easy, no Equipment Required	1. Only for surface defects 2. No quantitative result.
ROCKWELL HARDNESS	1. Hardness (Strength)	1. Testing the strength of metals	1. Non-destructive	1. Not exact value of Strength
RADIOGRAPHIC (RT)	1. Internal Defects 2. Density Variations	1. Welds 2. Forgings 3. Castings	1. Gives Permanent record. 2. Great Penetration 3. Good on most geometries 4. Portable 5. Sensitive to density variations	1. Costly 2. Radiation Hazard 3. Need highly skilled operators
DYE PENETRANT (DT)	1. Surface Defects 2. Porosities open to the surface	1. Welds 2. Forgings 3. Castings	1. Low COST 2. Portable 3. Easily interpreted	1. Surface defects only 2. Must clean surface before and after test
MAGNETIC PARTICLE (MT)	1. Surface, shallow subsurface flaws 2. Cracks and Porosities	1. Ferrous Materials 2. Forgings and Castings	1. Can locate very tight cracks which might not see with Dye 2. Low Cost 3. Fairly portable 4. Subsurface capability	1. Alignment of magnetic field is critical 2. Must demagnetize after the test 3. Must clean magnetic dust after test 4. Surface coating masks results.
EDDY CURRENT	1. Surface and shallow Subsurface defects 2. Alloy content	1. Tubes 2. Wires 3. Ball Bearings	1. High Speed 2. Automated 3. Gives Permanent Record	1. Need a Conductive material 2. Requires reference standard 3. Shallow defects only 4. Standard Geometry only
ULTRASONIC (UT)	1. Internal Defects 2. Material Thickness 3. Delaminations in Composites 4. Young's Modulus	1. Welds/Brazed Joints 2. Wrought Metals 3. Hull Thickness 4. In-Service Parts	1. Most sensitive to Cracks 2. Results known Immediately 3. Permanent record 4. Portable 5. High Penetration	1. Only on limited Geometries 2. Need Trained Operators

Fig. 19 Comparison of Non-Destructive Testing Techniques

11 - 19

CHAPTER 12

FATIGUE

12.1 Fatigue Failure of Materials
12.2 Fatigue Testing Procedures
12.3 S-N Fatigue Curves
12.4 Effect of Mean Stress using Goodman-Soderberg Relation
12.5 Stress concentrations
12.6 Miner's Rule for Fatigue Under Varying Stress Levels.
12.7 Fatigue Under Combined Stress
12.8 Specialized Formulae for Two Dimensions
12.9 Equivalent Stresses in Terms of Maximum Shear
12.10 Connection Between Fatigue and Failure.

12.1 Fatigue Failure of Materials

Fatigue failure of materials refers to their failure under the action of cyclic elastic stress. Fatigue generally involves the formation and gradual growth of cracks and ultimately to fracture as a result of reduced load carrying capacity.

Definitions. We consider uniaxial cyclic stress loading as shown below in figure 1.
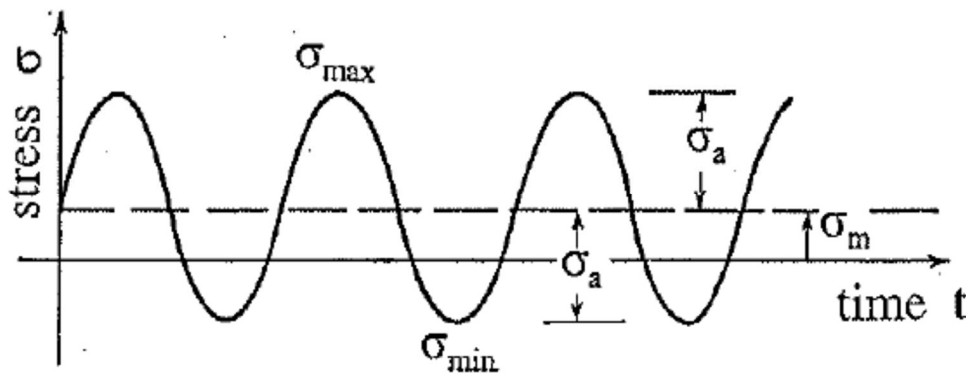
Figure 1: Definitions associated with cyclic stress

The mean stress σ_m and stress amplitude σ_a are defined as

$$\sigma_m = \tfrac{1}{2}(\sigma_{max} + \sigma_{min})$$
$$\sigma_a = \tfrac{1}{2}(\sigma_{max} - \sigma_{min})$$

When the mean stress σ_m equals zero we have completely reversed stress. The stress variation $\Delta\sigma_a$ is referred to as the range of stress. For sinusoidal loading, the stress-time relation is given simply as

12 - 1

$$\sigma = \sigma_m + \sigma_a \sin(2\pi/T)t$$

where T denotes the period of the stress cycle. The stress-time variation need not necessarily be sinusoidal for fatigue failure, though in many practical cases it is.

12.2 Fatigue Testing procedures

The are two basic testing procedures used to study fatigue: the Rotatory-Bending Test and the Deflection-Bending Test. These are illustrated in figure 2.

(a) Rotatory Bend   (b) Deflection Bend
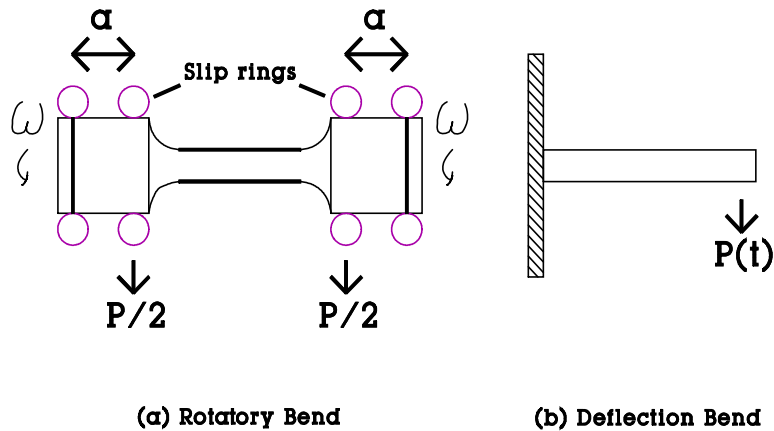
Figure 2: Fatigue Testing Procedures

In the rotatory-bending test, the internal moment M in the specimen between the slip-rings is constant and equal to pa/2. Therefore the maximum stress is

$$\sigma = \frac{My}{I} = \frac{(Pa)}{2} \frac{y}{I}$$

Where I denotes the moment of inertial of the cross-section about the neutral axis and y denotes the vertical distance from the section centroid. for a rotating beam with non-rotating forces, as in this case, y is related to the radius r of a ring of material by

$$y = r \sin\theta = r \sin (2\pi/T)t.$$
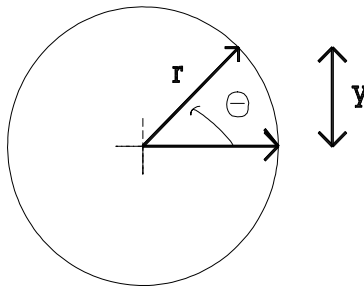
Figure 3: Coordinates for Rotary Bend Test

12 - 2

Taking r = R = outside radius, we have the stress in the rotating beam experiment given by

$$\sigma = \frac{MR}{I}\sin(\frac{2\pi}{T})t$$

Thus, the mean stress σ_m is zero and the amplitude is equal to MR/I.

In the case of the Deflection - Bending test, the tip of the cantilever beam is subjected to a sinusoidal force variation and we have (at the clamped end)

$$\sigma = \frac{P_o lC}{I}\sin(\frac{2\pi}{T})t$$

Where p_o is the amplitude of the applied force, l is the length of the beam, and C the distance from neutral axis to outer surface. Again the mean stress σ_m is zero and the amplitude σ_a is given as $P_o lC/I$.

12.3 S-N Fatigue Curves.
Using this test, the stress amplitudes associated with fatigue failure after N cycles can be determined and plotted as shown for the case of steel in Figure 4.
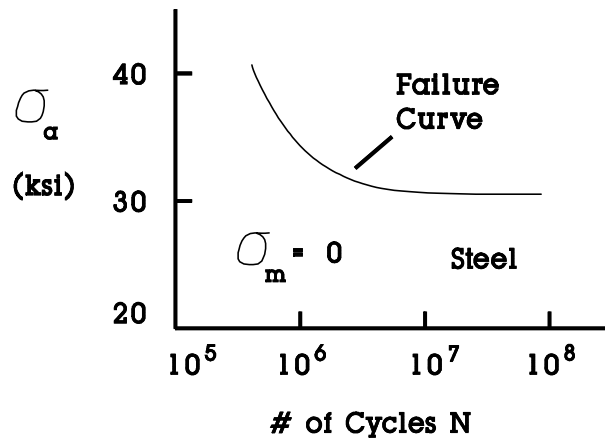
Figure 4: Example S-N Curve for Steel

The curve of figure 4 is sometimes referred as the S-N curve. We denote the value of σ_a for failure after N cycles as σ_N. Note that for steels, there is a stress level below which no failure is observed. This is known as the <u>endurance limit</u>. It generally does not exist for other materials such as aluminum, etc. Figure 5 shows a comparison of two S-N curves for steel, with an endurance limit, and aluminum, without an endurance limit.

12 - 3
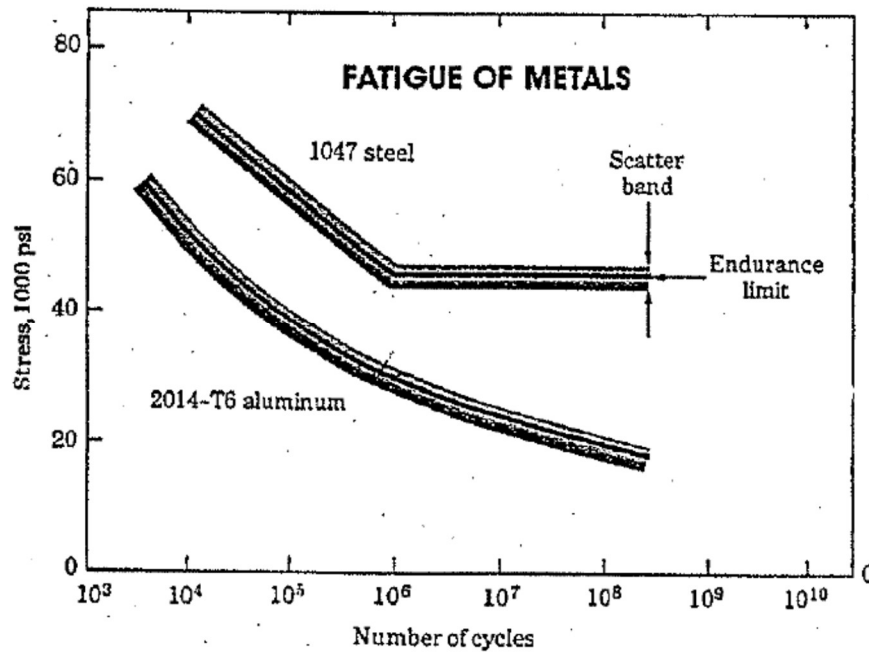
Figure 5: Comparison of Aluminum and Steel SN curves

It is to be emphasized that fatigue failure can occur even though the stress never exceeds the elastic limit of the material. In the elastic range, the fatigue failure usually occurs after 10^5 cycles of stress (high cycle fatigue). For large stresses causing plastic deformation, much fewer cycles of stress are needed for failure (low cycle fatigue). In low-cycle fatigue, the strain vs. number of cycles is plotted, since the calculation of stress by elastic formulas is no longer valid.

12.4 Effect of mean stress using Goodman-Soderberg Relation

The effect of mean stress on modifying the stress amplitude σ_a needed for failure after N cycles is estimated using the Goodman-Soderberg relation. This assumes that when the mean stress equals the failure stress σ_u of the material, the additional stress amplitude σ_a for failure after N cycles is zero. It also uses the fact that the stress amplitude for failure at N cycles will be that from the usual S-N curve (σ_N) when the mean stress is zero and it assumes a linear relation between these two extremes as shown in figure 6.

$$\sigma_a = \sigma_N - \frac{\sigma_N}{\sigma_u}|\sigma_m|$$

12 - 4

$$\sigma_a = \sigma_N - \frac{\sigma_N}{\sigma_u}|\sigma_m|$$
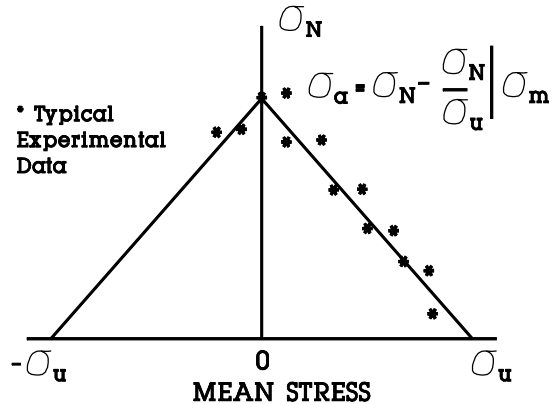
Figure 6: Mean stress effect on fatigue strength. The solid line denotes predictions from the Goodman-Soderberg relation

Example. A rod of 0.5 in² is subjected to static mean tensile load of 10 kips. What fatigue stress amplitude σ_a will produce failure after 10^6 cycles? Assume $\sigma_n = 32$ ksi, $\sigma_u = 60$ ksi.

Solution. We have $\sigma_m = 10/.5 = 20$ ksi. The Goodman-Soderberg relation then give

$$\sigma_a = \sigma_n - \frac{\sigma_n}{\sigma_u}|\sigma_m| = 32 - \frac{32}{60}20 = 21.3 \; ksi \; thus \; F_A = 21.3 \; ksi$$

12.5 Stress Concentrations.

In the case of a hole, fillet (a welding term), or other geometric differences, the applied stresses tend to concentrate and we must account for this. Letting k_s be the <u>static stress concentration factor</u>, we have:

$$\sigma_a = k_s\sigma_\varphi$$

where σ_a = the actual tensile stress and σ_φ = the nominal or applied stress.

In the case of fatigue, we have a fatigue strength reduction factor k_f such that

$$\sigma_{N\varphi} = \sigma_N/k_f$$

where $\sigma_{N\varphi}$ = the maximum allowable stress at N cycles and σ_N = the strength at N cycle regardless of the fatigue strength reduction factor (from the S-N curve).

As a result the Goodman-Soderberg relation can now be written as

$$\sigma_a = \frac{\sigma_N}{k_f} - \frac{\frac{\sigma_N}{k_f}}{\frac{\sigma_u}{k_s}}|\sigma_m| = \sigma_{N\varphi} - \frac{\sigma_{N\varphi}}{\frac{\sigma_u}{k_s}}|\sigma_m|$$

12 - 5

Example. A threaded steel rod of 2 in root diameter is subjected to a mean stress of 20 ksi and a variable stress σ_a. Determine the allowable σ_a if σ_N = 300 ksi, σ_u = 60 ksi, k_s = 2.0, and k_f = 1.5.

Solution. Using the Goodman-Soderberg relation,

$$\sigma_a = \frac{30}{1.5} - \frac{\frac{30}{1.5}}{\frac{60}{2.0}}20 = 6.7 \; ksi$$

12.6 Miner's Rule for Fatigue Under Varying Stress Levels.

Suppose a material is subjected to n_1 cycles of stress at stress amplitude σ_1 and n_2 cycles at amplitude σ_2, etc. Miner's Rules states that

$$\frac{n_1}{N_1} + \frac{n_2}{N_2} + \dots \frac{n_i}{N_i} = \sum_{i=1}^{i=\infty} \frac{n_i}{N_i} = 1$$

where n_i = number of cycles at a particular stress and N_i = the fatigue life at that stress. figure 7 shows the relationship between allowable stress σ_N and N cycles.
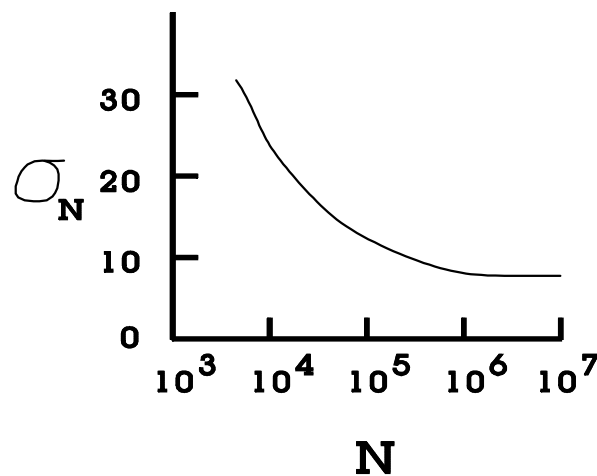
Figure 7: Example S-N curve

12 - 6

Example. A beam is subjected to 5×10^2 reversed cycles of stress at $\sigma_1 = 30$ ksi. How many additional cycles can the beam withstand at stress $\sigma_2 = 20$ ksi? ($N_{30ksi} = 10^4$, $N_{20ksi} = 10^5$).

Solution:

$$\frac{5 \times 10^2}{10^4} + \frac{n_2}{10^5} = 1 \qquad n_2 = 5 \times x10^4$$

Example. An off-shore structure is subjected to reversed stress loading by surface waves as shown in the table. Determine the total number of waves for failure.

σ (ksi)	30	20	10	
N		10^4	10^5	10^6
% of waves	**5%**	**15%**	**80%**	

From Miner's Rule

$$\frac{0.05N}{10^4} + \frac{0.15N}{10^5} + \frac{0.80N}{10^6} = 1 \quad N = 1.37 \times 10^5 \, Waves$$

Example. Suppose that in the previous example, the periods of the waves associated with σ_1, σ_2, and σ_3 are 5, 3, and 1 seconds respectively. Determine the life of the structure.

Solution. If T equals the life of the structure in seconds, we then have

$T = (0.05N)(5) + (0.15N)(3) + (0.80N)(1)$
$T = 2.055 \times 10^5 \, sec = 57.08 \, hours$

12.7 Fatigue Under Combined Stress.

The above considerations have been limited to fatigue under the action of a single stress component. To handle fatigue under combined stress, we use a Mises-type condition as in the case of yielding. For the case where the mean stress of each principal stress component is zero and the amplitudes of the principal stresses are σ_{1a}, σ_{2a}, and σ_{3a} we have

$$(\sigma_{1a} - \sigma_{2a})^2 + (\sigma_{2a} - \sigma_{3a})^2 + (\sigma_{3a} - \sigma_{1a})^2 = 2\sigma_N^2$$

(This formula is merely resolving the magnitude of the combined Von Mises stress)

Example: *If σ_N = 30 ksi, for failure after 10^6 cycles, determine the amplitude of a completely reversed shear stress for failure after 10^6 cycles.*
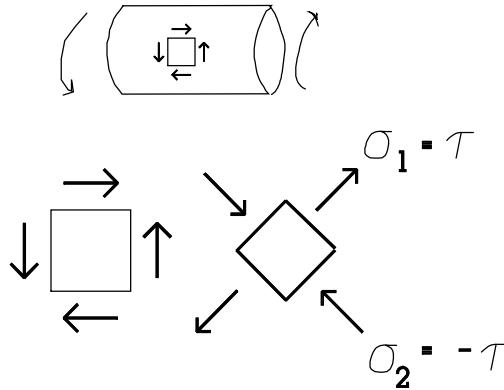
Solution: *The principal stresses are: σ_{1a} = τ_a, σ_{2a} = -τ_a, σ_{3a} = 0. Substituting into the above relation we have*

$$\tau_a = \frac{1}{\sqrt{3}}\sigma_N = 17.3 \ ksi$$

Next consider the more complex case of the non-zero mean stresses σ_{1m}, σ_{2m}, σ_{3m} together with amplitudes σ_{1a}, σ_{2a}, σ_{3a}. From the Mises-type relation we then define

$$\sigma_m^* = \frac{1}{\sqrt{2}}[(\sigma_{1m} - \sigma_{2m})^2 + (\sigma_{2m} - \sigma_{3m})^2 + (\sigma_{3m} - \sigma_{1m})^2]^{1/2}$$

$$\sigma_a^* = \frac{1}{\sqrt{2}}[(\sigma_{1a} - \sigma_{2a})^2 + (\sigma_{2a} - \sigma_{3a})^2 + (\sigma_{3a} - \sigma_{1a})^2]^{1/2}$$

where σ_m^* is the resolved mean stress and σ_a^* is the resolved stress amplitude. Substituting into the Goodman-Soderberg relation,

$$\sigma_a^* = \sigma_N - \frac{\sigma_N}{\sigma_u}\sigma_M^*$$

We thus obtain an equation relating the "equivalent" stress amplitude σ_a^* to the "equivalent mean stress σ_M^*.

Example. *A rod of circler cross section is subjected to tension and torsion such that the tension stress is constant and equal to 20 ksi and a shear stress which cyclically varies from 0 to S. If σ_N = 40 ksi for failure after 10^6 cycles, determine the allowable value of S for failure after this number of cycles. Assume σ_u = 80 ksi.*
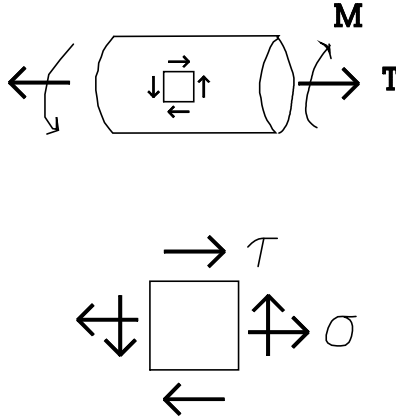
Solution.

The mean and amplitude stresses are σ_m = 20 ksi, σ_a = 0, τ_m = S/2, and τ_a = S/2. We also have the principal stress formula

$$\sigma_{1,2} = \frac{\sigma}{2} \pm \sqrt{\left(\frac{\sigma}{2}\right)^2 + \tau^2}$$

Substituting for the "equivalent" mean stress $\sigma_m{}^*$ and the stress amplitude $\sigma_a{}^*$ we find

$$\sigma_{1m} = 10 + \sqrt{100 + \left(\frac{S}{2}\right)^2} \quad \sigma_{2m} = 10 - \sqrt{100 + \left(\frac{S}{2}\right)^2}$$

$$\sigma_{1a} = \frac{S}{2} \quad \sigma_{2a} = -\frac{S}{2}$$

Using the Goodman-Soderberg relation we find

$$\sigma_m^* = \frac{1}{\sqrt{2}}\left(800 + \frac{3}{2}S^2\right)^{\frac{1}{2}} \quad \sigma_a^* = \frac{1}{\sqrt{2}}\left(\frac{3}{2}S^2\right)^{\frac{1}{2}} = \sqrt{\frac{3}{4}}S$$

$$\sqrt{\frac{3}{4}}S = \sigma_N - \frac{\sigma_N}{\sigma_u}\frac{1}{\sqrt{2}}\left(800 + \frac{3}{2}S^2\right)^{\frac{1}{2}}$$

With the above values of σ_N and σ_u, this reduces to

$$S^2 - 123.2S + 2669 = 0$$

The solutions to which are

$$S = 28 \text{ ksi}, S = 95.2 \text{ ksi}$$

to decide which root is appropriate, again consider the Goodman-Soderberg relation

$$\sigma_a^* = \sigma_N - \frac{\sigma_N}{\sigma_u}\sigma_m^*$$

Taking $\sigma_a = (3/4)^{\frac{1}{2}}S$ and solving for σ_m with $S = 28$ ksi, we find that $\sigma_m = 31.5$ ksi. For $S = 95.2$ ksi we find that $\sigma_m = - 84. 9$ ksi. Since σ_m must be positive in the Goodman-Soderberg relation, the only acceptable solution is $S = 28$ ksi.

Example. A proposed scuba air bottle may be idealized as a closed cylinder of 8 in. diameter with a wall thickness of 0.10 inches. Determine the maximum safe internal pressure loading for 10^4 cycles of loading if $\sigma_N = 30$ ksi and $\sigma_u = 60$ ksi.

Solution. We assume the pressure varies from 0 to P during a cycle of loading. We have

$$\sigma_\theta = \frac{Pa}{t} = 40P = \sigma_1 \quad \sigma_z = \frac{Pa}{2t} = 20P = \sigma_2$$

Hence

$$\sigma_{1m} = 20P, \sigma_{2m} = 10P$$
$$\sigma_{1a} = 20P, \sigma_{2a} = 10P$$

The equivalent σ_m^* and σ_a^* stresses are

$$\sigma_m^* = \sigma_a^* = 17.32P$$

Substituting into the Goodman Soderberg relation

$$17.32P = 30 - (30/60)(17.32P) \text{ or } P = 1.15 \text{ ksi}$$

12.8 Specialized Formulas for Two-Dimensions

The equivalent stress formulas are in terms of principal stresses. For two-dimensional stress problems, it is convenient to express the formulas in terms of non-principal stress components. Those relations may be written as:

$$\sigma_m^* = [\sigma_{xm}^2 + \sigma_{ym}^2 - \sigma_{xm} \sigma_{ym} + 3 \tau_m^2]^{1/2}$$

$$\sigma_a^* = [\sigma_{xa}^2 + \sigma_{ya}^2 - \sigma_{xa} \sigma_{ya} + 3 \tau_a^2]^{1/2}$$

Example Use the above relations to solve the problem of the earlier example where a rod is

subjected to a constant tensile stress of 20 ksi and a cyclic shear stress between 0 and S, with the value of S required for failure after 10^6 cycles.

Solution: With $\sigma_m = 20$ ksi $\sigma_a = 0$ $\tau_m = S/2$ and $\tau_a = S/2$, we find directly

$$\sigma_m^* = \frac{1}{\sqrt{2}}(800 + \frac{3}{2}S^2)^{\frac{1}{2}}$$

$$\sigma_a^* = \frac{1}{\sqrt{2}}(\frac{3}{2}S^2)^{\frac{1}{2}} = \sqrt{\frac{3}{4}}S$$

And the Goodman-Soderberg relation then provided the relation

$$\sqrt{\frac{3}{4}}S = \sigma_N - \frac{\sigma_N}{\sigma_u}\frac{1}{\sqrt{2}}(800 + \frac{3}{2}S^2)^{\frac{1}{2}}$$

The solution for S is 28 ksi, as before.

12.9 Equivalent Stresses in Terms of Maximum Shear

The maximum shear condition, introduced earlier in connection with yielding, may also be used in place of the Mises condition to define equivalent stresses. With $\sigma_1 > \sigma_2 > \sigma_3$, we have the relations

$$\sigma_m^* = \left| \sigma_{1m} - \sigma_{3m} \right| \tag{42}$$

$$\sigma_a = \left| \sigma_{1a} - \sigma_{3a} \right| \tag{43}$$

Example : Use the above relations to solve the problem of Example 1 where a rod is subjected to constant tensile stress of 20 ksi and a cyclic shear stress between 0 and S, with the value of S required for failure after 10^6 cycles.

Solution: From Example 1, we have the principal stresses

$$\sigma_{1m} = 10 + \sqrt{100 + (\frac{S}{2})^2} \qquad \sigma_{3m} = 10 - \sqrt{100 + (\frac{S}{2})^2}$$

$$\sigma_{1a} = \frac{S}{2} \qquad \sigma_{3a} = -\frac{S}{2}$$

Hence, from equations (42) and (43)

$$\sigma_m^* = 2\sqrt{100 + \left(\frac{S}{2}\right)^2} \qquad\qquad \sigma_a^* = S$$

Substitution into the Goodman-Soderberg relation of equation (39), we then find

$$S = \sigma_N - 2\frac{\sigma_N}{\sigma_U}\sqrt{100 + \left(\frac{S}{2}\right)^2}$$

The solution of this equation is $S = 24$ ksi , which is somewhat less than the value of $S = 28$ ksi found in Example 1 using equivalent stresses based on the Mises condition. As in the case of yielding prediction, the maximum shear condition provides a conservative estimate to the more accurate Mises formulation.

12.10 Connection Between Fatigue and Failure.

We have previously noted that fatigue failure ultimately results from the growth of small cracks and flows with cyclic loading until such time that the cracks are of such size that fracture occurs. It is of interest to establish a quantitative relationship to describe the crack growth. Experimental measurements indicate a relation of the form

$$\frac{da}{dN} = C(\Delta k)^n$$

where a denotes crack size after N cycles of stress, C and n denote constants and Δk, for a thumb-nail surface flaw is given approximately by

$$\Delta k = \Delta\sigma\sqrt{\pi a}$$

$$\frac{da}{dN} = c(\Delta\sigma\sqrt{\pi a})^n$$

Example. A structural member contains surface flaws of initial depth 0.01 inches. Determine the life of the member in cycles if it is repeated loaded from 0 to 70 ksi. Assume $K_{IC} = 90$ ksi - $(in)^{1/2}$, n = 2, and C= 4 x 10^{-10} (ksi²-cycle)^{-1}.

Solution.

$$\frac{da}{dN} = C(\Delta\sigma)^2\pi a$$

$$\int_{a_o}^{a_c} \frac{da}{a} = \int_0^N C(\Delta\sigma)^2\pi \; dN$$

$$ln(\frac{a_c}{a_o}) = c(\Delta\sigma)^2\pi N$$

Since Δσ = 70 ksi, a_o = the initial crack depth, and a_c denotes the crack depth at fracture and is given by

$$a_c = \frac{K_{1C}^2}{\pi\sigma_{max}^2} = \frac{90^2}{\pi 70^2} = 0.526 inches$$

using this value we thus find that with a_c/a_u = 52.6, N = 6.4 x 10^5 cycles.

Table of Value
(units of kips, inches)

Material	n	C
mild steel	3	3.6×10^{-10}
High strength steel	2.25	6.6×10^{-9}

CHAPTER 13

WOOD

13.1 Directionality (isotropy)
13.2 Mechanical Properties
13.3 Typical Uses in the Marine Environment
13.4 Structural Analysis Equations
13.5 Fastening
13.6 Control of Degradation
13.7 Plywood

Wood has been used as a shipbuilding and offshore structure material since the earliest days of each industry. The USS *Constitution* and the Standard Oil Company's California Rig #1 are both examples of wood's long-term presence in the industry. On the shipbuilding side, over 40,000 wooden ships and small craft were built for the US Navy in WWII. The last Navy wooden-hull purchases were the YP's in the '80's and the Avenger-class minesweepers (Figure 1) in the '90's. At 224 feet, the Avengers are the longest wooden hulls built for the Navy.

Figure 1: USS *Chief*, Avenger-class wooden minesweeper
Commissioned in 1994

Although it is unlikely that the Navy will ever again purchase wooden hulled vessels (mostly because of high initial costs compared to composites), wood's properties make it a viable material for structural use in the Navy for many years to come. In EN380 we will briefly explore these properties.

First is a description of the microscopic properties. Wood consists mainly of hollow fiber cells (sort of like short soda straws) made of lignin and cellulose (Figure 2). The lignin acts as an adhesive holding the cells together. The cellulose is a fibrous material that is hygroscopic, or attracts water like a sponge. (And just like a sponge, wood will swell when moist.) The lignin is very strong, so much so that wood typically fails by crushing of the cellulose structure rather than failure of the lignin.

13 - 1
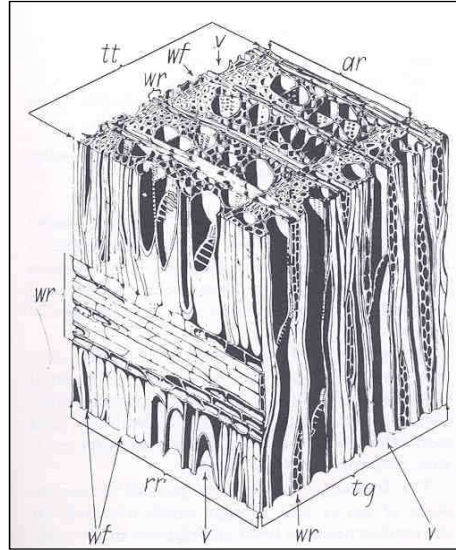
Figure 2: Wood microstructure – tt = tg = transverse, rr = radial, wr = wood ray

Wood is typically grouped into two classes: hardwoods and softwoods, although unfortunately there is no correlation between these terms and the wood's surface hardness. Hardwoods have broad leaves and small fiber (cell) sizes (about 0.01" diameter and 0.05" length). Softwoods are conifers (have cones) and large cell sizes (0.05" x 0.13"). Balsa and oak are hardwoods, Douglas fir, pine and cedar are softwoods.

13.1 Directionality (isotropy)

Continuing the soda straw analogy will explain wood's directional properties. If a soda straw is held in the hand and squeezed between two fingers, the straw's wall crushes. This is the *radial* direction of the wood and like the straw it is not very strong. If the straw is held between the hands in the long direction and pulled or pushed, it is strong as long as it does not buckle. This is the *longitudinal (axial) or with-the-grain* direction of the wood and is its strongest direction. The last property direction is the *tangential or hoop* direction. This direction can be visualized by the pressure built up in a straw if one end is capped and the other is blown in to. If the straw splits (or "checks"), it is a tangential failure, and this is typically the weakest of wood's three directions. The radial direction is slightly stronger than the tangential direction due to the presence of wood "rays" (wood fibers). Few species have rays in the tangential direction, but those that do are highly preferred in marine construction due to the increased splintering resistance. The most notable are Sitka Spruce, Live Oak, and Black Locust. The last two are fairly rare. On an historical footnote, the 1797 frigates were specified for Live Oak frames and planking. Due to a shortage, only two were built using Live Oak rather than the inferior White Oak. One of those was the *Constitution*.

In material science, a material which has the same properties in all directions is *isotropic* (metals are <u>usually</u> considered isotropic). One which has different properties in every direction is *anisotropic*. If it has the different properties in three perpendicular planes it is *orthotropic* (composites are orthotropic). If one of the planes has the same material

13 - 2

properties in all directions it is *transversely isotropic* (an example is a single fiber in a resin). These terms are important when using Hooke's Law. Wood is technically anisotropic but is usually modeled as transversely isotropic. Composites are technically orthotropic but are also modeled as transversely isotropic. Analytically, wood and composites share many characteristics.

The three directional properties of wood vary widely, but in general, if a wood species has a longitudinal strength of 100, its radial strength will be about 5-10 and its tangential strength about 2-10. Given the large difference in properties it is clear that making sure the load is arranged with the grain is critical to a structure's success! This is often not easy as most trees do not grow perfectly straight and lumber mills do not usually cut lumber for maximum strength.

Figure 3 shows a typical log undergoing the milling process. Depending on what part of the log the plank comes from it will have dramatically different properties when exposed to moisture. The "A" plank is quartersawn (or vertical grain – VG). This cut goes through the tree's center and gives planks that are warp stable. (See Figure 4.) Another advantage to this cut is that it minimizes the weakest hoop direction fibers. The major disadvantage is that if small trees are used, planks of a useful width for marine construction will often include sapwood, the outer rings that are rot prone. Plainsawed planks of low density woods like pine, fir and cedar will often warp as much as a plank thickness. The bottom line is that for any structural application exposed to moisture, quartersawn heartwood is specified.
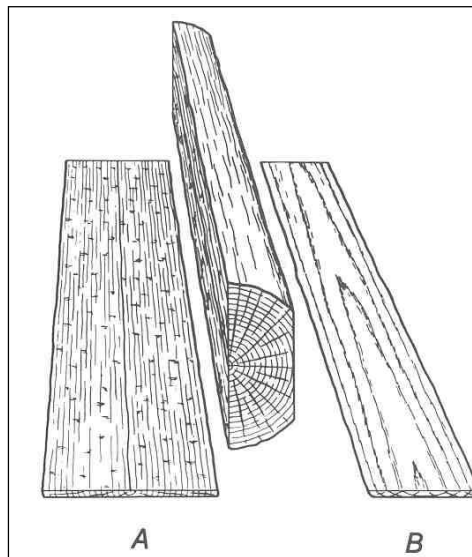
Figure 3: Quartersawed (A) and plainsawed (B) boards cut from a log. (From Ref. 2)

13 - 3
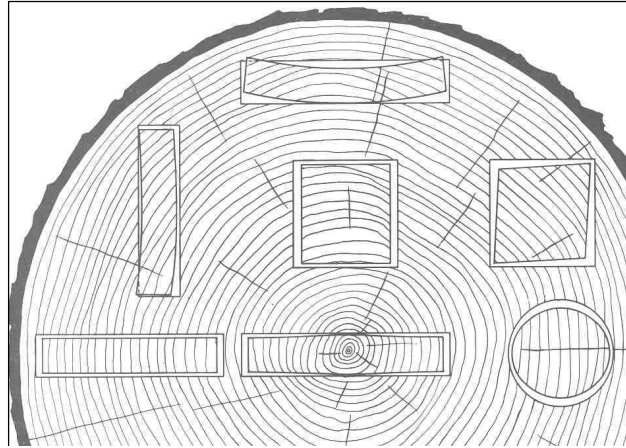
Figure 4: Distortion due to sawing location of planks from the log. (From Ref. 2)

13.2 Mechanical Properties

Material properties of wood are generally given for the longitudinal direction and are presented for a *standard moisture content of 12%*. Radial and tangential properties are occasionally given but are usually estimated from the previously mentioned ratio's. If given, then usually the tangential, being lower, is given. "*Green wood*", where the moisture content is above 18%, generally has strength properties about ½ of the dry wood properties. Wood can be "green" either because it has not dried sufficiently after harvesting, or because of exposure to water after construction. As the structures designed by naval architects and ocean engineers are often in a wet environment, it is also important that they understand what will be the equilibrium moisture content of the wood in their designs! The equation for moisture content is:

$$MC = \frac{wet\,weight - oven\,dry\,weight}{oven\,dry\,weight}$$

Table 1 shows the material properties for common woods used in ships and offshore structures. Tensile properties parallel to the grain are usually taken as equal to the compressive strength, although they are typically higher.

13 - 4

Species	green specific gravity	dry specific gravity	flexural strength psi	tensile strength* psi	compressive strength psi	modulus of elasticity msi
douglas fir	0.45	0.48	12,200	340	7,430	1.95
white oak	0.6	0.68	15,200	800	7,440	1.78
western red cedar	0.31	0.32	7,500	220	4,560	1.11
sitka spruce	0.37	0.4	10,200	370	5,610	1.57
mahogany	0.45	0.45	11,500	-	6,780	1.5
teak	0.55	0.55	14,600	-	8,410	1.55
lignumvitae	1.05	1.06	-	-	11,400	-
*tangential						
all properties are for oven dry samples						

Table 1: Mechanical Properties of Common Woods used
in the Marine Environment (from Refs. 1 & 2)

13.3 Typical Uses in the Marine Environment

Apart from recreational craft, wood is still commonly used in fishing vessels and other small commercial vessels worldwide. Its natural buoyancy, abundancy, and ability to be worked with simple tools lend itself to marine construction in developing countries. It has significant disadvantages for large commercial and naval applications however, including:

- Low modulus of elasticity
- Low fire resistance
- Susceptibility to biodegradation
- Splintering

In the US Navy, wood is still specified for well-decks of amphibious ships and as a damage control material. Figure 5 shows "4x4's" (four inch square lumber) stored on DDG-53. Typical species are White oak, Eastern pine and Douglas fir.

Figure 5: Damage Control Material on USS *Ramage* (DDG-51)

13.4 Structural Analysis Equations

Because wood is essentially *transversely isotropic*, equations governing stress and strain are different from isotropic materials. The most accurate way to analyze a wood structure would be to use the same methods as for composites. In the case of plywood this is especially true as it is a wood laminate. The mechanics approach for plywood and composites uses the *plane stress* assumption which assumes that stresses through-the-thickness are zero.

In general practice though, as lumber is typically used in plank form, one axis dominates the properties and the stresses in the other two directions are assumed zero. Little additional error is created in using the resulting *isotropic beam* formulas.

For example, in axial loading, the deflection is given by:

$$\delta = \frac{PL}{AE}$$

where P is the axial force, L is the length, A is the cross-sectional area and E is the Young's modulus of the axial direction.

In bending the deflection of a straight beam of constant cross-section is:

$$\delta = \frac{k_b W L^3}{EI} + \frac{k_s WL}{GA'}$$

where the bending and shear constants (k_b and k_s) are based on the loading and boundary conditions (see Table 2), W is the total beam load acting perpendicular to the beam neutral axis, L is the span, I is the moment of inertia, G is the shear modulus and A' is a modified shear area.

$$I = \frac{bh^3}{12} \text{ for rectangular beams, } I = \frac{\pi d^4}{64} \text{ for circular beams}$$

$$A' = \tfrac{5}{6} bh \text{ for rectangular beams, } A' = \tfrac{9}{40} \pi d^2 \text{ for circular beams}$$

Loading	Beam ends	Deflection at	k_b	k_s
Uniformly distributed	Both simply supported	Midspan	5/384	1/8
	Both clamped	do.	1/384	1/8
Concentrated at midspan	Both simply supported	do.	1/48	1/4
	Both clamped	do.	1/192	1/4
Concentrated at outer quarter span points	Both simply supported	do.	11/768	1/8
	do.	Load point	1/96	1/8
Uniformly distributed	Cantilever, one free, one clamped	Free end	1/8	1/2
Concentrated at free end	do.	do.	1/3	1

Table 2: k_b and k_s for beam deflection

13 - 6

Again, due to the beam assumption, stress formulas for wood are the same as those of isotropic materials:

$$\sigma = \frac{P}{A} \text{ for axial loads, and } \sigma = \frac{My}{I} \text{ for bending, and } \tau_{max} = k\frac{V}{A} \text{ for shear,}$$

where k is 3/2 for rectangular cross-sections and 4/3 for circular cross-sections

Typical lumber dimensions lead to the possibility of buckling under compressive loading. The critical buckling stress is:

$$\sigma_{cr} = \frac{\pi^2 E_L}{\left(\frac{L}{r}\right)^2} \text{ where r is the radius of gyration, } r = \frac{b}{\sqrt{12}} \text{ for a rectangular section with b as}$$

the smaller dimension and, $r = \frac{d}{4}$ for a circular section.

As wood will creep under long-term load it is customary to design to half the allowable deflection or stress.

13.5 Fastening

Wood is relatively easy to join compared to other materials. And as with other materials, joining can be broadly classified into two methods: *bonded* joints and *mechanically-fastened* joints. The trade-off between the two are that bonded joints are typically 1 ½ - 3 times stronger, but take longer to assemble and are regarded as permanent.

Due to fastener degradation, adhesive bonding is required for long-term, efficient joints in the marine environment. Adhesives transfer load from one member (called an adherend) to another, through the adhesive. In most cases the load transfer is designed as a shear load, as adhesives are typically much stronger in shear than in tension. Factors involved in adhesively bonded joints include:
- Type of wood
- Surface quality
- Adhesive
- Bonding process
- Joint geometry
- Service environment

All of the woods noted above can be glued, although teak, oak and lignumvitae all require specialized methods for satisfactory results. Figure 6 shows typical edge and axial joints and Figure 7 shows corner joints.
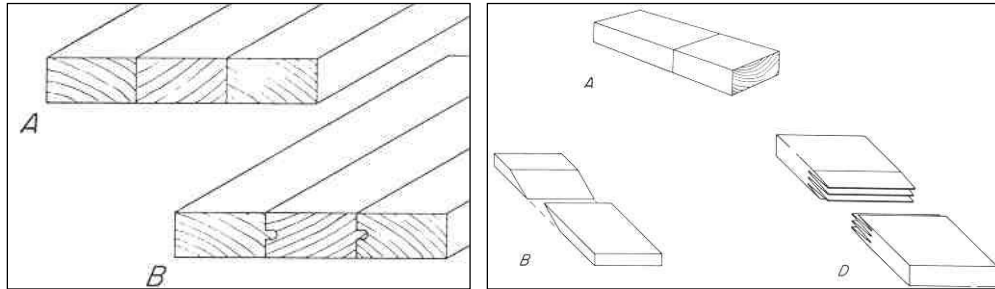
Figure 6: Edge (A-plain, B-tongue and groove) and
Axial (A-plain, B-scarf, D-finger) Bonded Wood Joints
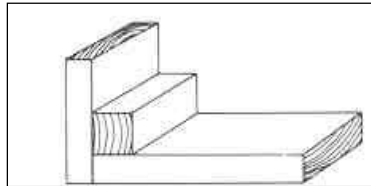
Figure 7: Corner Bonded Wood Joint

Mechanically-fastened joints in wood use a staggering variety of fasteners. (Just walk down an aisle at Home Depot.) Marine joints however, rely primarily on two types: wood screws and bolts. In general, screws are used for lightly loaded, watertight connections. Bolts are used for high-load conditions, but are significantly more difficult to make watertight. Thin planking on small craft is occasionally fastened with copper rivets.

An important corrosion issue is the reaction of wood fasteners. Traditionally the way to avoid fastener corrosion was to use wood trunnels (dowels). In the US the preferred trunnel material was Black Locust. These are relatively low-strength however and silicon bronze and monel are preferred. If cost is an issue stainless or galvanized steel is used, although service life is reduced. If cost is no object then titanium can be used.

13.6 Control of Degradation

Under ideal conditions wood structures can survive for centuries. The primary reasons wood structures fail include fungi, insects, bacteria and marine borers. In some cases large structures have been known to fail within a month of infestation.

Fungi (rot) requires moisture, oxygen and mild temperatures and is considered the largest source of marine decay. To get rot the moisture content must be above the fiber saturation point (30%), and the temperature must be between 50 and 90°F. The best prevention methods include ventilation, reduction of leaks, and preservatives. Note that most preservatives are toxic and make painting difficult.

Insect attack includes termites, beetles and carpenter ants. Rarely are marine structures infected by insects. Some vessels stored out of the water, or along infested docks, have become infected, and alongshore structures are susceptible.

13 - 8

Damage by marine borers is worldwide, and can occur in seawater, brackish and even fresh water. Attack can be rapid, with pilings destroyed in less than six months. The primary borers are the *toredo* (shipworm) which can grow to lengths of four feet in ideal conditions, and various species of *bankia*, *pholads*, and *limnoria*.

In all cases preservation techniques attempt to either impregnate the wood with toxic chemicals or provide an impregnable barrier. Preservatives include copper compounds and creosote tars. The allowable (by EPA or OSHA) versions change frequently. The US Navy currently favors a combination of epoxy/glass coatings and copper antifouling paint for vessels and concrete coverings for stationary structures.

13.7 Plywood

Plywood is a glued-up lamination of many layers of wood. Figure 8 shows typical 3, 4, and 5-ply construction. Compared to lumber, plywood is more stable and uniform. It's axial and transverse properties are similar and it is available in wider widths. Its primary disadvantage is that it is not easily formable. Compound curves (bending about two axes) is not possible. If formed in-place into a curved shape (such as a boat hull) it is commonly called "cold-molded" construction.
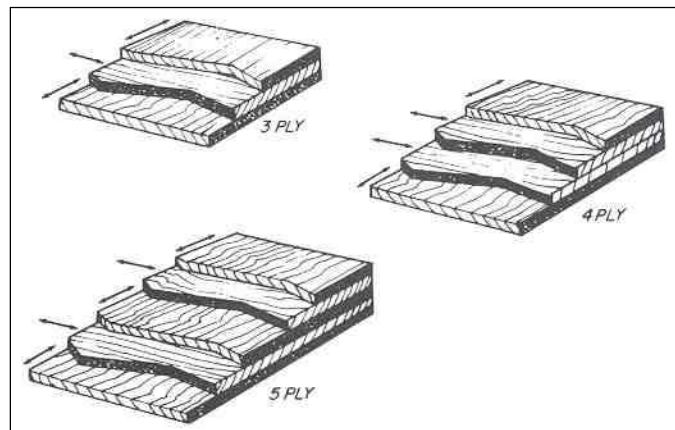
Figure 8: Plywood construction.

The individual plies are held together with various glues. Exterior, marine, and aircraft grade plywood are required to use waterproof grade. The difference between the three grades are the number of flaws in each ply, and the variation is quite wide. In general, the price is reflective of the ply quality and wood species. Many marine applications can use exterior-grade. Aircraft grade is rarely justified except in weight critical structures, and even then may not be desirable as many woods used in aircraft ply are not rot resistant.

Recommended References:
1. Wood: A Manual for it Use as a Shipbuilding Material, 4 Volumes, Bureau of Ships, Department of the Navy, 1957-1962
2. The Encyclopedia of Wood, Revised Edition, Sterling Publishing, New York, 1989 (Also called, *Wood Handbook: Wood as an Engineering Material* by the US Government Printing Office)

13 - 9

CHAPTER 14

CONCRETE

14.1 What is Concrete?
14.2 Variations of Concrete
14.3 Mechanical Properties of Concrete:
14.4 Design Options

Concrete has a wide range of uses in the marine environment, including applications for decks, buildings, seawalls, piles, pipelines, ships/barges.

Concrete Applications

14.1 What is Concrete?

A typical concrete mixture has 5 main components:

Portland Cement	7-15%
Water	14-21%
Air	0.5-8%
Fine Aggregate	24-30%
Coarse Aggregate	31-50%

14 - 1

Portland Cement (7-15%) Water (14-21%) Air (0.5-8%)

Fine Aggregate (24-30%) Coarse aggregate (31-50%)

Advantages	Disadvantages
Low Cost High Durability High Fatigue Resistance Easy to form/Shape	Low tensile strength Heavy Develops strength slowly Dimensions can change with time

Concrete ≠ Cement!
1. Concrete is a composite material composed of coarse granular material (Aggregate) within a matrix of cement paste (Portland Cement and water)

2. Cement is a mixture of lime, silica, alumina and iron oxide that forms the binder for concrete.

3. Portland cement is the most common type of cement, and has five types:
   a. Type I: **Common/General Purpose** - used for general construction, when not significant contact with soils or groundwater is expected. Examples:

   b. Type II: **Moderate Sulfate Resistance** - for concrete in contact with soil or groundwater and for large structures that may be subject to high temperatures.

   c. Type III: **High Early Strength** - develops significant compressive strength in ~7 days (same as 28 day strength for Types I and II). Often used when laying concrete in cold weather.

14 - 2

  d. Type IV: **Low Heat of Hydration** - low heat of hydration as concrete strengthens. Often used for dams and massive structures.

  e. Type V: **Sulfate Resistant** - prevents sulfate attack in highly alkaline soil or seawater.

14.2 Variations of Concrete

Reinforced Concrete - since the tensile strength of plain concrete is 10-15 times lower than its compressive strength, reinforcement can be added to carry the tensile load.
  1. Examples of reinforcement: Rebar (steel rods), wires, mesh, glass fibers, carbon fiber, etc.

Rebar

Glass Fiber Reinforcement

14 - 3

Mesh Reinforcement

Pre-stressed Concrete: place concrete under compression before supporting any loads (besides its own dead weight).
1. The process involves tensioning steel "tendons" that are located within or adjacent to the concrete form.
2. This improves structural capacity and serviceability.
3. Applications: long-span bridges, high rise buildings, names, foundation systems

Prestressed Concrete

14 - 4
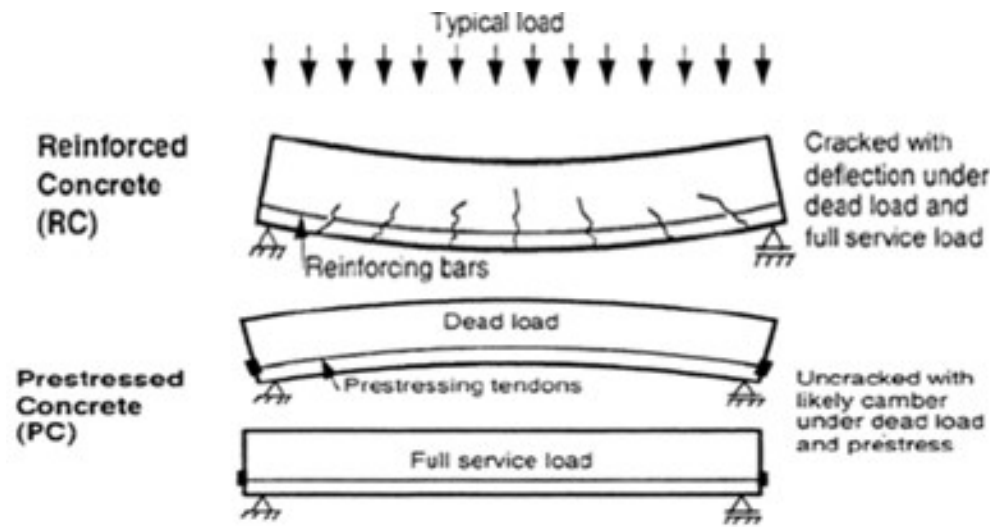
Prestressed concrete

<u>Post-tensioned concrete</u>: tendons are tensioned after the concrete has been cast.
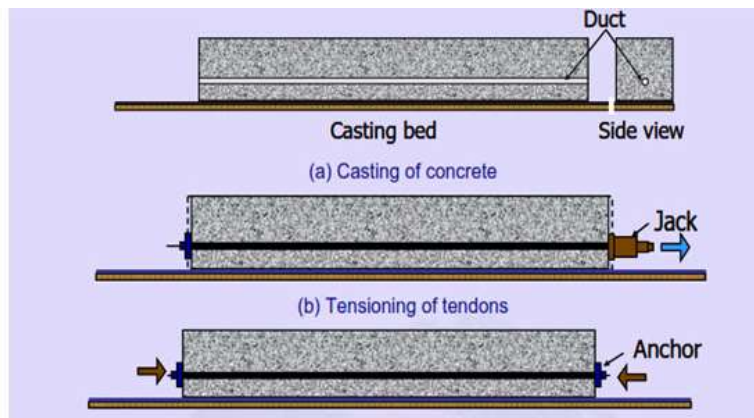
Post Tensioning

Post Tensioning

14 - 5

Shotcrete: Concrete is reinforced with 1-3 inch long glass, fibers, etcetera, and is sprayed through a nozzle/hose.
1. Wet and dry mix variations
2. Gunite is another variation that is a dry mix of sand and cement
3. Many applications in the mining industry

Shotcrete

Grout: a very fluid form of concrete
1. Used to fill gaps
2. The mixture includes water, cement, and fine aggregate (sand) - no coarse aggregate.
3. Applications: tiling

Grout

14 - 6

<u>Tremie concrete</u>: for underwater concrete placement.
1. Process involves placing concrete below the water level using a pipe. The lower end of the pipe is submerged in fresh concrete, and rising concrete from the bottom will displace water without washing out the cement content.
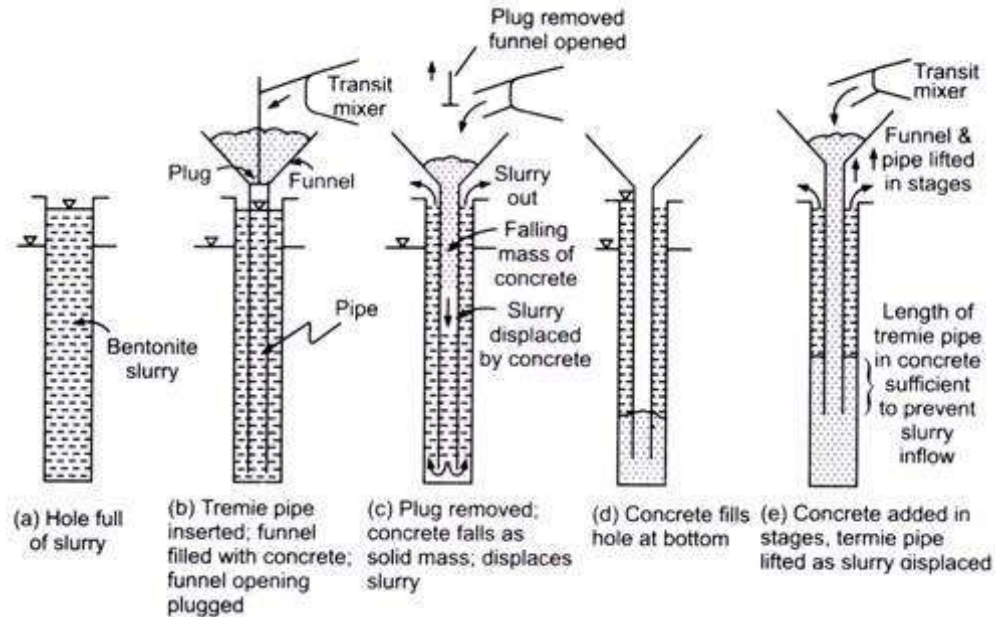
Tremie Concrete

14.3 Mechanical Properties of Concrete
Strength increases with time from 1-6 months after placement. It is often tested at 3, 7, and 28 days. The compressive strength varies from ≈ 3-14 ksi The tensile strength is about 10% of compressive strength.

The following empirical Equation can be used to estimate elastic modulus based on compressive strength:

$$E_C = \gamma_C^{1.5} 33 \sqrt{\sigma_C}$$

Where,
E_C = elastic modulus (psi)
σ_C = compressive strength (psi)
γ_C = unit weight of concrete (54-150 lb/cu ft)

Concrete Compression Test

14.4 Design Options

The tensile strength of concrete is a significant drawback. How can we increase the tensile strength of a structure?
> Add reinforcement
> Pre/Post Stress
> High-Strength Mix

To increase the durability of a concrete structure, the following may be considered:
> Minimum 2" cover for rebar to prevent corrosion of steel
> Low water/cement ratio (ph increases, permeability decreases)
> Coatings for rebar or the exterior of the concrete
> Admixtures that promote air entrainment – pores for capillary water in freeze-thaw cycles.

14 - 8

CHAPTER 15

COMPOSITES

15.1 Fiber Reinforced Polymers
15.2 What are Polymers?
15.3 FRP Fiber Orientation
15.4 FRP Fabrication
15.5 Vacuum Bagging
15.6 Mechanical Properties of FRP

A <u>composite</u> is simply a thing made up of different elements. Reinforced concrete, for instance, is a composite of steel rebar and concrete. They used to build "composite" wooden boats, with iron frames. Typically when the word "composite" is used today, it relates to some type of fiber reinforced polymer.

15.1 Fiber Reinforced Polymers

Fiber Reinforced Polymers are a composite material made of a polymer matrix that is reinforced with fibers.

The <u>matrix</u> is a resin that holds the fibers together. Three commonly used resins are:

- Epoxy – Strong and flexible to resist cracking. This resin is good for FRP-wood construction, in which the swelling and shrinking of the wood can cause delamination
- Polyester – This is very low cost, but somewhat more brittle than epoxy.
- Vinylester – This is in between epoxy and polyester for cost and performance.

The <u>reinforcing fibers</u> also vary, including
- Glass – inexpensive "fiberglass" Available in different types, like E-glass (standard) and S-glass (with higher strength)
- Carbon Fiber – Very high tensile strength, and high modulus of elasticity (stiffness)
- Kevlar – Similar tensile strength to carbon fiber, but more deflection

15.2 What are Polymers?

The matrix, or resin that holds the fibers together is made of polymers. Polymers are "repeating chains of organic material." A mer is the basic unit and there are many of them in a repeating structure. Natural polymers include wood, rubber, wool, leather and methane. Man-made polymers are made from small organic molecules and include plastic, rubber and fibers. Figure 1 represents a simple polymer. Because of the connection details, the polymer can bend in 3 dimensions.

15 - 1
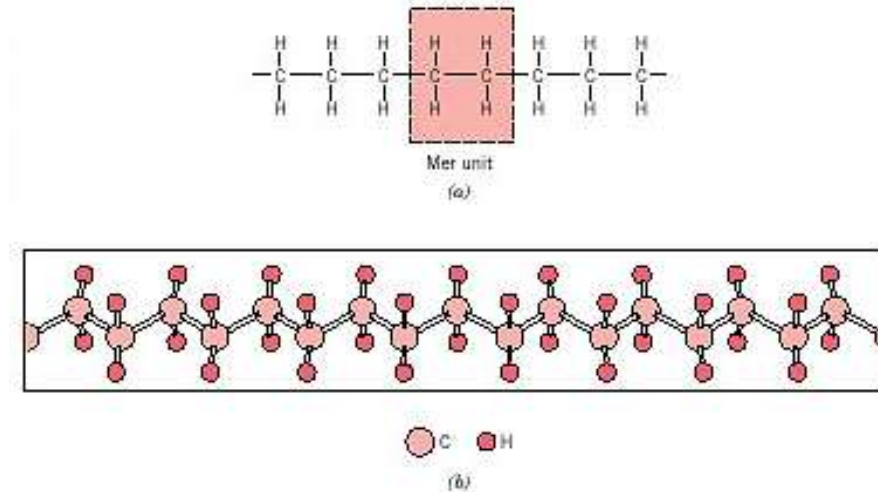
Figure 1: Notional Hydrocarbon

Polymers form very large molecules because of the repeating structure. The carbon atom is the backbone of the polymer. The average molecular weight of a polymer changes the melting temperature. For instance:

$$\overline{M} < 100\frac{g}{mole} \qquad \text{Liguid/Gas}$$

$$\overline{M} \approx 1000\frac{g}{mole} \qquad \text{Waxy solids}$$

$$\overline{M} \approx 10^4 to 10^6\frac{g}{mole} \qquad \text{Solids (high polymers)}$$

Figure 2 shows a typical polymer chain. The intertwining gives it elastic properties.
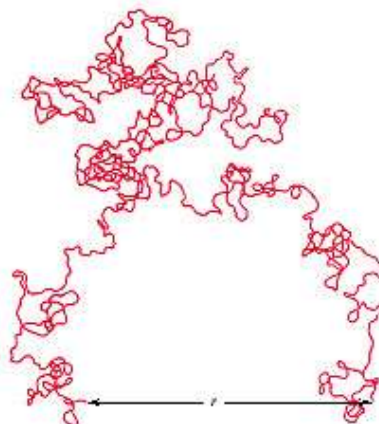
Figure 2: Typical Polymer Chain

15 - 2

Unlike metals, polymers do not create completely crystalline structures. There may be regions of crystallinity, along with amorphous regions. These variations affect how hard the structure is. Figure 3 shows the structure of a polymer solid.
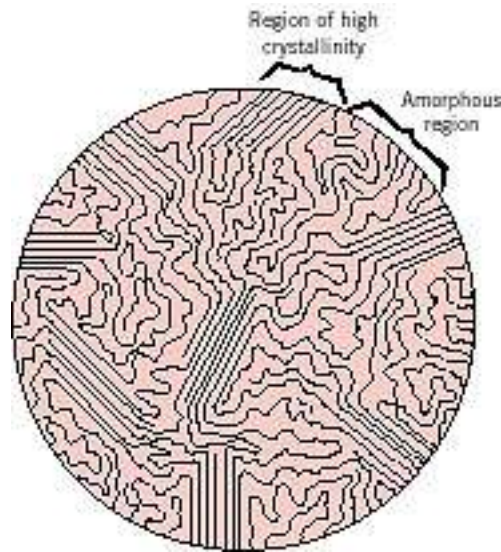
Figure 3: Crystalline and Amorphous structures of Polymers

15.3 FRP Fiber Orientation

can be varied, meaning composites are not isotropic. The strength can be increased in the direction needed by the design. Fiber can come in the following orientations:

- Chopper Gun – These are short fibers that are sprayed onto the inside of the mold along with the resin. This is the lowest strength-to-weight ratio, but the cheapest (many production boats are made this way)
- Chopped Strand Mat – This is like a roll of cloth, but with randomly oriented strands.
- Bi-axial – comes in a roll with two directions. Can be laid up "on the bias" at 45 degrees as well.
- Uni-axial – Strength in one-direction

15 - 3

Figure 4: Laying up a fiberglass boat with a chopper gun (Fibers and resin are sprayed on)
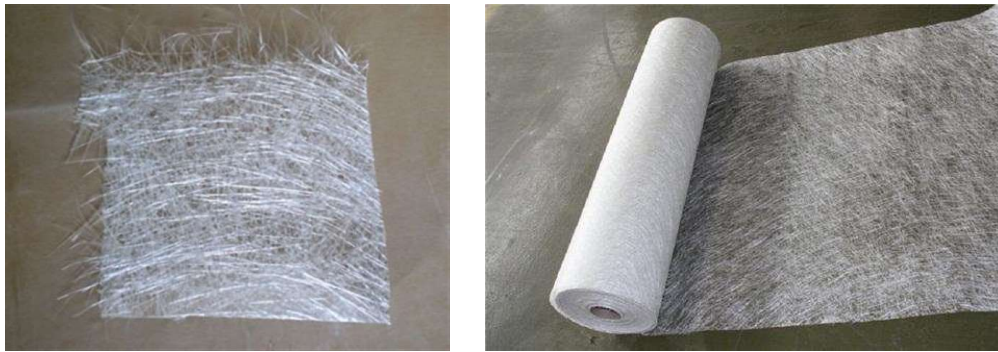
Figure 5: Chopped Strand Mat

Figure 6: Woven Roving – Bi-Axial   Figure 7:Uniaxial Fibers
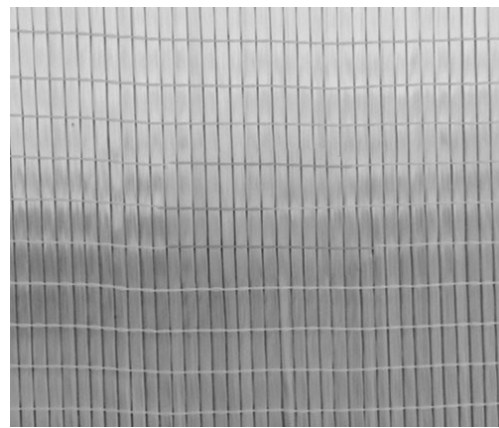
15.4 FRP Fabrication

For production boats, pools, hot tubs, etc, there is generally a female mold with a smooth interior surface.

- They first spray it with a **release agent** to keep the hull from sticking to the mold.

15 - 4

- Then they spray on "**gel coat**" which is a hard shiny surface that you see on the outside of the boat or the inside of the hot tub.
- If the boat is cheap (like most) then they get the **chopper gun** and spray. The inside will then be very rough.
- More expensive **hand layup** requires a layer of **chopped strand mat** first, so that the bi-axial fibers don't "**print through**." Then generally they alternate **woven roving** and chopped strand mat for each subsequent layer (this keeps the woven parts from bunching up and leaving voids).
- In specialized custom design boats, like racing yachts, they will use **uniaxial** fibers to increase the strength in particular directions. This requires careful design and understanding of the loads.
- Hulls sometimes include a **core** material so that there is strong fiberglass on the outside and the inside, with a core to space them apart. This increases the moment of inertia and hence the stiffness and strength.

Figure 8: Boat Molds in Shop

15.5 Vacuum Bagging

Once there is enough resin to bond the fibers together, more resin doesn't add strength. It costs money to buy and adds weight. As a result, efforts are sometimes taken to reduce the amount of resin in a particular layup. Vacuum bagging is used to put a suction over the layup to compress it and reduce the amount if resin. This works well, but increases the difficulty of the job. For very thin layups, it can sometimes result in pinhole leaks.

15 - 5
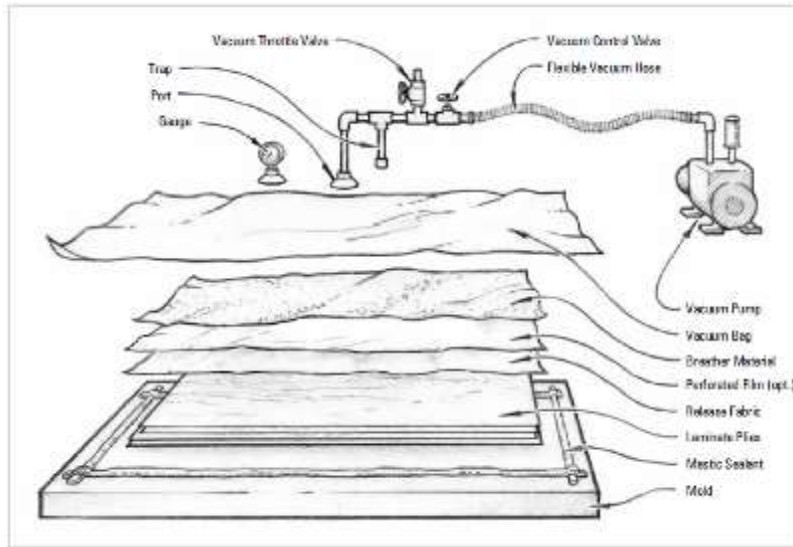
Figure 9: Vacuum Bagging (From Jamestown Distributers)

Figure 10: Small Vacuum Bagging   Figure 11:Vacuum Bagging a Wind Turbine Blade

15.6 Mechanical Properties of FRP

The matrix and the fibers have different strengths and elasticity. When the forces are in the same direction as the fibers, assume isostrain – the fibers and the matrix elongate the same amount.
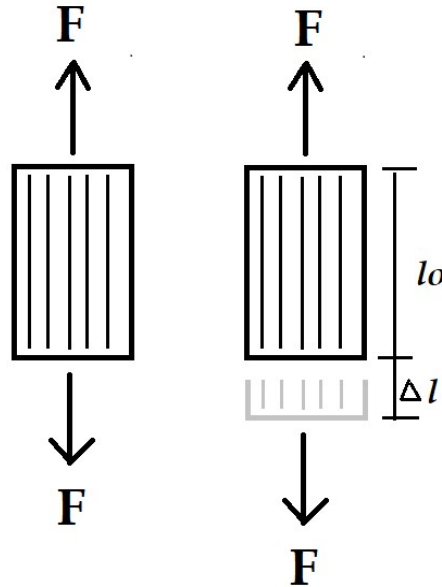
Figure 11: Elongation of Uni-axial Fiber

Using isostrain and the volume fraction of the fibers and matrix, we can use the <u>Rule of Mixtures</u>

$$E_{FRP} = E_M V_M + E_F V_F$$

Where, E_{FRP}, E_M, E_F is the modulus of elasticity of the FRP, the matrix and the fibers. V_M and V_F are the volume fractions of the matrix and the fibers.

$$V_M + V_F = 1$$

The ratio of the force carried by the fibers and the force carried by the matrix

$$\frac{F_F}{F_M} = \frac{E_F V_F}{E_M V_M}$$

Where, F_F and F_M = the force carried by the fibers and the matrix, in N or lb. The total load is then,

$$F_{FRP} = F_F + F_M$$

15 - 7

What if the loads are in the transverse direction? The fibers do not have significant strength in this direction, so it is not isostrain. Instead, assume isostress - -the same force per unit area.

$$E_{FRP-TRANSVERS} = \frac{E_M E_F}{E_M V_M + E_F V_F}$$

Example 1a: A continuous uniaxial glass FRP has 40% by volume fibers ($E_F = 10 \times 10^6$ psi) in a polyester resin ($E_M = 0.5 \times 10^6$ psi). Compute the longitudinal elastic modulus of the composite.

Answer

$$E_{FRP} = E_M V_M + E_F V_F$$

$$V_F = 0.4 \text{ so } V_M = 1 - V_F = 0.6$$

$$E_{FRP} = 0.5 \times 10^6 psi \times 0.6 + 10 \times 10^6 psi \times 0.4 = 4.3 \times 10^6 psi$$

Example 1b: If the cross-section area of the composite in the previous example of 0.4 square inches and a longitudinal stress of 7250 psi is applied, find the load carried by the fibers and by the matrix.

Answer:

① load Ratio $\dfrac{F_F}{F_m} = \dfrac{E_F V_F}{E_m V_m} = \dfrac{10 \cdot 10^6 psi \times 0.4}{0.5 \times 10^6 psi \times 0.6} = 13.3$

$$\boxed{F_F = 13.3 \, F_m}$$

② we also know that

$$F_{FRP} = F_F + F_m$$

$$\sigma_{FRP} A_{FRP} = F_F + F_m$$

$$7250 psi \times 0.4 in^2 = 13.3 F_m + F_m$$

$$2900 lb = 14.3 F_m \rightarrow \boxed{F_m = 202 lb}$$

$$\therefore F_F = 13.3 \times 202 lb = \boxed{2698 lb = F_F}$$

15 - 8

Example 1c: *For the previous example, what is the strain sustained by each of the fibers and the matrix?*

Answer:

① $E = \frac{\sigma}{\varepsilon} \Rightarrow \quad \varepsilon = \frac{\sigma}{E} = \boxed{\varepsilon = \frac{F}{AE}}$

② $\varepsilon_{FRP} = \varepsilon_F = \varepsilon_m$

$\rightarrow \varepsilon_{FRP} = \frac{F_{FRP}}{A_{FRP} E_{FRP}} \quad = \quad \hat{\varepsilon}_F = \frac{F_F}{\underbrace{A_F E_F}_{V_F A_{FRP}}}$

$\therefore \quad \varepsilon = \frac{2900 \, lb}{0.4 in^2 \times 4.3 \times 10^6 psi} = 0.000169 \, \frac{in}{in}$

$\varepsilon_F = \frac{F_F}{A_F E_F} = \frac{2,698 \, lb}{(0.4 \times .4 in^2) \times 10 \cdot 10^6 psi} = \underline{\quad\quad}$

    $\uparrow$
    V_F

Example 1d: *What if we load in the transverse direction?*

Solution:

a. Fibers do not have significant strength in this direction → **not** isostrain

b. instead assume isostress – same force per area

c. $E_{FRP}^{TRAN} = \frac{E_m E_F}{V_m E_F + V_F E_m}$

d. For example:

$E_{TRAN}^{FRP} = \frac{0.5 \times 10^6 psi \times 10 \times 10^6 psi}{.6 \times 10 \cdot 10^6 psi + 0.4 \times 0.5 \times 10^6 psi}$

$\boxed{E_{TRAN}^{FRP} = 0.81 \times 10^6 \, psi}$ (~20% of longitudinal modulus)

Example 2: For a uniaxial FRP that has a 50-50 ratio by volume of fibers ($E_F = 10 \times 10^6$ psi) in a polyester resin ($E_M = 0.5 \times 10^6$ psi).

a. Find the strain felt by the composite fibers and matrix if the applied force is 4500 lb and the total cross-section area is 0.6 sq inches.

(1) ISOStrain → $\varepsilon_{FRP} = \varepsilon_F = \varepsilon_m = \dfrac{\sigma}{E} = \dfrac{F}{AE}$

ⓐ $E_{FRP}^{ION} = E_F V_F + E_m V_m = 10 \cdot 10^6 \text{psi} \times 0.5 + 0.5 \times 10^6 \text{psi} \times 0.5$

$\boxed{E_{FRP}^{ION} = 5.25 \times 10^6 \text{psi}}$

ⓑ ∴ $\varepsilon_{FRP} = \dfrac{F_{FRP}}{A_{FRP} E_{FRP}} = \dfrac{4500 \text{lb}}{0.6 \text{in}^2 \times 5.25 \times 10^6 \text{psi}}$

$\boxed{\varepsilon = 0.00143 \text{ in/in}}$

b. Find the load carried by the fibers in the matrix.

(2) ⓐ $\dfrac{F_F}{F_m} = \dfrac{E_F V_F}{E_m V_m} = \dfrac{10 \cdot 10^6 \text{psi} \times 0.5}{0.5 \times 10^6 \text{psi} \times 0.5} = 20 \rightarrow \underline{F_F = 20 F_m}$

ⓑ $F_F + F_m = F_{FRP} = 4500 \text{lb}$

$21 F_m = 4500 \rightarrow \boxed{\begin{array}{l} F_m = 214 \text{lb} \\ F_F = 4,286 \text{lb} \end{array}}$

c. The longitudinal elastic modulus of the composite

(3) ✓ $E_{FRP}^{ION} = 5.25 \times 10^6 \text{psi}$

d. The transverse elastic modulus of the composite.

(4) $E_{FRP}^{TRAN} = \dfrac{E_F E_m}{E_F V_m + E_m V_F} = \dfrac{10 \cdot 10^6 \text{psi} \times 0.5 \times 10^6 \text{psi}}{10 \cdot 10^6 \text{psi} \times 0.5 + 0.5 \times 10^6 \text{psi} \times 0.5}$

$\boxed{E_{FRP}^{TRAN} = 0.95 \times 10^6 \text{psi}}$

Note: $\dfrac{E_{ION}}{E_{TRAN}} = \dfrac{5.25 \cdot 10^6}{0.95 \cdot 10^6} = 5.5$

15 - 10

APPENDIX

CATHODIC PROTECTION DESIGN

from Swain Classnotes (1996)

```
┌─────────────────────────────────────────┐
│              STRUCTURE                   │
│  Metal, Design Life, Dimensions,         │
│            Coatings, Other               │
└─────────────────────────────────────────┘
                    ↓
┌─────────────────────────────────────────┐
│               LOCATION                   │
│  Environmental Conditions,               │
│           Other Structures               │
└─────────────────────────────────────────┘
                    ↓
┌─────────────────────────────────────────┐
│             C.P. CRITERIA                │
│    Potential for Cathodic Protection     │
└─────────────────────────────────────────┘
                    ↓
┌─────────────────────────────────────────┐
│          C.P. CURRENT DEMAND             │
│           Initial, Mean, Final           │
└─────────────────────────────────────────┘
                    ↓
┌─────────────────────────────────────────┐
│               C.P. TYPE                  │
│  Impressed Current, Sacrificial Anode    │
└─────────────────────────────────────────┘
                    ↓
┌─────────────────────────────────────────┐
│     ANODE AND  HARDWARE SELECTION        │
│  Current Output, Design Life, Placement  │
└─────────────────────────────────────────┘
                    ↓
┌─────────────────────────────────────────┐
│        COST AND IMPLEMENTATION           │
│                                          │
└─────────────────────────────────────────┘
```

Appendix: Cathodic Protection Design - 1

Table of Contents

1.0   INTRODUCTION

Metallic structures in contact with water, soil, concrete, and moist air are subject to corrosion.   Cathodic protection (CP) is one of the few methods that successfully mitigates corrosion.   It can be applied in any situation where the environment surrounding the metal acts as a conductor for electric current.   It has been successfully applied to offshore structures, ships, boats, propellers, moorings, pipelines, storage tanks, piers, jetties, bridges, aquaria, instrumentation etc.

This handout is designed as an introduction to CP design. As such, it does not cover all aspects of the subject. Therefore, the student should realize the limitations of his/her knowledge and consult other literature or experts in the field when necessary.

2.0   STRUCTURE

CP design begins with a thorough understanding of the structure to be protected.   This includes the following information:

- Metal type(s)
- Operating conditions
- Dimensions and surface area
- Coatings
- Data from previous structures and CP systems
- Design life

3.0   LOCATION

The environmental conditions are determined by the location of the proposed installation.   Factors such as climate, electrolyte conductivity and chemistry, physical loading, and biological activity, all impact CP requirements.   These factors are generally allowed for in the CP current demand and polarization potential criteria.

3

4.0   CP CRITERIA

Potential measurements are the most commonly used criteria to ascertain the level of CP afforded to metals and alloys. CP potential values vary according to the metal and the environment. Corrosion is likely to occur at potentials which are more positive than the protected value. Damage may also occur if the metal is overprotected (i.e. the potential too negative). The most common error associated with potential measurements is a result of IR drop. This is the displacement of measured metal potential due to current flow through the electrolyte. High electrolyte resistivity and high current densities can cause significant differences between the measured and actual metal potential.

4.1   Potential Values

The measurement of potential with respect to a standard reference electrode is probably the most common method of evaluating the degree of cathodic protection afforded to a structure. Typical cathodic protection potentials for commonly used metals ref. Ag/AgCl reference electrode (seawater) are provided in Table 4.1. A more detailed summary of protection potentials for steel in seawater is provided in Table 4.2.

Table 4.1   Approximate freely corroding and protected potentials of metals in seawater (may vary according to velocity and conditions).

Metal or Alloy	Freely Corroding Potential (V) ref. Ag/AgCl	Protected Potential (V) ref. Ag/AgCl
316,304 Stainless (passive)	-0.10	-0.75
Copper Alloys	-0.35	-0.70
316,304 Stainless (active)	-0.50	-0.75
Steel	-0.60	-0.80
Aluminum Alloys	-0.75	-1.00
Zinc/Aluminum Anodes	-1.05	
Magnesium Anodes	-1.50	

4

Table 4.2   Potential values for corrosion and protection of steel in seawater

V ref. Ag/AgCl	Condition	V ref. Zn
	Heavy Corrosion	
-0.60	Freely Corroding Steel	+0.50
-0.70	Some Protection	+0.40
-0.80	Cathodic Protection	+0.30
-0.90	Some Over	+0.20
-1.00	Protection	+0.10
-1.10		0.00
-1.20	Over Protection	-0.10
-1.30	May Cause	-0.20
-1.40	Paint Blistering and Flaking	-0.30
-1.50		-0.40

4.2   300 mV Shift

The NACE Standard, RP-02-85 states that a minimum negative (cathodic) voltage shift of 300mV, produced by the application of protective current should provide CP to iron and steels. The voltage shift is measured between structure surface and a stable reference electrode contacting the electrolyte. This criteria does not apply to structures in contact with dissimilar metals.

4.3   100 mV Shift

The NACE Standard, RP-02-85 states that a minimum negative (cathodic) voltage shift of 100mV measured between the structure surface and a stable reference electrode contacting the electrolyte should provide CP to iron and steel. This polarization voltage shift is determined by interrupting the protective current and measuring the instant off and polarization decay. The instant off value is obtained immediately following the interruption of the CP current. The voltage shift is equivalent to the IR drop created by the CP current and electrolyte resistance. The polarization decay is measured as the change in potential over a period of time from the instant off value.

5

4.4   E-log-I Curve

The NACE Standard, RP-02-85 states that a structure-to-electrolyte voltage at least as negative (cathodic) as that originally established at the beginning of the Tafel segment of the E-log-I-curve should provide CP to iron and steel. This structure-to-electrolyte voltage shall be measured between the structure surface and a stable reference electrode contacting the electrolyte at the same location where voltage measurements were taken to obtain the E-log-I curve.

4.5   Anodic Current Discharge Points

The NACE Standard, RP-02-85 states that a net protective current from the electrolyte into the structure surface as measured by an earth current technique applied to predetermined current discharge (anodic) points of the structure should provide CP to iron and steel.

5.0   CATHODIC PROTECTION CURRENT DEMAND

The cathodic protection current demand is the amount of electricity required to polarize the structure to a level that meets the criteria described in Section 4. This may be obtained from a trial polarization of the structure at the installation site, a trial polarization of a metal test coupon at the installation site, or from conservative estimates obtained from historical information obtained from previous structures operating under the prescribed conditions.

For planning and design purposes, it is often possible to rely on conservative estimates provided by recommended practice. There are several sources for this information. The most current one is Recommended Practice RP B401, Cathodic Protection Design, Det Norske Veritas Industri Norge AS, 1993.

5.1   Recommended Practice RP B401, Det Norske Veritas

The CP current densities are calculated for different environmental conditions and conditions of the steel (i.e. uncoated, coated, concrete reinforcing steel, pipeline).

6

5.1.1 Uncoated Steel

Three design current densities are given: initial, final, and average.

Initial   This is the current density required to effect polarization of the initially exposed bare steel surface. It assumes some atmospheric rusting and/or millscale.   The initial current density is higher because of lack of calcareous scales (cathodic chalks). A proper initial current density enables rapid formation of protective calcareous scales.

Final   This is the current density required to protect the metal surface with established marine growth and calcareous layers. It takes into account the current density required to repolarize the structure in the event of removal of these layers by storms, cleaning operations etc.

Average   This is the anticipated current density required once the cathodic protection system has reached its steady state. The average or maintenance current density is used to calculate the minimum mass of anode material required to protect the structure throughout the design life.

Table 5.1   Initial, final, and average current densities for various climatic conditions and depths (climatic conditions are based on yearly range of average surface water temperatures).

	Design Current Densities (A/m^2)											
	Tropical >20ºC			Sub-Tropical 12º-20ºC			Temperate 7º-12ºC			Arctic <7ºC		
Depth (m)	Initial	Final	Average	Initial	Final	Average	Initial	Final	Average	Initial	Final	Average
0 - 30	0.150	0.090	0.070	0.170	0.110	0.080	0.200	0.130	0.100	0.250	0.170	0.120
>30	0.130	0.080	0.060	0.150	0.090	0.070	0.180	0.110	0.080	0.220	0.130	0.100

5.1.2 Coated Steel

The use of coatings on steel dramatically reduces the current demand on the cathodic protection system. This can save on the cost and structural weight associated with sacrificial anode systems. The CP current demand of a coated offshore jacket may be estimated by multiplying the bare steel current demand by a coating breakdown factor (f_c). The coating breakdown factor does not allow for mechanical damage to paint

7

coatings. These areas are treated as bare metal surface. For CP design purposes the average and final coating breakdown factors for a design life of t_r years are as follows:

$$f_c(average) = k_1 + k_2 \frac{t_r}{2}$$
$$f_c(final) = k_1 + k_2 t_r$$

When the design life of the CP system exceeds that of the coating system then f_c (average) is calculated as follows:

$$f_c(average) = 1 - \frac{\left(1 - k_1^2\right)}{2k_2 t_r}$$

If the calculated value exceeds 1, then $f_c = 1$ shall be applied to the design.

Table 5.2   Constants (k_1 and k_2) for calculation of paint coating breakdown factors.

Category	Description	k_1	k_2 0-30m	k_2 >30m
I	One layer of primer coat, about 50 μm nominal DFT.	0.10	0.10	0.05
II	One layer of primer coat, plus minimum one layer of intermediate top coat, 150 - 250 μm nominal DFT.	0.05	0.03	0.02
III	One layer of primer coat, plus minimum two layers of intermediate/top coats, 300 μm nominal DFT.	0.02	0.015	0.012
IV	One layer of primer coat, plus minimum three layers of intermediate/top coats, 450 μm nominal DFT.	0.02	0.012	0.012

5.1.3 Pipeline Coatings

The coating breakdown factors as shown in table 5.2 apply equally to both buried and non-buried pipelines. It is assumed that coatings and field joint systems have been chosen to be compatible with the maximum design temperature of the pipeline.

For pipelines with the following coating systems, another coating breakdown factor is calculated.

$\Rightarrow$ asphalt + concrete weight coating

$\Rightarrow$ fusion bonded epoxy + adhesive + polyethylene or polypropylene

$\Rightarrow$ polychloroprene rubber

$\Rightarrow$ equivalent coating systems based on an inner layer dedicated to corrosion protection and one or more outer layers for mechanical protection.

This is as follows:

$$f_c(average) = 0.05 + 0.002(t_r - 30)$$

$$f_c(final) = 0.07 + 0.004(t_r - 20)$$

5.1.4 Concrete

It is now recognized that cathodic protection of concrete reinforcing steel is necessary to ensure the long term integrity of the structure. Also, any CP system designed to protect metallic appendages and components must be designed to allow for current drain from CP to the reinforcement. The cathodic current density is determined by transport of oxygen to the steel by capillary action of pore water driven by evaporation in the atmospheric zone and internal dry compartments. The current densities are, therefore, dependent on depth and climatic conditions.

9

Table 5.4   Design current densities for concrete reinforcing steel.

(NOTE: design currents refer to the area of the reinforcing steel)

	Design Current Densities (A/m^2)			
Depth (m)	Tropical >20°C	Sub-Tropical 12°-20°C	Temperate 7°-12°C	Arctic <7°C
5 to -10	0.0030	0.0025	0.0015	0.0010
<-10	0.0020	0.0015	0.0010	0.0008

5.2   Current Requirements for Pipelines in Soils of Different Types

The current demands for steel pipelines are determined by the soil type (conductivity, pH, moisture, temperature) and the condition of the steel (coating type). An example of typical CP current demand for a pipeline with different coating conditions is presented as follows.

Table 5.3   Range of current required to protect 10 miles of 36" diameter pipe in soil with average resistivity of 1000 ohm-centimeters. Current required is that needed to cause a 0.3 Volt drop across the effective resistance between pipeline and remote earth. [from A.W.Peabody, Control of Pipeline Corrosion,NACE, 1967]

Effective Coating Resistance in Ohms for One Average Square Foot	Current Required, Amps
Bare Pipe (minimum 1 mA/ft^2)	500
10,000	14.91
25,000	5.964
50,000	2.982
100,000	1.491
500,000	0.2982
1,000,000	0.1491
5,000,000	0.0298
Perfect Coating	0.000058

5.3   Current Requirements for Ship Protection

Information with regard to current density requirements for ship hull protection is limited. One source of information is the Technical and Research Report R-21, Fundamentals of Cathodic Protection for Marine Service, The Society of Naval Architects and Marine Engineers, January 1976. It must be remembered that this was compiled before the development of modern day bottom coatings. It may, therefore, be better to use the DNV practice for coated steel and to include an allowance for damaged surfaces.

Table 5.5   Protective current densities for ships. [from Technical and Research Report R-21, Fundamentals of Cathodic Protection for Marine Service, The Society of Naval Architects and Marine Engineers, January 1976]

Specific Area	Current Density, mA/m^2
External Hull	22-54
Rudders (Coated and for velocities not exceeding 5 knots. Current demand maybe 3 or more times greater underway)	490
Propellers (For velocities not exceeding 5 knots. Current demand maybe 3 or more times greater underway)	150 -170
Coated Tanks	11
Segregated Ballast	150
Washed Cargo / Clean Ballast	130
Dirty Ballast Tanks	86

11

6.0   CP TYPE

The CP type determines how the cathodic current is supplied to the structure. CP can be applied by either an impressed current system or by a sacrificial anode system. Impressed current CP systems use an external DC current source and a variety of anode materials to supply the cathodic current. Sacrificial anode CP systems generate the cathodic current from the corrosion of metals less noble than the metal to be protected.

The choice between impressed and sacrificial cathodic protection depends many factors and may be just personal preference. There are, however, situations where one or the other provides the correct choice. The advantages and disadvantages of each type of CP system are described in Table 6.1.

Table 6.1   Advantages and disadvantages of impressed current and sacrificial anode CP systems.

Impressed Current	Sacrificial Anodes
Advantages	
Variable control of current and potential	Self contained
Can be automated	Can be self adjusting
Light weight and fewer anodes	Polarity of connections always correct
Varied anode geometry	Needs no supervision
Long life with inert anodes	Simple to install
Disadvantages	
Complex installation and maintenance	Expensive method of generating electricity
Requires external power source	No variable control
Anodes require dielectric shields	Anodes add weight
Anodes may be damaged	Anodes have finite life
Probability of stray current corrosion	Small lead resistance reduces current

7.0   ANODE SELECTION

Anodes, for both impressed current and sacrificial anodes, are selected according to their size and chemical composition. This determines the current output and design life. Specifications for impressed current anodes are provided in Table 7.1 and for sacrificial anodes in Tables 7.2 and 7.3.

Table 7.1   Impressed current anodes.

Anode Material	Recommended Current density A/m^2	Maximum Voltage, V	Consumption Rate, g/A-yr	Comments
Scrap Steel	Varies	-	200 - 9,000	Difficult life prediction
Graphite	10	-	30 - 450	Very brittle
Silicon-Chromium-Cast Iron	10 - 100	-	90 - 250	Very brittle
Lead-Silver	250 - 500	-	30 - 90	Heavy, Poor mechanical properties
Lead-Platinum	100	-	2 - 60	
Magnetite	10 - 500	-	40	Very Brittle
Platinized Titanium	250 - 700	9	0.01	5 μm thick Pt film provides 10 year life
Platinized Tantalum	500 - 1000	100	0.01	5 μm thick Pt film provides 10 year life
Platinized Columbium	500 - 1000	100	0.01	5 μm thick Pt film provides 10 year life
Lithium-Ferrite Ceramic	15 - 2000	9.7	1-2	Lightweight and tough

Table 7.2   Sacrificial anode types and use.

Anode	Preferred Use	Approx. Potential Volts ref. Ag/AgCl
Magnesium, High Potential	Soils with resistance > 2000 Ω-cm	-1.75
Magnesium, Standard	Soils with resistance < 2000 Ω-cm, and in aqueous environments with controllers if necessary	-1.50
Zinc, Hi-Amp	Seawater, brackish water, saline mud. Temps < 60°C	-1.05
Zinc, Hi-Purity	Underground, fresh water, and saline environments > 60°C	-1.05
Galvalum I	Submerged seawater, max. temp 25 °C	-1.05
Galvalum II	Saline mud	-1.04
Galvalum III	Seawater, brackish water, saline mud	-1.10
Reynode		-1.05
Al-Sn-In Alloy		-1.05

Table 7.3   Sacrificial anode properties.

Property	Anode Material Type				
	Magnesium	Zinc	Galvalum 1	Galvalum II	Galvalum III
Density, kg/m^3	1940	7130	2700	2700	2700
Electrochem Equiv, g/coulomb	0.126E-3	0.339E-3	0.093E-3	0.093E-3	0.093E-3
Theoretical Ah/Kg	2,205	819	2,987	2,987	2,987
Current Efficiency %	0.55	0.95	0.95	0.57	0.85
Actual Ah/Kg	1,212	780	2,830	1,698	2,535
Actual Kg / Amp / Year	7.95	11.25	3.10	5.16	3.46
Potential V, ref. Ag/AgCl	-1.75	-1.05	-1.05	-1.04	-1.10

Table 7.4 Sacrificial Anode Composition.
Percent of Total Weight

	Mg	Zn	Al	Cd	Cu	Fe	Hg	In	Mn	Ni	Pb	Si
Magnesium, High Potential	rem		0.01		0.02	0.03			0.50 - 1.30	0.001		
Magnesium, Standard	rem	2.5 - 3.5	5.3 - 6.7		0.05	0.003			0.15	0.003		0.30
Zinc, Hi-Amp		rem	0.1 - 0.4	0.025 - 0.060		0.005					0.006	
Zinc, Hi-Purity		rem		0.003		0.0014					0.003	
Galvalum I		0.35 - 0.48	rem				0.035 - 0.048					0.14 - 0.21
Galvalum II		3.5 - 5.0	rem				0.035 - 0.048					
Galvalum III		2.8 - 3.5	rem					0.01 - 0.02				0.08 - 0.12

Appendix: Cathodic Protection Design - 15

7.1 Anode Resistance to Ground

The current output from an anode is determined by its shape, electrolyte resistance, and driving potential. The shape and electrolyte resistance determine the anode resistance to ground which is calculated from standard anode resistance formulae. The most commonly used formulae are presented in Table 7.4 and seawater conductance values in Table 7.5.

Table 7.4   Anode resistance to ground formulae.

Anode Type	Resistance Formula
Long Slender stand-off L ≥ 4r	$R = \dfrac{\rho}{2\pi L}\left(\ln\left(\dfrac{4L}{r}\right) - 1\right)$ (Modified Dwight)
Long Slender stand-off L < 4r	$R = \dfrac{\rho}{2\pi L}\left[\ln\left\{\dfrac{2L}{r}\left(1 + \sqrt{1 + \left(\dfrac{r}{2L}\right)^2}\right)\right\} + \dfrac{r}{2L} - \sqrt{1 + \left(\dfrac{r}{2L}\right)^2}\right]$
Long flush mounted L ≥ 4 x width and thickness	$R = \dfrac{\rho}{2S}$ (Lloyds)
Short flush-mounted, bracelet and other flush mounted shapes	$R = \dfrac{0.315\rho}{\sqrt{A}}$ (McCoy)

where: R is anode resistance, ohms

ρ is electrolyte resistivity, ohm-cm

L is anode length, cm

S is the mean of the anode sides $= \dfrac{a+b}{2}$

r is equivalent radius, cm, $= \sqrt{\dfrac{\text{anode cross - sectional area}}{\pi}}$

A is the exposed surface area of anode, cm^2

Appendix: Cathodic Protection Design - 16

Table 7.5   Specific Conductance of Seawater

Note: Resistivity, ρ, is the reciprocal of conductance. Tabled values are expressed in in $(\Omega^{-1}\text{-cm}^{-1})$.

Chlorinity, ppt	Temperature, °C					
	0	5	10	15	20	30
1	0.001839	0.002134	0.002439	0.002763	0.003091	0.003431
2	0.003556	0.004125	0.004714	0.005338	0.005971	0.006628
3	0.005187	0.006016	0.006872	0.007778	0.008702	0.009658
4	0.006758	0.007845	0.008958	0.010133	0.011337	0.012583
5	0.008327	0.009653	0.011019	0.012459	0.013939	0.015471
6	0.009878	0.011444	0.013063	0.014758	0.016512	0.018324
7	0.011404	0.013203	0.015069	0.017015	0.019035	0.021121
8	0.012905	0.014934	0.017042	0.019235	0.021514	0.023868
9	0.014388	0.016641	0.018986	0.021423	0.023957	0.026573
10	0.015852	0.018329	0.020906	0.023584	0.026367	0.029242
11	0.017304	0.020000	0.022804	0.025722	0.028749	0.031879
12	0.018741	0.021655	0.024684	0.027841	0.031109	0.034489
13	0.020167	0.023297	0.026548	0.029940	0.033447	0.037075
14	0.021585	0.024929	0.028397	0.032024	0.035765	0.039638
15	0.022993	0.026548	0.030231	0.034090	0.038065	0.042180
16	0.024393	0.028156	0.032050	0.036138	0.040345	0.044701
17	0.025783	0.029753	0.033855	0.038168	0.042606	0.047201
18	0.027162	0.031336	0.035644	0.040176	0.044844	0.049677
19	0.028530	0.032903	0.037415	0.042158	0.047058	0.052127
20	0.029885	0.034454	0.039167	0.044114	0.049248	0.054551
21	0.031227	0.035989	0.040900	0.046044	0.051414	0.056949
22	0.032556	0.037508	0.042614	0.047948	0.053556	0.059321

7.2   Anode Ground Beds

Anode ground beds are used to increase the anode current output in soils. They typically comprise an excavation which is filled with low conductance carbonaceous material into which the anode(s) are placed. The total resistance of the system then becomes the resistance of the anode to the carbonaceous backfill plus the resistance to earth of the backfill itself. The anode resistance is reduced by the low resistance of the backfill (typically 50 ohm-cm for coke breeze), and the resistance of the backfill to earth is reduced by the large surface area of the backfill in contact with the soil. Standard anode to ground resistance formulae are used to obtain the resistance values.

Because of the variables involved in ground bed sites, experience is invaluable in attaining competence in their design. They are designed with regard to the current demand of the structure to be protected, to the soil resistance, and to other structures and stray current effects.

7.3   Anode Current Output

Anode current output is calculated using Ohm's Law:

$$I = \frac{V}{R}$$

This is where V is the driving potential, and R is the anode resistance. The driving potential is determined by the anode type. The driving potential for sacrificial CP systems is determined by the environment (Table 7.2), but for impressed current systems it is determined by the rectifier and controller voltage output (Table 7.1). The anode resistance to ground is found from the anode resistance formulas (Table 7.4).

7.4   Anode Size, Weight, Number, Distribution and Design Life

The CP system must be designed to provide the required current to every part of the structure for the required design life. This requires determining anode size, weight, number, and distribution.

18

The calculations for impressed current CP systems are relatively simple. In this case, it is only necessary to match the number of anodes of known current output to the total current demand of the structure, and to be sure that the anode distribution insures an even and well balanced current distribution.

The calculations for sacrificial CP systems are a little more complex. Not only must the number of anodes satisfy the current demand of the structure, but they must also have sufficient mass to provide electricity for the design life of the structure.

Anode size and shape are determined by the following factors:
- Requirements for minimum and maximum current output
- Requirement for mounting and attachment
- Requirement for streamlining
- Requirement for weight of anode material (sacrificial)
- Commercial availability

The minimum and maximum current outputs are calculated as described in sections 7.1 and 7.2. The types of mounting methods range from welding steel cores, cast into the anode materials, directly to the structure, to mounting complex dielectric shields with screw in platinized titanium impressed current anodes. Where streamlining is required, recesses may be built into the structure to house both impressed and sacrificial anode types.

Sacrificial CP design requires that the weight of anode material is sufficient to supply current for the design life of the structure. This is calculated by the following formula:

19

$$W = \frac{\left(8760\,\frac{h}{yr}\right)YC}{ZU}$$

where :

W = weight of anode material

Y = design life (yrs)

C = current demand (Amps)

Z = anode capacity

U = utilization factor (0.9 for aluminum and zinc)

Finally, due to practical considerations, anode selection may ultimately be determined by commercial availability. It is often too expensive to customize anode size and geometry for one job. Therefore, except for large and specialized requirements, CP design centers around standard, commercially available anode types.

8.0   COST AND IMPLEMENTATION

There are many permutations possible in CP design, however to be successful it must satisfy economic constraints and be easy to install and operate.   Examples of CP designs are presented for an oil platform and ship.

8.1   Oil Platform Example
8.1.1 Structural Details

Water Depth	110m
No. of Legs	4
No. Horizontal Frames	5
No. of Nodes Below Surface	75
Total Submerged Surface Area	63,000 m^2
Total Pile Surface Area in Mud	6,000 m^2
Allowance for Risers, Conductors, Wells	220 Amps
Design Life	35 years

8.1.2. Current Demand

$Total = (\text{submerged S. A.})(\text{CP current density}) + (\text{pile S. A.})(\text{CP current density}) + \text{allowance}$

	Submerged Steel (A)	Piles (A)	Allowance (A)	Total (A)
North Sea				
Initial	11,340	150	220	11,710
Mean	5,670	120	220	6,010
Final	7,560	90	220	7,870
Gulf of Mexico				
Initial	6,930	150	220	7,300
Mean	3,780	120	220	4,120
Final	5,040	90	220	5,350

The following design current densities were used for calculating the current demand shown in the previous table:

	Submerged Steel (mA/m²)	Piles (mA/m²)
North Sea		
Initial	180	25
Mean	90	20
Final	120	15
Gulf of Mexico		
Initial	110	25
Mean	60	20
Final	80	15

Example calculation (for North Sea, Initial)

CP current for submerged steel $=$ (submerged S. A.)(CP current density) $= (63{,}000\text{m}^2)(0.180\,\frac{A}{m^2})$

CP current for submerged steel $= 11{,}340A$

CP current for piles $=$ (pile S. A.)(CP current density) $= (63{,}000\text{m}^2)(0.025\,\frac{A}{m^2})$

CP current for piles $= 150A$

Total CP current $= 11{,}340A + 150A + 220A$

Total CP current $= 11{,}710A$

8.1.3. Sacrificial Anode Design for Uncoated Structure

The following table is the weight required for 35 year CP design life (using mean current density)

Location	Zinc, kg	Aluminum, kg
NORTH SEA	2,624,880	723,462
GULF OF MEXICO	1,799,419	495,953

Example calculation for the weight of zinc required, North Sea:

$$W = \frac{\left(8760\,\frac{h}{yr}\right)YC}{ZU}$$

$$W = \frac{\left(8760\,\frac{h}{yr}\right)(35\,yr)(6{,}010\,A)}{\left(780\,\frac{Ah}{kg}\right)(0.9)}$$

$$W = 2{,}624{,}880\,kg$$

Number of Anodes Required to Provide Initial Current Demand to Polarize the Structure

Assume the following anode dimensions: 2,500 mm long

250 mm width

207 mm thick

	NORTH SEA	GULF OF MEXICO
Seawater Resistivity, ohm-cm	30	20
Anode Resistance, Ohms	0.0641	0.0427
Anode Current Output, Amps	3.900	5.855
Number of Anodes for Initial Current Demand	3003	1247
Mass of Zinc Anodes, kg	2,768,766	1,149,734
Mass of Aluminum Anodes, kg	1,048,047	435,203

23

The previous table was created using the following methodology:

Find Mass of One Anode, Zinc

$$m = \rho_{zinc} \forall$$
$$m = (7,130 \tfrac{kg}{m^3})(2.5m)(0.25m)(0.207m)$$
$$m = 922kg$$

Find Mass of One Anode, Aluminum

$$m = \rho_{Al} \forall$$
$$m = (2,700 \tfrac{kg}{m^3})(2.5m)(0.25m)(0.207m)$$
$$m = 349kg$$

Find the Resistance of the Anode Using Table 7.4 (example for North Sea)

$$R = \frac{\rho}{2\pi L}\left(\ln\left(\frac{4L}{r}\right) - 1\right)$$

$$R = \frac{30\Omega cm}{2\pi(250cm)}\left(\ln\left(\frac{4(250cm)}{\sqrt{\frac{(25cm)(20.7cm)}{\pi}}}\right) - 1\right)$$

$$R = 0.0641\Omega$$

Calculate single anode current output (example for North Sea):

$$I = \frac{V}{R}$$
$$I = \frac{(-0.800V - (-1.05V))}{0.0641\Omega}$$
$$I = 3.90A$$

Find the # of Anodes Necessary to Produce the Initial Current (example for North Sea):

$$\# \text{ of anodes} = \frac{\text{Initial current demand}}{\text{current output per anode}}$$

$$\# \text{ of anodes} = \frac{11,710A}{3.90 \tfrac{A}{anode}} = 3002.5 \text{ anodes} = 3003 \text{ anodes}$$

Find the Mass of the Anodes (example for zinc anodes, North Sea):

Total Mass of Zinc Anodes = (# of anodes)(mass per anode)

Total Mass of Zinc Anodes = (3003 anodes)(922 $\frac{kg}{anode}$) = 2,768,766 kg

Let us then compare the mass of anodes required for the design life and the mass required for the initial polarization of the structure:

	NORTH SEA	GULF OF MEXICO
Mass of Zinc to protect the structure for 35 years, kg	2,624,880	**1,799,419**
Mass of Zinc required to provide the initial current, kg	**2,768,766**	1,149,734
Mass of Aluminum to protect the structure for 35 years, kg	723,462	**495,953**
Mass of Aluminum required to provide the initial current, kg	**1,048,047**	435,203
# of Zinc Anodes Needed	3003	1952
# of Aluminum Anodes Needed	3003	1421

Anode Distribution and Spacing

For sacrificial anodes this maybe based on the current demand of the structure and the maximum current output of the anode.

NORTH SEA

Maximum Current Output   3.900 Amps

Maximum Current Demand   180 mA/m^2

Maximum Area Protected   3.900 A/(0.180A/m^2) = 21.7m^2

GULF OF MEXICO

Maximum Current Output $\quad\quad$ 5.855 Amps

Maximum Current Demand $\quad\quad$ 110 mA/m^2

Maximum Area Protected $\quad\quad$ 5.855 A/(0.110 A/m^2) = 53.2m^2

If the structural member is relatively large, say 3 m diameter, then a single anode placed in the center of a 22 or 53 m^2 area will not be too far from the extremities of the cathode it is protecting. For smaller members, allowances have to be made for attenuation, and anode sizes must be selected to ensure that the anode protects half way to the next anode.

8.1.4 Sacrificial Anode Design Coated Structure

The effect of coating a structure on CP design can be seen by applying the DNV criteria to Example 1. It can be seen that significant savings in anode material can be achieved if a Category 2, 3 or 4 coating is used. The category 1 coatings are only helpful for short design life. This interpretation of the interaction between coatings and CP is still open to debate with many experts in the Oil Industry questioning the low performance criteria assigned to Category I coatings.

26

Structure Area, m^2:			63,000					
Allowance, Amps			220					
Piles, Amps:			120					
Zinc Anodes, Ah/kg			780		Cost, $/tonne, Feb 1995			1,025
Aluminum Anodes, Ah/kg			2,830		Cost, $/tonne, Feb 1995			2,000
CD mA/m^2	tr, years	Category	k1	k2	f (ave)	f (final)	CP (ave) mA/m^2	CP (final) mA/m^2
North Sea								
90	35	1	0.1000	0.1000	1.8500	3.6000	90	90
90	35	1	0.1000	0.0500	0.9750	1.8500	88	90
90	35	2	0.0500	0.0300	0.5750	1.1000	52	90
90	35	2	0.0500	0.0200	0.4000	0.7500	36	68
90	35	3	0.0200	0.0150	0.2825	0.5450	25	49
90	35	3	0.0200	0.0120	0.2300	0.4400	21	40
90	35	4	0.0120	0.0120	0.2220	0.4320	20	39
90	35	4	0.0120	0.0120	0.2220	0.4320	20	39
Category			I	II	III	IV		
Total Current Demand, Amps			6,010	3,600	1,942	1,599		
Wt Aluminum, kg			723,465	433,387	233,745	192,451		
Cost Aluminum			1,446,931	866,774	467,490	384,903		
Number of Anodes			3,003	3,000	2,500	2,500		
Weight/Anode, kg			482	289	187	154		
Cost, $ / Anode			1,156	693	449	370		
Cost Installation $ / Anode			450	400	400	400		
Total Cost CP, $			**4,823,983**	**3,280,258**	**2,121,975**	**1,923,767**		
Gulf of Mexico								
60	35	1	0.1000	0.1000	1.8500	3.6000	60	60
60	35	1	0.1000	0.0500	0.9750	1.8500	59	60
60	35	2	0.0500	0.0300	0.5750	1.1000	35	60
60	35	2	0.0500	0.0200	0.4000	0.7500	24	45
60	35	3	0.0200	0.0150	0.2825	0.5450	17	33
60	35	3	0.0200	0.0120	0.2300	0.4400	14	26
60	35	4	0.0120	0.0120	0.2220	0.4320	13	26
60	35	4	0.0120	0.0120	0.2220	0.4320	13	26
Category			I	II	III	IV		
Total Current Demand			4,120	2,514	1,408	1,179		
Wt Aluminum			233,535	142,473	79,802	66,839		

8.1.5 Impressed Current Anode Design

Assuming the use of platinized titanium anodes with the following dimensions.

length = 1000 mm

diameter = 25 mm

Maximum driving potential = 9V

Then the surface area of the anode is:

27

πdL   = 0.078m^2

	NORTH SEA	GULF OF MEXICO
Anode Resistance, Ohms	0.2277	0.1518
Maximum Anode Current Output, Amps	39.5	59.3
Maximum current density on anode surface, A/m^2	506	760
Number of anodes required	296	123

The distribution of the anodes is critical.

8.2   Ship Hull Protection

Ship Hulls require protection from both corrosion and the development of biofouling accumulations.   The former is achieved by both coating and cathodic protection systems and the latter by antifouling coatings.   In addition to the basic costs of the coating and cathodic protection systems, allowances must be made for dry dock costs, loss of revenue, and increased fuel consumption and lost performance due to the increase in skin friction drag caused by poor hull maintenance and biofouling.

SHIP HULL COATING

GRIT BLAST

NACE #1, with 1 - 2 mil anchor profile

BARRIER COAT

Hard Boiled Mastic, two component epoxy amine

Two coats, 3 mils D.F.T.

Coverage per one mil dry - 564 sq.ft./gal.

Cost, $23.00/gal.

Cost for 6 mils D.F.T. $0.24/sq.ft.

CATHODIC PROTECTION DESIGN

SHIP	ORIANA
TYPE	PASSENGER
LENGTH, m	245
BREADTH, m	30
DRAFT, m	9.75
BLOCK COEFFICIENT, C_b	0.6
WETTED SURFACE AREA $(1.7xLxD)+(C_bxLxB)$ m^2	8,471
CURRENT DEMAND FOR HULL, (@22mA/m^2) Amps	186
CURRENT DEMAND FOR RUDDERS, Amps	15
CURRENT DEMAND FOR PROPELLERS, Amps	35
TOTAL CURRENT DEMAND, AMPS	236

29

Sacrificial Anode Calculations

Current Output per Anode

Assume anode dimensions: 500mm x 115mm x 65mm

The current output, $I = \dfrac{V}{R}$

R =   the anode resistance calculated using Lloyds' Formula for plate anodes

      Lloyds' Formula

$$R = \frac{\rho}{2S}$$
$$R = \frac{20\Omega - cm}{2(30.75cm)}$$
$$R = 0.325\Omega$$

Current output per anode,

$$I = \frac{V}{R}$$
$$I = \frac{0.25V}{0.325\Omega} = 0.769A$$

Number of anodes required to supply current,

$$\text{\# of anodes needed} = \frac{\text{Total current required}}{\text{Current output per anode}}$$
$$\text{\# of anodes needed} = \frac{236A}{0.384\frac{A}{anode}} = 307 \text{ anodes}$$

The total current capacity for one anode is:

$$\text{Volume of Anodes * Density * Capacity of Galvalum 1}$$
$$= 3.738\text{x}10^{-3} \text{ m}^3 * 2{,}700 \text{ kg/m}^3 * 2{,}830 \text{ Ah/kg} = 28{,}558 \text{ Ah}$$

The design life of the system will be

$$= \frac{28{,}558 \text{ A hrs * 307 anodes * (0.9)}}{236 \text{ Amps}} = 33{,}435 \text{ hrs or 3.8 years}$$

APPENDIX

Some Commonly Used Marine Materials

from Dexter, S.C. (1985), <u>Handbook</u> <u>of</u> <u>Oceanographic</u> <u>Materials</u>, Krieger Publishing, Malabar, FL.

Aluminum Alloys

Material	Composition	Density, ρ (lb/in^3)
Aluminum alloy 5052	97.25% Al, 2.5% Mg, 0.25% Cr	0.097
Elastic Modulus, E (psi)	**Yield Strength, σ_y (ksi)**	**Tensile Strength, σ_u (ksi)**
10 x 10^6	31 (H34)	38 (H34)
Potential in Seawater, ref. Ag-AgCl (V)	**Corrosion Types Suffered**	**Uses**
-0.92 to -1.1	Crevice and sometimes pitting attack.	Applications demanding good corrosion resistance and fatigue strength. These include fuel lines, tanks, and sheets.
Special Notes: Severe galvanic attack can occur when placed in contact with steel, stainless steel, copper alloys, nickel alloys, and titanium. Corrosion protection is desired for submerged applications.		

Material	Composition	Density, ρ (lb/in^3)
Aluminum alloy 6061	97.95% Al, 1.0% Mg, 0.6% Si, 0.25% Cu, 0.20% Cr	0.098
Elastic Modulus, E (psi)	**Yield Strength, σ_y (ksi)**	**Tensile Strength, σ_u (ksi)**
10 x 10^6	40 (T6)	45 (T6)
Potential in Seawater, ref. Ag-AgCl (V)	**Corrosion Types Suffered**	**Uses**
-0.72 to -1.07	Crevice and pitting attack. May also undergo intergranular attack and SCC.	Applications demanding adequate corrosion resistance and good mechanical properties. The most versatile aluminum alloy for marine use.
Special Notes: Severe galvanic attack can occur when placed in contact with steel, stainless steel, copper alloys, nickel alloys, and titanium. Cathodic protection and coating is desired for submerged applications.		

Material	Composition	Density, ρ (lb/in^3)
Aluminum alloy 7075	90% Al, 5.6% Zn, 2.5% Mg, 1.6% Cu, 0.3% Cr	0.101
Elastic Modulus, E (psi)	**Yield Strength, σ_y (ksi)**	**Tensile Strength, σ_u (ksi)**
10.4 x 10^6	73 (T6)	83 (T6)
Potential in Seawater, ref. Ag-AgCl (V)	**Corrosion Types Suffered**	**Uses**
-0.72 to -0.83	Severe crevice and pitting attack. Also susceptible to SCC and exfoliation.	Applications requiring high strength and low weight.
Special Notes: Severe galvanic attack can occur when placed in contact with steel, stainless steel, copper alloys, nickel alloys, and titanium. Must be anodized, coated, and cathodically protected for submerged applications.		

Copper and Copper alloys

Material	Composition	Density, ρ (lb/in^3)
Copper	99.9% Cu	0.322
Elastic Modulus, E (psi)	**Yield Strength, σ_y (ksi)**	**Tensile Strength, σ_u (ksi)**
17 x 10^6	50 (Fully hardened)	55 (Fully hardened)
Potential in Seawater, ref. Ag-AgCl (V)	**Corrosion Types Suffered**	**Uses**
-0.12 to -0.30	Uniform attack and sometimes localized attack as a result of metal ion concentration cells. Velocity effects can also be quite marked.	Electrical and architectural applications. Resists biofouling at corrosion rates > 1 mpy.
Special Notes: None		

Material	Composition	Density, ρ (lb/in^3)
Beryllium-Copper, CDA 172	97.9% Cu, 1.9% Be, 0.2% Co	0.298
Elastic Modulus, E (psi)	**Yield Strength, σ_y (ksi)**	**Tensile Strength, σ_u (ksi)**
18 x 10^6	150 - 190 (HT and 75% Cold Worked)	195 - 205 (HT and 75% Cold Worked)
Potential in Seawater, ref. Ag-AgCl (V)	**Corrosion Types Suffered**	**Uses**
-0.10 to -0.25	Uniform corrosion and slight crevice attack.	Applications requiring good corrosion resistance and high strength. These include springs, bearings, and bushings.
Special Notes: As in most copper alloys, metal ion concentration cells may form.		

Material	Composition	Density, ρ (lb/in^3)
Red Brass, CDA 230	85% Cu, 15% Zn	0.316
Elastic Modulus, E (psi)	**Yield Strength, σ_y (ksi)**	**Tensile Strength, σ_u (ksi)**
17 x 10^6	49 (50% Work Hardened)	57 - 72 (50% Work Hardened)
Potential in Seawater, ref. Ag-AgCl (V)	**Corrosion Types Suffered**	**Uses**
-0.20 to -0.40	Uniform corrosion and slight dezincification.	Applications requiring good corrosion resistance.
Special Notes: As in most copper alloys, metal ion concentration cells may form.		

Material	Composition	Density, ρ (lb/in^3)
Inhibited Admiralty Brass	71% Cu, 28% Zn, 1% Sn, 0.6% As, Sb, or Pb	0.308
Elastic Modulus, E (psi)	**Yield Strength, σ_y (ksi)**	**Tensile Strength, σ_u (ksi)**
16 x 10^6	72 (Fully Hardened)	88 - 97 (Fully Hardened)
Potential in Seawater, ref. Ag-AgCl (V)	**Corrosion Types Suffered**	**Uses**
-0.16 to -0.25	Uniform corrosion and crevice attack. Erosion corrosion at velocities > 6 fps.	Heat exchanger and condenser tubes and plates.
Special Notes: As in most copper alloys, metal ion concentration cells may form.		

Material	Composition	Density, ρ (lb/in³)
Naval Brass	60% Cu, 39% Zn, 1% Sn	0.304
Elastic Modulus, E (psi)	**Yield Strength, σ_y (ksi)**	**Tensile Strength, σ_u (ksi)**
15×10^6	66 (Hard-Drawn)	88 (Hard-Drawn)
Potential in Seawater, ref. Ag-AgCl (V)	**Corrosion Types Suffered**	**Uses**
-0.20 to -0.27	Uniform corrosion and dezincification (not completely eliminated with CP).	Condenser plates, prop shafts, fasteners.
Special Notes: Dezincification of this alloy may be severe, and, therefore, should be used with caution in submerged applications.		

Material	Composition	Density, ρ (lb/in³)
Aluminum Bronze D, CDA 614	91% Cu, 7% Al, 2% Fe	0.281
Elastic Modulus, E (psi)	**Yield Strength, σ_y (ksi)**	**Tensile Strength, σ_u (ksi)**
18×10^6	40 - 55 (Hardened)	75 - 85 (Hardened)
Potential in Seawater, ref. Ag-AgCl (V)	**Corrosion Types Suffered**	**Uses**
-0.09 to -0.26	Uniform corrosion and some dezincification and crevice corrosion	Corrosion resistant tubing, tanks, fasteners, and sheathing.
Special Notes: As in most copper alloys, metal ion concentration cells may form.		

Material	Composition	Density, ρ (lb/in³)
High Silicon Bronze A, CDA 655	94.8% Cu, 3.3% Si, 1.5% Mn, < 1.5% Fe and Zn	0.308
Elastic Modulus, E (psi)	**Yield Strength, σ_y (ksi)**	**Tensile Strength, σ_u (ksi)**
15×10^6	45 - 57 (Half-Hard)	78 - 98 (Half-Hard)
Potential in Seawater, ref. Ag-AgCl (V)	**Corrosion Types Suffered**	**Uses**
-0.17 to -0.23	Uniform corrosion and crevice corrosion.	Marine hardware, fasteners, shafting, and heat exchanger tubing.
Special Notes: As in most copper alloys, metal ion concentration cells may form.		

Material	Composition	Density, ρ (lb/in³)
90-10 Copper-Nickel	88.7% Cu, 10% Ni, 1.3% Fe	0.323
Elastic Modulus, E (psi)	**Yield Strength, σ_y (ksi)**	**Tensile Strength, σ_u (ksi)**
18×10^6	57 (Light Drawn)	60 (Light Drawn)
Potential in Seawater, ref. Ag-AgCl (V)	**Corrosion Types Suffered**	**Uses**
-0.15 to -0.30	Uniform corrosion and some surface attack.	Excellent resistance to marine fouling if allowed to freely corrode. Used for seawater tubing and boat hulls.
Special Notes: Susceptible to sulfide attack. Velocity effects at velocities > 10 fps.		

Appendix: Material Properties - 3

Material	Composition	Density, ρ (lb/in^3)
70-30 Copper-Nickel	68.9% Cu, 30% Ni, 0.5% Fe, 0.6% Mn	0.323
Elastic Modulus, E (psi)	**Yield Strength, σ_y (ksi)**	**Tensile Strength, σ_u (ksi)**
22 x 10^6	79 (Cold Drawn)	85 (Cold Drawn)
Potential in Seawater, ref. Ag-AgCl (V)	**Corrosion Types Suffered**	**Uses**
-0.17 to -0.23	Uniform corrosion and some surface attack.	Good strength. Used in heat exchangers with high water velocities.
Special Notes: Susceptible to sulfide attack. Velocity effects at velocities > 15 fps.		

Material	Composition	Density, ρ (lb/in^3)
Cast Silicon Brass and Bronze	82 - 91% Cu, 5 - 14% Zn, 4% Si	0.302
Elastic Modulus, E (psi)	**Yield Strength, σ_y (ksi)**	**Tensile Strength, σ_u (ksi)**
15 x 10^6 - 18 x 10^6	22 - 35 (As Cast)	55 - 70 (As Cast)
Potential in Seawater, ref. S.C.E. (V)	**Corrosion Types Suffered**	**Uses**
~ -0.27	Uniform corrosion.	Bearings, impellers, gears, props, pumps, fittings.
Special Notes: None		

Material	Composition	Density, ρ (lb/in^3)
Cast Aluminum Bronze	81 - 88% Cu, 9 - 13% Al, 1 - 5% Fe, others	0.272 - 0.281
Elastic Modulus, E (psi)	**Yield Strength, σ_y (ksi)**	**Tensile Strength, σ_u (ksi)**
14 x 10^6 - 20 x 10^6	40 - 80 (Heat Treated)	80 - 124 (Heat Treated)
Potential in Seawater, ref. S.C.E. (V)	**Corrosion Types Suffered**	**Uses**
-0.3 to -0.4	Uniform corrosion and dealloying.	Pump housings, bearings, impellers, gears, props, fittings.
Special Notes: None		

Nickel Alloys

Material	Composition	Density, ρ (lb/in³)
Monel 400	66.25% Ni, 31.5% Cu, 1.35% Fe, 0.9% Mn	0.319
Elastic Modulus, E (psi)	**Yield Strength, σ_y (ksi)**	**Tensile Strength, σ_u (ksi)**
26 x 10⁶	90 - 130 (Fully Hardened)	100 - 140 (Fully Hardened)
Potential in Seawater, ref. S.C.E. (V)	**Corrosion Types Suffered**	**Uses**
-0.04 to -0.14	Uniform corrosion, pitting, and crevice attack.	Valves, pumps, prop shafts, fixtures, fasteners.
Special Notes: Resists erosion corrosion to high velocities. May cause severe galvanic attack of less noble metals when coupled.		

Material	Composition	Density, ρ (lb/in³)
Inconel 625	65.3% Ni, 18.6% Cr, 9% Mo, 4% Cb, 3% Fe, 0.05% C	0.305
Elastic Modulus, E (psi)	**Yield Strength, σ_y (ksi)**	**Tensile Strength, σ_u (ksi)**
29.8 x 10⁶	201 (70% Cold Worked)	219 (70% Cold Worked)
Potential in Seawater, ref. S.C.E. (V)	**Corrosion Types Suffered**	**Uses**
-0.04 to +0.10	Highly resistant to most forms of attack.	Wire rope, propeller blades, fittings, springs, fasteners. Parts where little to no corrosion can be accepted.
Special Notes: Resists erosion corrosion to high velocities.		

Material	Composition	Density, ρ (lb/in³)
Incoloy 825	41.8% Ni, 21.5% Cr, 30% Fe, 3% Mo, 1.8% Cu, 1% Ti, 0.03% C	0.294
Elastic Modulus, E (psi)	**Yield Strength, σ_y (ksi)**	**Tensile Strength, σ_u (ksi)**
28 x 10⁶	35 - 45 (Cold Drawn)	85 - 101 (Cold Drawn)
Potential in Seawater, ref. S.C.E. (V)	**Corrosion Types Suffered**	**Uses**
-0.03 to +0.05	Crevice corrosion and pitting.	Components in desalination plants and heat exchangers.
Special Notes: Resistant to chloride SCC.		

Iron and Steels

Material	Composition	Density, ρ (lb/in^3)
Ductile Cast Iron	3.3 - 4.0% C, 2 - 3% Si, 0.2 - 0.6% Mn, < 2.5% Ni, > 0.15% total P and Mg, remainder Fe	0.257
Elastic Modulus, E (psi)	**Yield Strength, σ_y (ksi)**	**Tensile Strength, σ_u (ksi)**
23 x 10^6 - 25 x 10^6	40 - 150	60 - 175
Potential in Seawater, ref. S.C.E. (V)	**Corrosion Types Suffered**	**Uses**
-0.60 to -0.72	Mostly uniform with some shallow pitting.	General machinery parts, props, piping.
Special Notes: Cathodic protection is needed for longer term submerged exposure.		

Material	Composition	Density, ρ (lb/in^3)
AISI 1040 Steel	99.6% Fe, 0.4% C	0.283
Elastic Modulus, E (psi)	**Yield Strength, σ_y (ksi)**	**Tensile Strength, σ_u (ksi)**
30 x 10^6	86 (Heat Treated)	113 (Heat Treated)
Potential in Seawater, ref. S.C.E. (V)	**Corrosion Types Suffered**	**Uses**
-0.60 to -0.70	Mostly uniform with slight crevice corrosion.	Multiple structural and mechanical uses.
Special Notes: Coatings and/or cathodic protection is needed for marine use. Galvanic attack may occur if this alloy is immersed in seawater and in contact with copper alloys, nickel alloys, stainless steels, or titanium alloys.		

Material	Composition	Density, ρ (lb/in^3)
AISI 1080 Steel	99.2% Fe, 0.8% C	0.283
Elastic Modulus, E (psi)	**Yield Strength, σ_y (ksi)**	**Tensile Strength, σ_u (ksi)**
30 x 10^6	142 (Heat Treated)	190 (Heat Treated)
Potential in Seawater, ref. S.C.E. (V)	**Corrosion Types Suffered**	**Uses**
-0.60 to -0.70	Mostly uniform with slight crevice corrosion. Also susceptible to SCC and hydrogen embrittlement.	Multiple structural and mechanical uses.
Special Notes: Coatings and/or cathodic protection is needed for marine use. Galvanic attack may occur if this alloy is immersed in seawater and in contact with copper alloys, nickel alloys, stainless steels, or titanium alloys.		

Material	Composition	Density, ρ (lb/in^3)
HY-80 Steel	2 - 3.25% Ni, 1 - 1.8% Cr, 0.2% - 0.6% Mo, 0.15 - 0.35% Si, <0.25% P and S, 0.1 - 0.4% Mn, 0.18% C, remainder Fe	0.284
Elastic Modulus, E (psi)	**Yield Strength, σ_y (ksi)**	**Tensile Strength, σ_u (ksi)**
30 x 10^6	80 - 100 (Quenched and Tempered)	103 (Quenched and Tempered)
Potential in Seawater, ref. S.C.E. (V)	**Corrosion Types Suffered**	**Uses**
-0.63	Mostly uniform.	Hull plating, offshore platforms, tanks pressure vessels, cranes, booms
Special Notes: Coatings and/or cathodic protection is needed for marine use. Galvanic attack may occur if this alloy is immersed in seawater and in contact with copper alloys, nickel alloys, stainless steels, or titanium alloys.		

Material	Composition	Density, ρ (lb/in^3)
HY-100 Steel	2.25 - 3.5% Ni, 1 - 1.8% Cr, 0.2% - 0.6% Mo, 0.15 - 0.35% Si, <0.25% P and S, 0.1 - 0.4% Mn, 0.2% C, remainder Fe	0.284
Elastic Modulus, E (psi)	**Yield Strength, σ_y (ksi)**	**Tensile Strength, σ_u (ksi)**
30 x 10^6	100 - 105 (Quenched and Tempered)	110 - 118 (Quenched and Tempered)
Potential in Seawater, ref. S.C.E. (V)	**Corrosion Types Suffered**	**Uses**
-0.63	Mostly uniform. Some tendency towards SCC and hydrogen embrittlement.	Hull plating, offshore platforms, tanks pressure vessels, cranes, booms
Special Notes: Coatings and/or cathodic protection is needed for marine use. Galvanic attack may occur if this alloy is immersed in seawater and in contact with copper alloys, nickel alloys, stainless steels, or titanium alloys.		

Material	Composition	Density, ρ (lb/in^3)
Low Alloy-High Strength Steels (ASTM A-242 and A-441)	0.18 - 0.22% C, 0.5 - 1.5% (each) Mn, Ni, Cr, ~0.25% (each) P, Si, S, Cu, remainder Fe	0.283
Elastic Modulus, E (psi)	**Yield Strength, σ_y (ksi)**	**Tensile Strength, σ_u (ksi)**
30 x 10^6	40 - 60 (Annealed)	60 - 80 (Annealed)
Potential in Seawater, ref. S.C.E. (V)	**Corrosion Types Suffered**	**Uses**
-0.57 to -0.63	Mostly uniform with some crevice corrosion and pitting.	Structural sections and members.
Special Notes: Coatings and/or cathodic protection is needed for marine use. Galvanic attack may occur if this alloy is immersed in seawater and in contact with copper alloys, nickel alloys, stainless steels, or titanium alloys.		

Appendix: Material Properties - 7

Material	Composition	Density, ρ (lb/in^3)
Maraging 300 Steel	18 - 19 % Ni, 8.5 - 9.5% Co, 4.7 - 5.2% Mo, 0.5 - 0.7% Ti, 0.05 - 0.15% Al, < 0.03% C, remainder Fe	0.290
Elastic Modulus, E (psi)	**Yield Strength, σ_y (ksi)**	**Tensile Strength, σ_u (ksi)**
29 x 10^6	295 - 303 (Heat Treated)	297 - 306 (Heat Treated)
Potential in Seawater, ref. S.C.E. (V)	**Corrosion Types Suffered**	**Uses**
-0.57 to -0.58	Uniform, SCC, and hydrogen embrittlement. SCC and embrittlement can be controlled with cathodic protection.	High strength weldable structural pieces.
Special Notes: Coatings and/or cathodic protection is needed for marine use. Galvanic attack may occur if this alloy is immersed in seawater and in contact with copper alloys, nickel alloys, stainless steels, or titanium alloys.		

Titanium and Titanium Alloys

Material	Composition	Density, ρ (lb/in^3)
Unalloyed Titanium	98.9 - 99.5% Ti	0.163
Elastic Modulus, E (psi)	**Yield Strength, σ_y (ksi)**	**Tensile Strength, σ_u (ksi)**
15 x 10^6	up to 90 (Cold Worked)	up to 100 (Cold Worked)
Potential in Seawater, ref. S.C.E. (V)	**Corrosion Types Suffered**	**Uses**
-0.05 to +0.06	None.	Structural members, marine parts requiring immunity, impressed current anodes.
Special Notes: SCC is possible if titanium contains higher levels of oxygen.		

Material	Composition	Density, ρ (lb/in^3)
Titanium 6Al-4V	5.5 - 6.5% Al, 3.5 - 4.5% V, <0.25% Fe, remainder Ti	0.160
Elastic Modulus, E (psi)	**Yield Strength, σ_y (ksi)**	**Tensile Strength, σ_u (ksi)**
16.5 x 10^6	155 (Age Hardened)	165 - 170 (Age Hardened)
Potential in Seawater, ref. S.C.E. (V)	**Corrosion Types Suffered**	**Uses**
-0.05 to +0.06	None, except some tendency for SCC.	Pumps, impellers, structural members, marine hardware and parts requiring immunity.
Special Notes: None		

Stainless Steels

Material	Composition	Density, ρ (lb/in^3)
302 Stainless Steel	70.85 - 74.85% Fe, 17 - 19% Cr, 8 - 10% Ni, 0.15% C	0.290
Elastic Modulus, E (psi)	**Yield Strength, σ_y (ksi)**	**Tensile Strength, σ_u (ksi)**
28 x 10^6	75 (Quarter Hard)	125 (Quarter Hard)
Potential in Seawater, ref. S.C.E. (V)	**Corrosion Types Suffered**	**Uses**
-0.05 to -0.10 (passive) -0.45 to -0.57 (active)	Crevice and pitting corrosion. Susceptible to local attack in areas covered by fouling	General purpose in non-submerged applications.
Special Notes: Local attack minimized in water velocities > 5 fps, but not generally recommended for submerged use due to pitting.		

Material	Composition	Density, ρ (lb/in^3)
303 Stainless Steel	17 - 19% Cr, 8 - 10% Ni, > 0.15% S or Se, 0.15% C, remainder Fe	0.290
Elastic Modulus, E (psi)	**Yield Strength, σ_y (ksi)**	**Tensile Strength, σ_u (ksi)**
28 x 10^6	75 (Cold Worked)	110 (Cold Worked)
Potential in Seawater, ref. S.C.E. (V)	**Corrosion Types Suffered**	**Uses**
-0.05 to -0.10 (passive) -0.45 to -0.57 (active)	Severe crevice and pitting corrosion. Susceptible to local attack in areas covered by fouling	Generally not recommended for seawater application.
Special Notes: This grade may be substituted for others by suppliers with devastating consequences. Non-magnetic, austenitic alloy.		

Material	Composition	Density, ρ (lb/in^3)
304 Stainless Steel	67.92 - 72.92% Fe, 18 - 20% Cr, 9 - 12% Ni, 0.08% C	0.290
Elastic Modulus, E (psi)	**Yield Strength, σ_y (ksi)**	**Tensile Strength, σ_u (ksi)**
28 x 10^6	75 (Cold Worked)	110 (Cold Worked)
Potential in Seawater, ref. S.C.E. (V)	**Corrosion Types Suffered**	**Uses**
-0.09 to -0.15 (passive) -0.20 to -0.57 (active)	Crevice and pitting corrosion. Susceptible to local attack in areas covered by fouling. Heat effected zones may be sensitized.	Topside wire rope and general purpose submerged use where velocities are > 5 fps.
Special Notes: Cathodic protection is necessary for submerged structural applications when exposure is greater than two months. Non-magnetic, austenitic alloy.		

Material	Composition	Density, ρ (lb/in^3)
316 Stainless Steel	64.92 - 71.92% Fe, 16 - 18% Cr, 10 - 14% Ni, 2 - 3% Mo, 0.08% C	0.290
Elastic Modulus, E (psi)	**Yield Strength, σ_y (ksi)**	**Tensile Strength, σ_u (ksi)**
28 x 10^6	30 - 42 (Annealed)	80 - 90 (Annealed)
Potential in Seawater, ref. S.C.E. and Ag-AgCl (V)	**Corrosion Types Suffered**	**Uses**
-0.00 to -0.15 (passive) -0.35 to -0.60 (active)	Crevice and pitting corrosion. Susceptible to local attack especially in areas covered by fouling. Heat effected zones may be sensitized.	Topside wire rope and general purpose where velocities are > 5 fps.
Special Notes: Cathodic protection is necessary for submerged structural applications when exposure is greater than six months. This is the most corrosion resistant 300 series stainless. Non-magnetic, austenitic alloy.		

Material	Composition	Density, ρ (lb/in^3)
17-4 PH Stainless Steel	16.5% Cr, 4% Ni, 4% Cu, 0.3% Nb and Ta, 0.07% C, remainder Fe	0.280 - 0.282
Elastic Modulus, E (psi)	**Yield Strength, σ_y (ksi)**	**Tensile Strength, σ_u (ksi)**
28.5 x 10^6	178 - 185 (Hardened)	200 (Hardened)
Potential in Seawater, ref. Ag-AgCl (V)	**Corrosion Types Suffered**	**Uses**
-0.10 to -0.20 (passive) -0.20 to -0.40 (active)	Crevice and pitting corrosion. Weld bead attack.	Parts with moderate corrosion resistance and high strength to weight ratio.
Special Notes: Cathodic protection should be from impressed current or mild steel sacrificial anodes. Problems arise with aluminum, zinc, and magnesium anodes. Cathodic protection may lead to hydrogen embrittlement and cracking.		

Material	Composition	Density, ρ (lb/in^3)
410 Stainless Steel	85.35 - 87.35% Fe, 11.5 - 13.5% Cr, 1% Mn, 0.15% C	0.280
Elastic Modulus, E (psi)	**Yield Strength, σ_y (ksi)**	**Tensile Strength, σ_u (ksi)**
29 x 10^6	140 - 145 (Heat Treated)	180 - 190 (Heat Treated)
Potential in Seawater, ref. S.C.E. (V)	**Corrosion Types Suffered**	**Uses**
-0.24 to -0.35 (passive) -0.45 to -0.57 (active)	Severe crevice and pitting corrosion.	Applications where a high strength alloy is important. Submerged applications require cathodic protection to prevent localized attack.
Special Notes: Magnetic, martensitic alloy.		

Appendix: Material Properties - 10

Other Metals

Material	Composition	Density, ρ (lb/in³)
Commercially Pure Magnesium	99.98% Mg	0.063
Elastic Modulus, E (psi)	**Yield Strength, σ_y (ksi)**	**Tensile Strength, σ_u (ksi)**
5.7×10^6 - 6.5×10^6	3 (As Cast)	13 (As Cast)
Potential in Seawater, ref. S.C.E. (V)	**Corrosion Types Suffered**	**Uses**
-1.60 to -1.63	Rapid uniform corrosion. Severe galvanic effects when coupled with all common marine metals.	Sacrificial anodes and corrosive links.
Special Notes: Not suitable for structural applications in seawater.		

Material	Composition	Density, ρ (lb/in³)
Zinc	99.92% Zn, 0.08% Pb	0.258
Elastic Modulus, E (psi)	**Yield Strength, σ_y (ksi)**	**Tensile Strength, σ_u (ksi)**
----	----	19 - 23 (Hot Rolled)
Potential in Seawater, ref. S.C.E. (V)	**Corrosion Types Suffered**	**Uses**
-0.98 to -1.03	Uniform corrosion with some pitting in anaerobic conditions.	Galvanizing, sacrificial anodes and corrosive links.
Special Notes: None.		

Material	Composition	Density, ρ (lb/in³)
Lead	----	0.410
Elastic Modulus, E (psi)	**Yield Strength, σ_y (ksi)**	**Tensile Strength, σ_u (ksi)**
2.0×10^6	----	2.0 (As Cast)
Potential in Seawater, ref. S.C.E. (V)	**Corrosion Types Suffered**	**Uses**
-0.19 to -0.25	Uniform corrosion.	Galvanizing, sacrificial anodes and corrosive links.
Special Notes: None.		

Material	Composition	Density, ρ (lb/in³)
Gold	99.5 - 99.99% Au	0.698
Elastic Modulus, E (psi)	**Yield Strength, σ_y (ksi)**	**Tensile Strength, σ_u (ksi)**
10.8×10^6 - 11.6×10^6	30 (60% Cold Worked)	32 (60% Cold Worked)
Potential in Seawater, ref. S.C.E. (V)	**Corrosion Types Suffered**	**Uses**
----	Completely resistant to marine corrosion.	Specialty applications and electrical contacts.
Special Notes: None.		

Appendix: Material Properties - 11

Material	Composition	Density, ρ (lb/in^3)
Platinum	99.85% Pt	0.775
Elastic Modulus, E (psi)	**Yield Strength, σ_y (ksi)**	**Tensile Strength, σ_u (ksi)**
21×10^6 - 25×10^6	27 (50% Cold Worked)	28 - 30 (50% Cold Worked)
Potential in Seawater, ref. S.C.E. (V)	**Corrosion Types Suffered**	**Uses**
+0.20 to +0.35	Completely resistant to marine corrosion.	Impressed current anodes and electrical contacts.
Special Notes: None.		

Material	Composition	Density, ρ (lb/in^3)
Silver	99.9% Ag	0.379
Elastic Modulus, E (psi)	**Yield Strength, σ_y (ksi)**	**Tensile Strength, σ_u (ksi)**
10.3×10^6 - 11.3×10^6	44 (50% Cold Worked)	up to 54 (50% Cold Worked)
Potential in Seawater, ref. S.C.E. (V)	**Corrosion Types Suffered**	**Uses**
-0.09 to -0.14	Slight uniform corrosion. Increased tarnish with sulfur compounds present.	Electrical conductors and radar applications. Solder when alloyed.
Special Notes: None.		

Appendix: Material Properties - 12

Polymers, Rubbers, and Elastomers

Material	Description	Specific Gravity
ABS, Medium Impact	Thermoplastic (acrylonitrile butadiene styrene)	1.05 - 1.07
Elastic Modulus, E (psi)	**Water Absorption**	**Tensile Strength, σ_u (ksi)**
3.0×10^5 - 4.1×10^5	0.2 - 0.45% in 24 hrs.	5.9 - 8.0
Behavior in the Marine Environment		**Uses**
Slight yellowing and embrittlement in direct sunlight. No chemical degradation in seawater. Not attacked by borers unless in contact with wood.		Multiple structural uses. Pipe, tubing, instrument housings, bearings.

Material	Description	Specific Gravity
Acetal, Standard Homopolymer	Thermoplastic (tradenames - Delrin, Celcon)	1.43
Elastic Modulus, E (psi)	**Water Absorption**	**Tensile Strength, σ_u (ksi)**
5.2×10^5	0.25% in 24 hrs.	10.0
Behavior in the Marine Environment		**Uses**
Slight chalking in sunlight. No chemical degradation in seawater. Usually not attacked by borers unless in contact with wood or tape. It is attacked by strong acids and bases. Excellent resistance to many organic solvents.		Gears, bushings, levers, shafts, springs, hardware.

Material	Description	Specific Gravity
Cast Acrylics	Polymethyl methacrylate (tradenames - Lucite, Perspex, Plexiglas)	1.17 - 1.28
Elastic Modulus, E (psi)	**Water Absorption**	**Tensile Strength, σ_u (ksi)**
2.7×10^5 - 5.0×10^5	0.2 - 0.5% in 24 hrs.	5.5 - 8.0 (High Impact Sheet)
Behavior in the Marine Environment		**Uses**
Usually not affected by sunlight. No chemical degradation in seawater. Usually not attacked by borers unless in contact with wood or tape. Water absorption can lead to a 10% reduction in hardness and up to a 30% reduction in tensile strength. It is attacked by strong acids and bases. Soluble in ketones, esters, and aromatic and chlorinated hydrocarbons. Excellent resistance to many organic solvents.		Lenses, windows, housings and many general purpose applications.

Material	Description	Specific Gravity
Epoxy	Diglycidal ether of bisphenol A	1.1 - 2.0
Elastic Modulus, E (psi)	**Water Absorption**	**Tensile Strength, σ_u (ksi)**
5×10^5 - 15×10^5	0.1 - 1.0% in 24 hrs.	5 - 15
Behavior in the Marine Environment		**Uses**
Resistant to sunlight with UV inhibitors. Usually not attacked by borers unless in contact with wood or tape. May be attacked by sulfuric and acetic acid. Some attack by stong bases. Resistant to organic solvents and weak acids and bases.		Potting material for electical components, castings, marine coatings, adhesives, patching compounds.

Material	Description	Specific Gravity
Nylon, Type 6	Thermoplastic, polyamide	1.14
Elastic Modulus, E (psi)	**Water Absorption**	**Tensile Strength, σ_u (ksi)**
3.8×10^5	1.3 - 1.9% in 24 hrs.	9.5 - 12.5
Behavior in the Marine Environment		**Uses**
Embrittled by prolonged exposure to sunlight. Usually not attacked by borers unless in contact with wood. May be attacked by strong acids, phenols, and formic acid. Resistant to bases, weak acids, and most common solvents. Water absorption and swelling may alter dimensions and mechanical properties		Bearings, gears, bushings, housings, rods, ropes, coatings.

Material	Description	Specific Gravity
Polycarbonate (unfilled)	Tradenames - Lexan, Merlon	1.19 - 1.25
Elastic Modulus, E (psi)	**Water Absorption**	**Tensile Strength, σ_u (ksi)**
3.0×10^5 - 4.5×10^5	0.12 - 0.19% in 24 hrs.	9.0 - 10.5
Behavior in the Marine Environment		**Uses**
Sunlight may lead to a slight color change and some embrittlement. No chemical degradation in seawater. Usually not attacked by borers unless in contact with wood. Low water absorption leads to good dimensional stability and retention of properties. It is attacked by strong acids and bases, organic solvents, and fuels. Resistance to weak acids, oils, and greases.		Lenses, windows, housings, impellers and parts requiring high impact resistance.

Material	Description	Specific Gravity
Polyethylene, High Density	Thermoplastic (Tradenames - Marlex, Norchem, Rulan)	0.95 - 0.96
Elastic Modulus, E (psi)	**Water Absorption**	**Tensile Strength, σ_u (ksi)**
3.0×10^5 - 4.5×10^5	< 0.01% in 24 hrs.	4.4
Behavior in the Marine Environment		**Uses**
Greatly degraded by sunlight if inhibitors are not used. Usually not attacked by borers unless in contact with wood. Generally shows excellent resistance to the marine environment. Good chemical resistance. Slowly attacked by strong acids.		Wire and cable insulation, pipe, housings.

Material	Description	Specific Gravity
Polypropylene	General purpose and high impact thermoplastic	0.89 - 0.91
Elastic Modulus, E (psi)	**Water Absorption**	**Tensile Strength, σ_u (ksi)**
1.6×10^5 - 2.2×10^5	< 0.01 - 0.03% in 24 hrs.	4.3 - 5.5
Behavior in the Marine Environment		**Uses**
Greatly degraded by sunlight if inhibitors are not used. Usually not attacked by borers unless in contact with wood. Generally shows excellent resistance to the marine environment. Good chemical resistance. Slowly attacked by strong acids.		Wire and cable coatings, film, packaging, hinges housings.

Material	Description	Specific Gravity
Teflon, PTFE	Polytetrafluoroethylene (tradenames - Teflon, Fluon, Halon, Rulon)	2.1 - 2.3
Elastic Modulus, E (psi)	**Water Absorption**	**Tensile Strength, σ_u (ksi)**
0.38×10^5 - 0.65×10^5	0.01% in 24 hrs.	2.0 - 6.5
Behavior in the Marine Environment		**Uses**
Not degraded by sunlight. Usually not attacked by borers unless in contact with wood. Generally shows excellent resistance to the marine environment. Excellent chemical resistance. May be attacked by the alkali metals.		Pipes, valves, bearings, impellers, electrical insulators, non-stick coatings.

Material	Description	Specific Gravity
Polyvinyl Chloride, PVC	Polytetrafluoroethylene (tradenames - Teflon, Fluon, Halon, Rulon)	1.30 - 1.45
Elastic Modulus, E (psi)	**Water Absorption**	**Tensile Strength, σ_u (ksi)**
3.5×10^5 - 6.0×10^5	0.03 - 0.04% in 24 hrs.	5.5 - 9.0
Behavior in the Marine Environment		**Uses**
Sunlight produces minor effects. Generally shows good resistance to the marine environment. Attacked by strong acids, ketones, esters, and aromatic hydrocarbons. Resistant to alcohols, aliphatic hydrocarbons, oils, bases, and weak acids.		Pipes, tanks, molded and extruded parts, housings.

Material	Description	Specific Gravity
Butyl Rubber	Isobutylene-isoprene	0.90
Tear Resistance	**Abrasion Resistance**	**Tensile Strength, σ_u (ksi)**
Good	Good to Excellent	2.5 - 3.0
Behavior in the Marine Environment		**Uses**
Very good resistance to sunlight produces. Excellent resistance to swelling in water. Resistant to acids, oxidation and heat aging. Vulnerable to many solvents, oils, and fuels.		Flexible electrical insulation, hose, shock absorption, diaphragms.

Material	Description	Specific Gravity
Natural and Synthetic Rubber	Polyisoprene	0.93
Tear Resistance	**Abrasion Resistance**	**Tensile Strength, σ_u (ksi)**
Excellent	Excellent	2.5 - 4.5
Behavior in the Marine Environment		**Uses**
Fair to poor resistance to sunlight. Marine exposure may cause some swelling. Microorganisms and hydrogen sulfide may lead to severe cracking. Resistant to oxidation and heat aging. Vulnerable to many solvents, oils, and fuels. Shows fair to good resistance to organic acids.		Seals, gaskets, hose, chemical tank linings.

Appendix: Material Properties - 15

Material	Description	Specific Gravity
Neoprene Rubber	Chloroprene	1.25
Tear Resistance	**Abrasion Resistance**	**Tensile Strength, σ_u (ksi)**
Fair to Good	Good	3.0 - 4.0
Behavior in the Marine Environment		**Uses**
Very good resistance to sunlight. Marine exposure may cause some swelling. May be degraded by aromatic hydrocarbons. Good to excellent resistance to other organic solvents, oils, fuels, acids, and heat.		Seals, gaskets, chemical tank linings, wetsuits.

Material	Description	Specific Gravity
Fluorocarbon Elastomers	Trade names: Kel-F, Viton	1.40 - 1.95
Tear Resistance	**Abrasion Resistance**	**Tensile Strength, σ_u (ksi)**
Poor to Fair	Good	1.5 - 3.0
Behavior in the Marine Environment		**Uses**
Very good resistance to sunlight and swelling. May be degraded by alkalies, synthetic lubricants, hydraulic fluids containing phosphates. Excellent resistance to high temperature air and oils.		O-rings, seals, gaskets, hose, shaft seals.

Material	Description	Specific Gravity
Urethane Elastomers	Trade names: Adiprene, Cyanaprene, Elastothane, Roylar	1.07
Tear Resistance	**Abrasion Resistance**	**Tensile Strength, σ_u (ksi)**
Excellent	Superior	5.0 - 8.0
Behavior in the Marine Environment		**Uses**
Very good resistance to sunlight and swelling (except at high temperatures). May be degraded by acids, alkalies, oxygenated alcohols. Excellent resistance to hydrocarbon solvents, oils.		Components requiring superior abrasion resistance.

Appendix: Material Properties - 16

Concrete and Glass

Material	Composition	Density, ρ (lb/ft^3)
Concrete	Varied	140 - 150
Elastic Modulus, E (psi)	**Compressive Strength, (ksi)**	**Flexural Strength, (ksi)**
3×10^6 - 6×10^6	3.5 - 7.5	0.4 - 0.8
Porosity (% by volume)	**Marine Attack Suffered**	**Uses**
5 - 10	Water absorption up to 2.4% @ 550 ft head. Degraded by high sulfate waters, causing cracking and softening.	Large structural members (with and without steel reinforcement), ship hulls, moorings.
Special Notes: Deterioration of concrete can lead to lowering of pH at the rebar, causing corrosion and spalling of the concrete. For longer term durability concrete, it is desirable to use low permeability types with reduced alkalinity and low 3 CaO Al$_2$O$_3$ content.		

Material	Composition	Specific Gravity
Glass (Borosilicate and Soda Lime)	Trade names: Kimax, Pyrex	2.13 to 2.55
Elastic Modulus, E (psi)	**Abrasion Resistance**	**Tensile Strength, σ_u (ksi)**
7.4×10^6 - 10.0×10^6	Excellent	0.5 - 40.0
Refractive Index	**Behavior in Marine Environment**	**Uses**
1.468 - 1.525	Generally unaffected by weathering or marine exposure.	Containers, plates, buoyancy spheres, lenses, housings.
Special Notes: May be attacked by hydrofluoric acid and sodium hydroxide.		

Wood

Material	Moisture Content (%)	Specific Gravity
Hardwood, Seasoned Maple and Oak	12	0.63 to 0.68
Elastic Modulus in Bending (psi)	**Modulus of Rupture (ksi)**	**Behavior in Marine Environment**
1.8×10^6	15.8 (maple) 14.3 - 15.2 (oak)	Left untreated these woods can be severely damaged by marine borers in as little as six months exposure when placed within six feet of bottom sediments. The borer attack is generally most rapid in warm coastal and lower latitude waters.

Material	Moisture Content (%)	Specific Gravity
Teak and Mahogany	52 (teak)	0.50 (mahogany)
Elastic Modulus in Bending (psi)	**Modulus of Rupture (ksi)**	**Behavior in Marine Environment**
1.4×10^6 - 1.7×10^6	11.1 - 11.4	These woods are susceptible to borer attack.

Material	Moisture Content (%)	Specific Gravity
Softwood, Seasoned Cedar and Cypress	12	0.46 to 0.47
Elastic Modulus in Bending (psi)	**Modulus of Rupture (ksi)**	**Behavior in Marine Environment**
0.9×10^6 - 1.4×10^6	8.8 (cedar) 10.6 (cypress)	Left untreated these woods can be severely damaged by marine borers in as little as six months exposure when placed within six feet of bottom sediments. The borer attack is generally most rapid in warm coastal and lower latitude waters.

Material	Moisture Content (%)	Specific Gravity
Softwood, Seasoned Pine and Spruce	12	0.35 to 0.40
Elastic Modulus in Bending (psi)	**Modulus of Rupture (ksi)**	**Behavior in Marine Environment**
1.2×10^6 - 2.0×10^6	8.6 - 10.1 (pine) 10.2 (spruce)	Left untreated these woods can be severely damaged by marine borers in as little as six months exposure when placed within six feet of bottom sediments. The borer attack is generally most rapid in warm coastal and lower latitude waters.

Fiber Reinforced Plastics (FRP)

from Agarwal, B.D and L.J. Broutman (1990), <u>Analysis</u> <u>and</u> <u>Performance</u> <u>of</u> <u>Fiber</u> <u>Composites</u>, Wiley Publishing, New York.

Material	Composition	Specific Gravity
E-Glass Reinforced Epoxy	57% E-Glass, 43% Epoxy	1.97
Tensile Modulus, E (psi)	**Tensile Strength, σ_u (ksi)**	**Longitudinal Poisson's Ratio**
3.1×10^6	82.5	0.25
Uses:		
Applications demanding excellent corrosion resistance and high strength to weight ratio. These include structural members, boat hulls, tanks, specialty items.		
Special Notes: Can be degraded by sunlight if inhibitors or barrier coat protection is not used. May also be somewhat degraded by water absorption if not protected.		

Material	Composition	Specific Gravity
Kevlar 49 Reinforced Epoxy	60% Kevlar 49, 40% Epoxy	1.40
Tensile Modulus, E (psi)	**Tensile Strength, σ_u (ksi)**	**Longitudinal Poisson's Ratio**
5.8×10^6	94.3	0.34
Uses:		
Applications demanding excellent corrosion resistance and high strength to weight ratio. These include structural members, boat hulls, tanks, specialty items.		
Special Notes: Can be degraded by sunlight if inhibitors or barrier coat protection is not used. May also be somewhat degraded by water absorption if not protected.		

Material	Composition	Specific Gravity
Carbon Fiber Reinforced Epoxy	58% Carbon Fiber, 42% Epoxy	1.54
Tensile Modulus, E (psi)	**Tensile Strength, σ_u (ksi)**	**Longitudinal Poisson's Ratio**
12.0×10^6	55.1	0.38
Uses:		
Applications demanding excellent corrosion resistance and high strength to weight ratio. Excellent stiffness properties. Uses include structural members, boat hulls, tanks, specialty items.		
Special Notes: Can be degraded by sunlight if inhibitors or barrier coat protection is not used. May also be somewhat degraded by water absorption if not protected.		